RADC-TR-82-286, Vol IVe (of six)
Final Technical Report
August 1984

AD-A150 652

BASIC EMC TECHNOLOGY ADVANCEMENT FOR C^3 SYSTEMS - Modeling of Transmission Lines: A Comparison of Lumped-Circuit Iterative Models and the Transmission Line Model

Southeastern Center for Electrical Engineering Education

Woodrow W. Everett III and Clayton R. Paul

ELECTE
FEB 2 7 1985

APPROVED FOR PUBLIC RELEASE; DISTRIBUTION UNLIMITED

DTIC FILE COPY

ROME AIR DEVELOPMENT CENTER
Air Force Systems Command
Griffiss Air Force Base, NY 13441

85 02

This report has been reviewed by the RADC Public Affairs Office (PA) and is releasable to the National Technical Information Service (NTIS). At NTIS it will be releasable to the general public, including foreign nations.

RADC-TR-82-286, Volume IVe (of six) has been reviewed and is approved for publication.

APPROVED: Roy F. Stratton

ROY F. STRATTON
Project Engineer

APPROVED:

W. S. TUTHILL, Colonel, USAF
Chief, Reliability & Compatibility Division

FOR THE COMMANDER: John A. Ritz

JOHN A. RITZ
Acting Chief, Plans Office

If your address has changed or if you wish to be removed from the RADC mailing list, or if the addressee is no longer employed by your organization, please notify RADC (RBCT) Griffiss AFB NY 13441. This will assist us in maintaining a current mailing list.

Do not return copies of this report unless contractual obligations or notices on a specific document requires that it be returned.

DISCLAIMER NOTICE

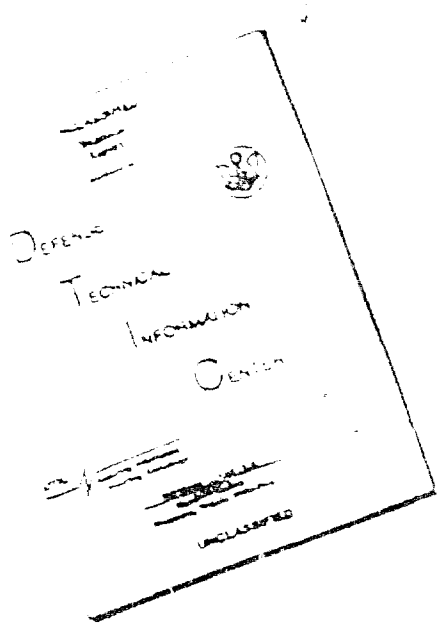

THIS DOCUMENT IS BEST QUALITY AVAILABLE. THE COPY FURNISHED TO DTIC CONTAINED A SIGNIFICANT NUMBER OF PAGES WHICH DO NOT REPRODUCE LEGIBLY.

REPRODUCED FROM BEST AVAILABLE COPY

THIS DOCUMENT CONTAINED BLANK PAGES THAT HAVE BEEN DELETED

UNCLASSIFIED
SECURITY CLASSIFICATION OF THIS PAGE

REPORT DOCUMENTATION PAGE

1a. REPORT SECURITY CLASSIFICATION UNCLASSIFIED	1b. RESTRICTIVE MARKINGS N/A
2a. SECURITY CLASSIFICATION AUTHORITY N/A	3. DISTRIBUTION/AVAILABILITY OF REPORT Approved for public release; distribution unlimited.
2b. DECLASSIFICATION/DOWNGRADING SCHEDULE N/A	
4. PERFORMING ORGANIZATION REPORT NUMBER(S) N/A	5. MONITORING ORGANIZATION REPORT NUMBER(S) RADC-TR-82-286, Volume IVe (of six)
6a. NAME OF PERFORMING ORGANIZATION Southeastern Center for Electrical Engineering Education 6b. OFFICE SYMBOL (If applicable)	7a. NAME OF MONITORING ORGANIZATION Rome Air Development Center (RBCT)
6c. ADDRESS (City, State and ZIP Code) 1101 Massachusetts Ave St. Cloud FL 32706	7b. ADDRESS (City, State and ZIP Code) Griffiss AFB NY 13441
8a. NAME OF FUNDING/SPONSORING ORGANIZATION Rome Air Development Center 8b. OFFICE SYMBOL (If applicable) (RBCT)	9. PROCUREMENT INSTRUMENT IDENTIFICATION NUMBER F30602-81-C-0062
8c. ADDRESS (City, State and ZIP Code) Griffiss AFB NY 13441	10. SOURCE OF FUNDING NOS. PROGRAM ELEMENT NO. 62702F; PROJECT NO. 2338; TASK NO. 03; WORK UNIT NO. 35

11. TITLE (Include Security Classification) BASIC EMC TECHNOLOGY ADVANCEMENT FOR C^3 SYSTEMS - Modeling of Transmission Lines: A Comparison of Lumped-Circuit Iterative Models and the (Cont'd)

12. PERSONAL AUTHOR(S)
Woodrow W. Everett III and Clayton R. Paul

13a. TYPE OF REPORT	13b. TIME COVERED	14. DATE OF REPORT (Yr., Mo., Day)	15. PAGE COUNT
Final	FROM Sep 82 TO Dec 83	August 1984	

16. SUPPLEMENTARY NOTATION
The work was performed at the Electrical Engineering Department, University of Kentucky, Lexington KY. Project Engineers: Roy F. Stratton and Gerard T. Capraro.

17. COSATI CODES			18. SUBJECT TERMS (Continue on reverse if necessary and identify by block number)
FIELD	GROUP	SUB. GR.	
09	03		Electromagnetic Compatibility, Crosstalk, Cable Coupling, Computer Modeling, Transmission Lines.
09	01		

19. ABSTRACT (Continue on reverse if necessary and identify by block number)

A Comparison between the predictions of various lumped-circuit iterative models of transmission lines and that of the transmission line model is given for both the two and three-conductor cases. For frequencies such that the line length is approximately 1/10 of a wavelength or less one section of the lumped-circuit models yield predictions which are within $\pm$3dB of the transmission line model predictions, and which are essentially independent of the value of load impedance. For frequencies where the line length is greater than approximately 1/10 of a wavelength, more than one section of the lumped models must be used to yield accurate predictions, but the prediction accuracy may be significantly effected by the load impedance value. The range of accurate predictions (in terms of electrical length) may be increased by adding more sections of a lumped-circuit model, but this range increases in a nonlinear fashion. Because of this nonlinear relationship, it is difficult to find a satisfactory method for estimating the number of sections of a particular lumped-circuit model that must be used in order to obtain a desired range of accurate predictions.

20. DISTRIBUTION/AVAILABILITY OF ABSTRACT	21. ABSTRACT SECURITY CLASSIFICATION	
UNCLASSIFIED/UNLIMITED ☒ SAME AS RPT. ☐ OTIC USERS ☐	UNCLASSIFIED	
22a. NAME OF RESPONSIBLE INDIVIDUAL Roy F. Stratton	22b. TELEPHONE NUMBER (Include Area Code) (315) 330-2563	22c. OFFICE SYMBOL RADC (RBCT)

DD FORM 1473, 83 APR EDITION OF 1 JAN 73 IS OBSOLETE.

UNCLASSIFIED
SECURITY CLASSIFICATION OF THIS PAGE

Block 11 (Continued)

Transmission Line Model

TABLE OF CONTENTS

DTIC COPY INSPECTED

A-1

LIST OF FIGURES

LIST OF TABLES

CHAPTER 1

INTRODUCTION

Electronic equipment and devices are interconnected by cables or by traces on printed circuit (P. C.) boards. Since the overall cost, and thus space conservation, is a high priority, these cables are formed into bundles, and the traces on P. C. boards are placed as close to one another as possible. This close proximity makes it impossible to avoid some interference (crosstalk) between these cables or traces.

Since crosstalk is unavoidable, the occurrence of crosstalk is not the major concern. The problem is determining when the crosstalk is large enough to cause an equipment malfunction. Also, since it is very expensive to find and eliminate an interference problem once the manufacturing process is underway or finished, it would be a great advantage to develop a method which will accurately predict the crosstalk (interference). This would make it possible to discover and correct any crosstalk problems during the design process, where the costs of modifications are much less.

One method of predicting the crosstalk between cables is by developing and solving the transmission line equations [1]. Figure 1-1 shows an (n+1)-conductor, uniform transmission line of total length L. (A uniform line is one whose cross-sectional configuration is constant for the

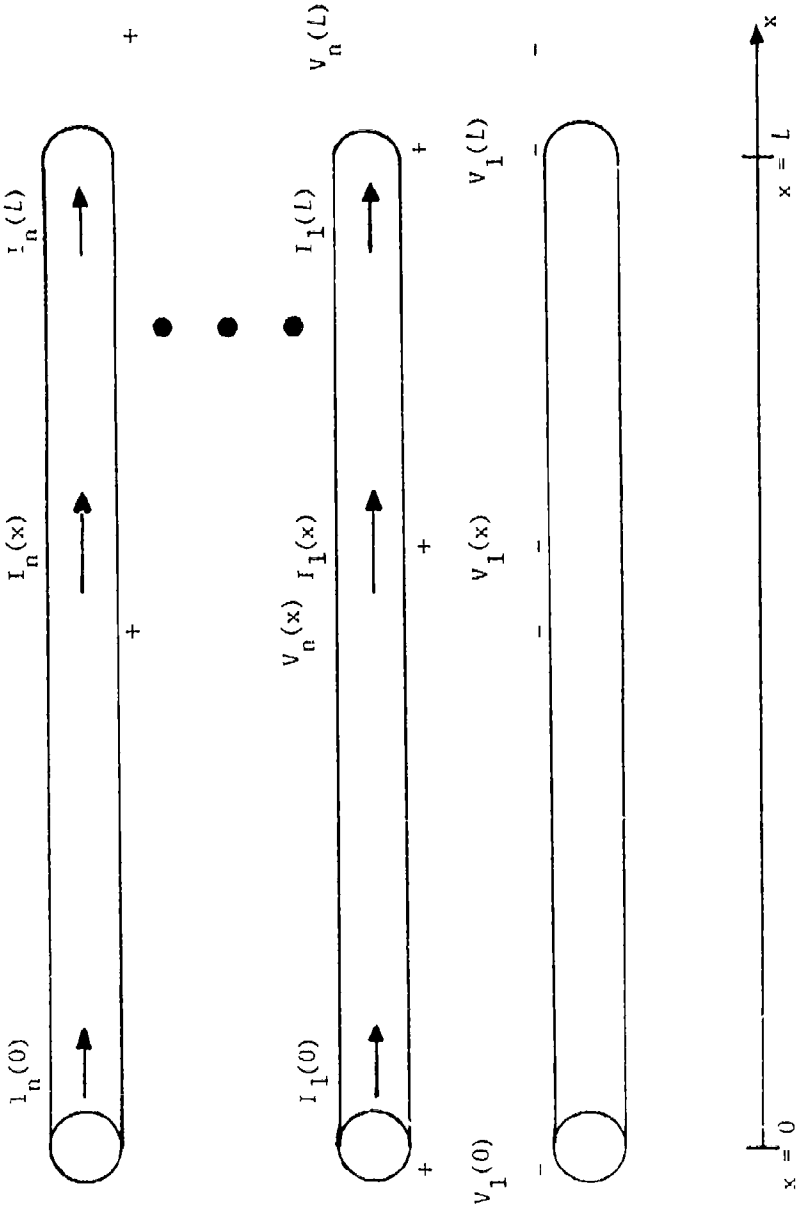

Figure 1-1 (n+1)-Conductor Transmission Line

entire length of the line). A Δx section of this line can be represented as shown in Figure 1-2. The per-unit-length inductances and capacitances are denoted by ℓ and c, respectively. It should be noted that the subscripts i and j refer to which lines are involved. For example ℓ_{ii} denotes the self inductance of the i^{th} line, while c_{ij} denotes the mutual capacitance between the i^{th} and j^{th} lines. Losses in the i^{th} conductor are represented by the per-unit-length resistance, r_i, while losses between the j^{th} line and the reference line are denoted as g_j, the per-unit-length conductance.

The transmission line equations, which are derived from this model of a Δx section of line, in the limit as $\Delta x \to 0$, are an exact representation of the line only for the TEM (Transverse Electro-Magnetic) mode of propagation. For only the TEM mode to be present, the transmission line of Figure 1-1 must consist of perfect conductors, a homogeneous surrounding medium, and have electrically small cross-sectional dimensions [1]. Therefore, in order for only the TEM mode of propagation to be present, the per-unit-length resistances, r_i, in Figure 1-2 must be zero (the conductors must be perfect). Since the medium is assumed to be linear, isotropic, and homogeneous, it can be described by μ (permeability) and ε (permittivity) [1]. It should be noted that an imperfect dielectric (medium) does not preclude the possibility for the existence of only the TEM mode of propagation, but it does complicate the problem

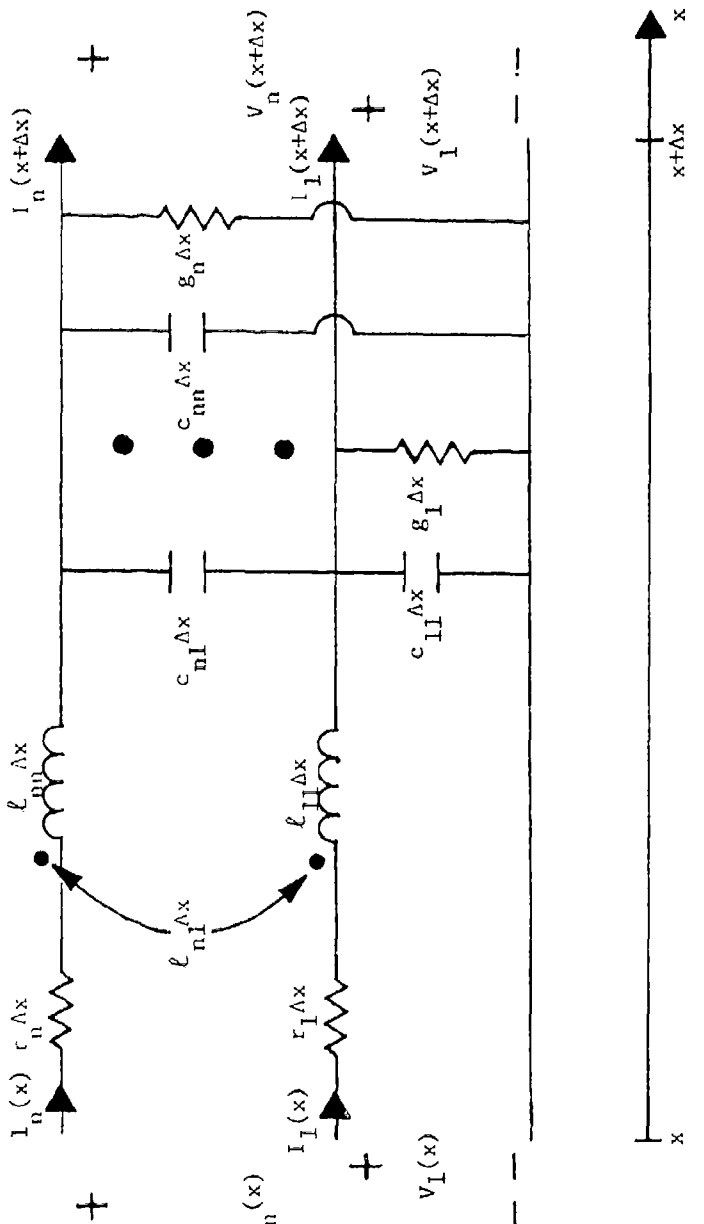

Figure 1-2 Δx Section of an (n+1)-Conductor Transmission Line

somewhat (by the inclusion of a complex value for the permittivity (ϵ)). For simplicity, a perfect dielectric will be assumed. This results in the per-unit-length conductances, g_j, being zero. These assumptions (TEM mode of propagation and perfect dielectric) result in the exact model of a Δx section of an n-conductor line shown in Figure 1-3. It should be noted that inclusion of good, but not perfect conductors (small conductor losses) results in what is called "quasi-TEM" mode propagation, where the longitudinal fields are small but non-zero. These loss terms, r_i, can be included in the per-unit-length transmission line model (Figure 1-3), but the resulting model is no longer exact.

The idea of deriving/solving the transmission line equations, and then calculating the crosstalk between the lines is a simple one in principal, but in practice this is not always, the case. The derivation of the transmission line equations may be lengthy for a large number of conductors, but it is reasonably straight forward. The solution of these equations, on the other hand, is sometimes far from straight forward. For example, if conductor losses are included, the solution involves calculating the eigenvalues and eigenvectors of an n x n matrix (recall that n is the number of lines minus the reference conductor) at each frequency of interest. Also, once the transmission line equations have been solved, the calculation of the actual crosstalk is not always an easy matter. For a large

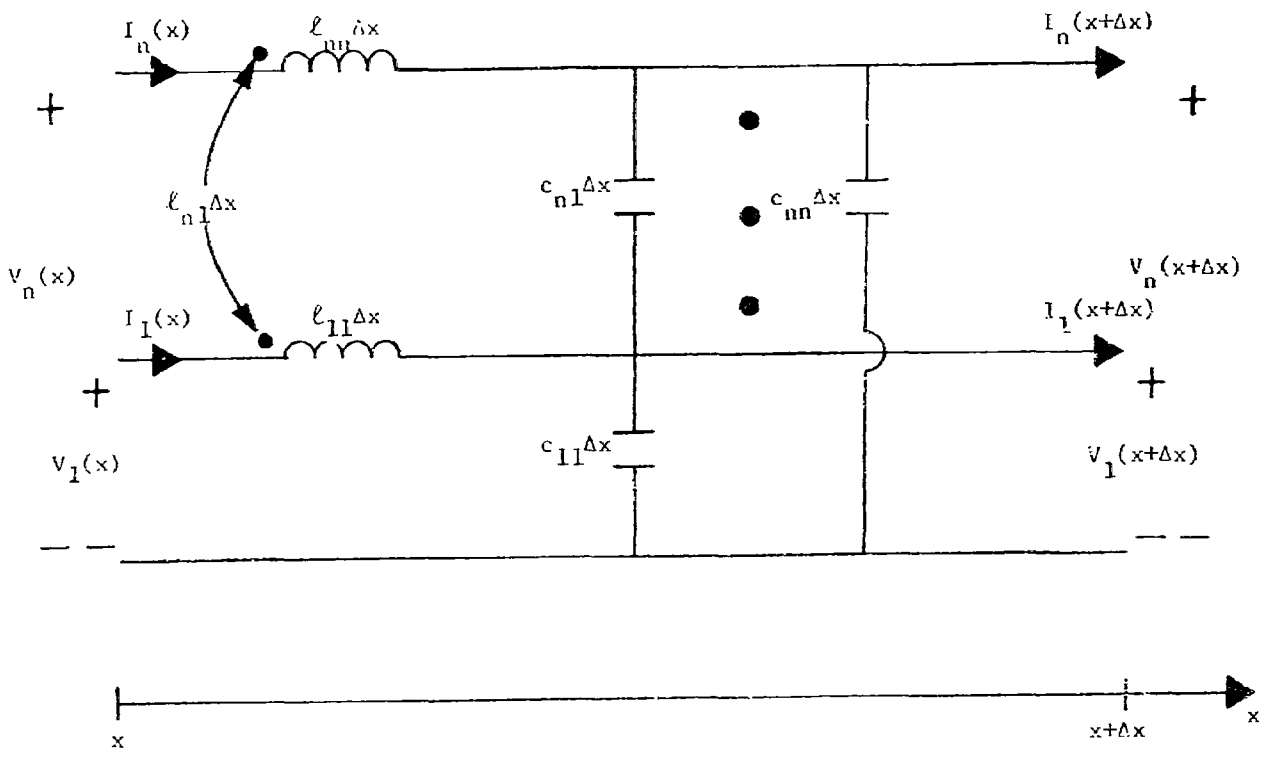

Figure 1-3 Δx Section of an Exact (n+1)-Conductor Transmission Line

number of conductors, incorporation of the terminal (boundary) conditions is possible, but is somewhat lengthy, and if nonlinear loads are present (such as transistors or gates, for example) a closed form solution cannot be obtained. Transient (time domain) analysis is also quite cumbersome at best.

For these reasons, iterative lumped circuit models have been used to represent transmission lines [1-3]. These lumped models are directly suitable for use with circuit analysis programs such as PCAP, SPICE, NCAP, SCEPTOR and ASTAP [4-8], with which most engineers are already quite familiar. (This opens the analysis of transmission lines, and crosstalk, to a larger number of analysts.) These codes eliminate the need for the solution of the transmission line equations, and incorporation of the terminal conditions is done directly. They also eliminate the problem introduced by the most common nonlinear loads (gates, line drivers etc.) in either the frequency, or time domain, because these circuit analysis codes model these loads when the basic circuit elements of the load are modeled (BJT's, FET's etc.).

The basic idea of an iterative lumped model is a simple one. Break up the total line length, L, into N "electrically short" ($L/\lambda << 1$, where λ is the wavelength $\lambda=v/f$, v = velocity of propagation and f is the frequency of excitation in Hz) sections, and model each of these sections with one section of a particular lumped model. If

the line is "electrically short" one section of the lumped model will produce accurate prediction results. They are called iterative models, because the range of accurate prediction (in terms of electrical length (L/λ)) is increased by adding (cascading) more sections of that lumped model.

Since we are attempting to model a transmission line it only makes sense to choose a lumped model whose architecture is similar to that of the per-unit-length transmission line model shown in Figure 1-3. Figure 1-4 shows one section of the four possible lumped models (for the two-conductor case) that will be discussed, in depth, in this report. It should be noted that the names given to these lumped models were chosen to match their architectures. For example, the BGAM and FGAM lumped models are the Backward GAMma and the Forward GAMma, respectively. The PI and TEE lumped models were so named because they are shaped like a π, or a T, respectively. Figure 1-5 shows the two-conductor per-unit-length transmission line model, so that the architectural similarities of the lumped models can be seen. The structural similarities are the same for multi-conductor lines, but the two-conductor case is used because of its simplicity.

At present, the relationship between the number of sections and the resulting accuracy is not known. Exactly when a section is "electrically short" is also unknown, but

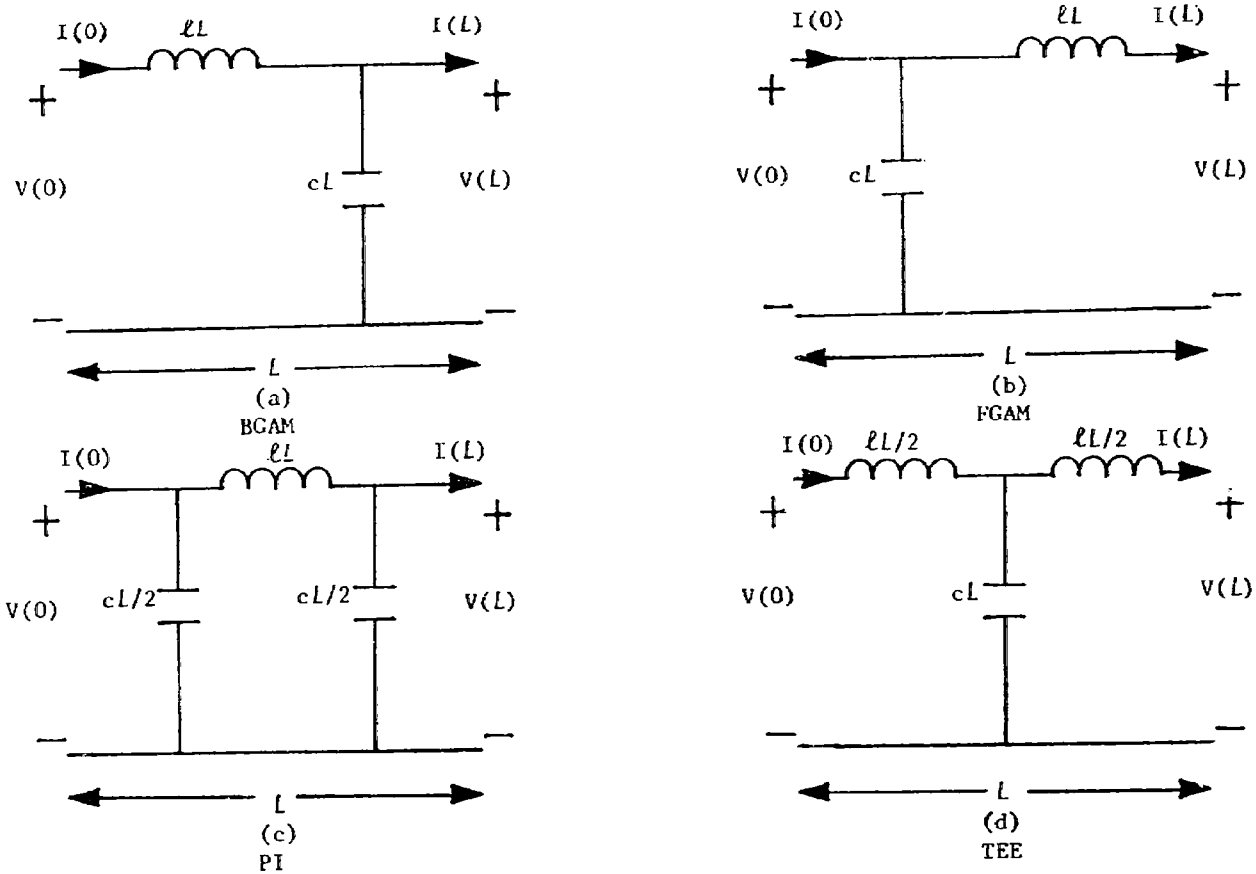

Figure 1-4 One Section of Four 2-Conductor Lump Models

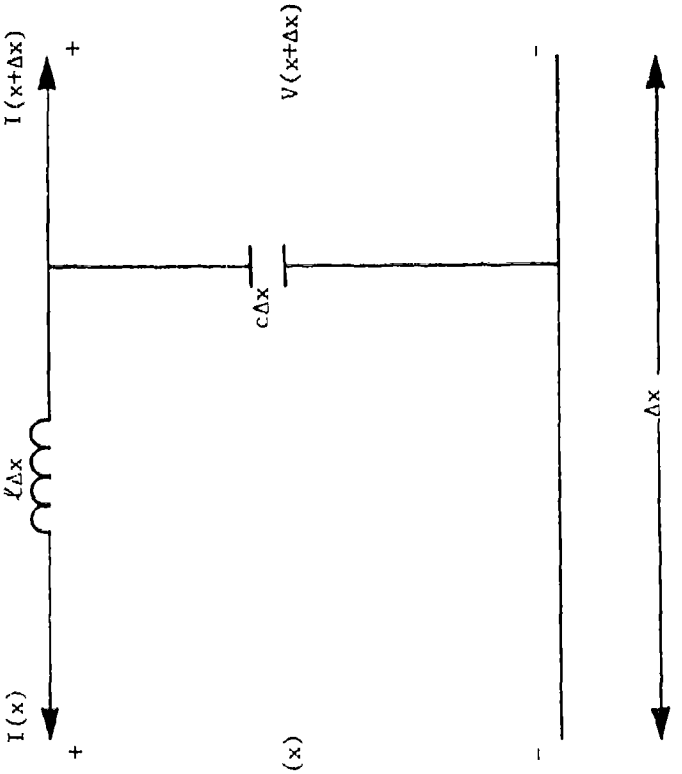

Figure 1-5 2-Conductor Transmission Line Model

there seems to be a general rule of thumb that one section will yield accurate approximations until frequencies are reached where the line length is in the vicinity of 1/20 to 1/10 of a wavelength. It is also unknown whether load impedance values have any effect on the lumped model prediction accuracy, or the number of sections needed to obtain a desired prediction accuracy. These problems have received only minimal attention [1,2,9].

In this report we compare the prediction accuracies of the four lumped models shown in Figure 1-4 for various numbers of sections and various values of load impedances to the exact transmission line equation results for both the two-conductor and three-conductor cases. It will be shown that one section of any of the four lumped models will accurately model (within ± 3dB) a transmission line, regardless of load impedance values, until frequencies are reached where L/λ is approximately 1/10. It will also be shown that the value of load impedance may significantly affect the prediction accuracies of the lumped models for values of $L/\lambda > 1/10$ (where more than one section must be used to accurately model the entire line). It will also be shown that any relationship between the desired prediction accuracy and the number of sections required to obtain this accuracy is difficult to obtain since the relationship between the range of coverage (in terms of electrical length) and the number of sections used is a nonlinear one.

Since the two-conductor case is much simpler than the

three-conductor one, it will be analyzed first. Therefore, Chapter two contains the analytical development of the two-conductor line. That is, the exact transmission line equations will be derived and solved, and the lumped model results will be expressed in such a way as to make it relatively simple to use any number of sections of a particular lumped model.

Chapter three consists of the comparisons of the corresponding prediction accuracies of the different lumped models for the two-conductor case. Plots for various numbers of sections and load impedance values are shown in Appendices A and B.

The fourth chapter contains the analytical development for the three-conductor line. The fifth chapter compares the corresponding three-conductor results in the same manner as Chapter three compared the two-conductor results. Plots of the three-conductor results for various numbers of sections and load impedance values are shown in Appendices C-F.

CHAPTER 2

Two-Conductor Analytical Development

Figure 2-1 shows a Δx section of a lossless, uniform two-conductor transmission line in a homogeneous medium. Since the TEM mode of propagation is assumed, this Δx section of line can be modeled exactly as shown in Figure 1-5. The per-unit-length inductance and capacitance of the line are denoted by ℓ and c, respectively. As stated before, the assumption of a perfect dielectric results in the per-unit-length conductance being zero.

The transmission line equations can be derived from the model of a Δx section of line shown in Figure 1-5. The sinusoidal, steady-state version of these transmission line equations become, in the limit as $\Delta x \to 0$,

$$\frac{dV(x)}{dx} = -j\omega \ell I(x) \qquad (2\text{-}1a)$$

and

$$\frac{dI(x)}{dx} = -j\omega c V(x). \qquad (2\text{-}1b)$$

These equations have solutions of the form

$$V(x) = V^{+}e^{-j\beta x} + V^{-}e^{j\beta x} \qquad (2\text{-}2a)$$

and

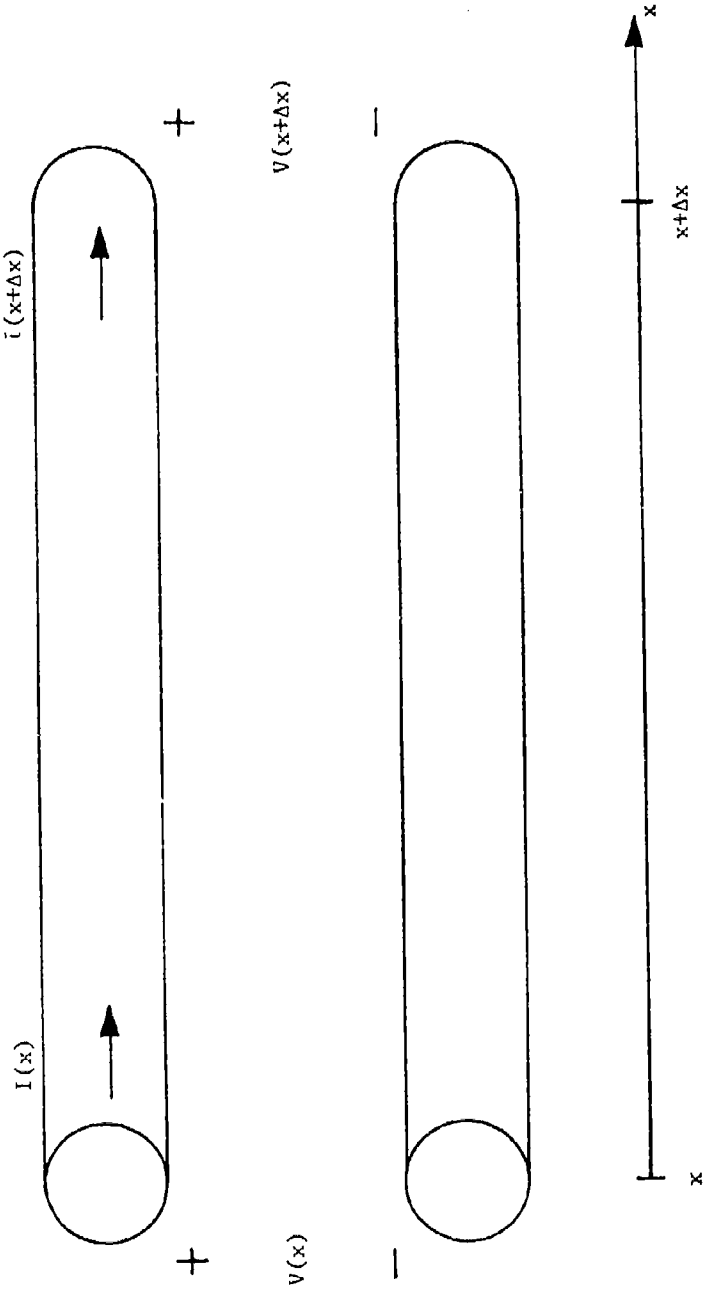

Figure 2-1 Δx Section of a 2-Conductor Transmission Line

$$I(x) = \frac{V^+}{Z_C} e^{-j\beta x} - \frac{V^-}{Z_C} e^{j\beta x} \qquad (2\text{-}2b)$$

where V^+ and V^- are undetermined constants, β is the propagation constant ($\beta=\omega/v$), v is the velocity of propagation ($v=1/\sqrt{\mu\epsilon}$), and Z_C is the characteristic impedance of the line ($Z_C=\sqrt{\ell/c}$).

The values of the constants V^+ and V^- can be determined in terms of the "near" end voltage and current by letting $x=0$ in equations (2-2). The "far" end voltage and current can be determined in terms of the "near" end voltage and current by letting $x=L$, and substituting the above determined values of V^+ and V^- into equations (2-2). The results are

$$V(L) = \text{Cos}(\beta L)V(0) - jZ_C \text{Sin}(\beta L)I(0) \qquad (2\text{-}3a)$$

and

$$I(L) = \{-j\text{Sin}(\beta L)/Z_C\}V(0) + \text{Cos}(\beta L)I(0). \qquad (2\text{-}3b)$$

In matrix notation, these become

$$\begin{bmatrix} V(L) \\ I(L) \end{bmatrix} = \underset{\sim}{\Phi}_{\text{TLINE}} \begin{bmatrix} V(0) \\ I(0) \end{bmatrix}, \qquad (2\text{-}3c)$$

where

$$\underset{\sim}{\Phi}_{\text{TLINE}} = \begin{bmatrix} \text{Cos}(\beta L) & -jZ_C \text{Sin}(\beta L) \\ -j\text{Sin}(\beta L)/Z_C & \text{Cos}(\beta L) \end{bmatrix} \qquad (2\text{-}3d)$$

$$\phi_{TLINE} = \begin{bmatrix} \phi_{11} & \phi_{12} \\ \phi_{21} & \phi_{22} \end{bmatrix} \qquad (2\text{-}3e)$$

is defined as the "chain parameter matrix", and V(0), I(0), V(L), I(L) are the "near" and "far" end voltages and currents, respectively.

Figure 2-2 shows a two-conductor line terminated with a load impedance of Z_L, and driven by a sinusoidal voltage source , V_S. For simplification we assume that the voltage source has zero internal impedance. Incorporation of the terminal (boundary) conditions:

$$V(0) = V_S \qquad (2\text{-}4a)$$

and

$$V(L) = Z_L I(L) \qquad (2\text{-}4b)$$

along with the relation, $\beta = 2\pi/\lambda$ (where λ is the wavelength, $\lambda = v/f$) into equations (2-3), yields the voltage transfer ratio

$$\frac{V(L)}{V_S} = \frac{z_L}{z_L\phi_{22} - \phi_{12}/z_C} = \frac{z_L}{z_L \cos(2\pi\alpha) + j\sin(2\pi\alpha)} \qquad (2\text{-}5)$$

In this result z_L is the ratio of load impedance to charac-

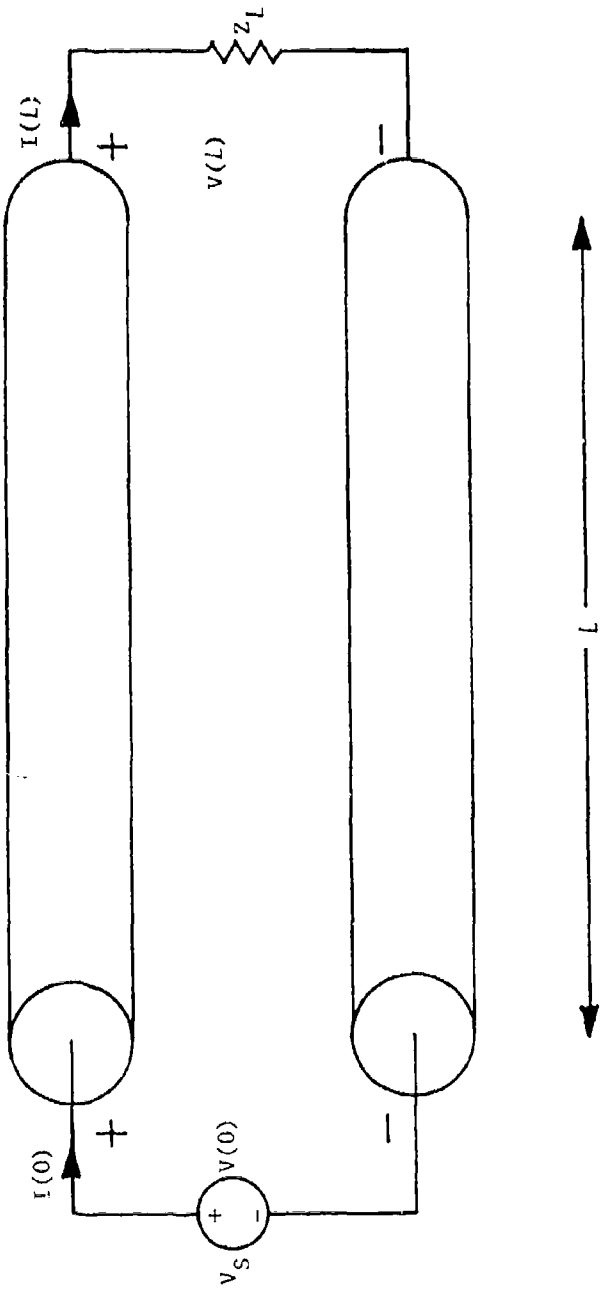

Figure 2-2 Terminated 2-Conductor Transmission Line

teristic impedance ($z_L = Z_L/Z_C$), and α is the "electrical length" of the line ($\alpha = L/\lambda$). As stated before, because of the TEM mode assumption, equation (2-5) is an exact result for a lossless, two-conductor transmission line.

Now the lumped model approximation results must be obtained so that a comparison between their predictions and those of the exact transmission line result (equation (2-5)) can be performed. Figure 1-4 shows one section of the four lumped models that have been chosen to model the lossless, uniform, two-conductor transmission line. As was discussed previously, these four lumped models were chosen from the infinite number of possible ones, because of their similarity to the transmission line model (shown in Figure 1-5).

Figure 2-3 shows several cascaded sections of a particular lumped model. Each section is identical, and the "far" end voltages and currents are related to the "near" end voltages and currents by $\underset{\sim}{\phi}$, the chain parameter matrix (as defined in equation (2-3c)). The chain parameter matrix is especially useful in this case, because the overall $\underset{\sim}{\phi}_T$, is equal to the product of the individual $\underset{\sim}{\phi}$'s. That is,

$$\underset{\sim}{\phi}_T = \underset{\sim}{\phi}\,\underset{\sim}{\phi} \cdots \underset{\sim}{\phi} \qquad (2\text{-}6)$$

$$= \underset{\sim}{\phi}^N$$

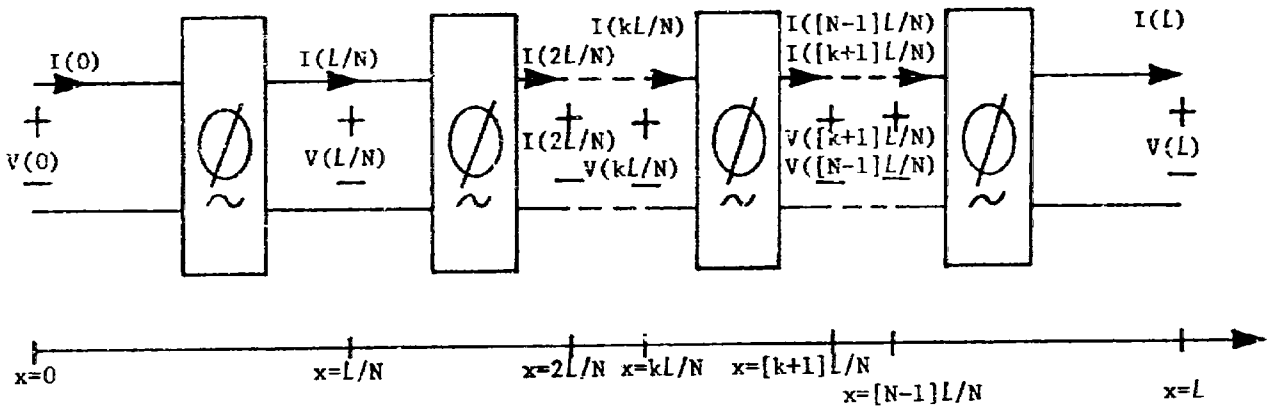

Figure 2-3 N Cascaded Lumped Model Sections

when N identical sections are cascaded. This is important, because once the $\underset{\sim}{\phi}$ for one section of the lumped model has been calculated, any number of sections may be cascaded simply by performing N matrix multiplications. It should be noted that since each individual $\underset{\sim}{\phi}$ is a function of N (the number of sections being used) one cannot add one more section by multiplying by the "old" $\underset{\sim}{\phi}$ one more time. That is, any time the number of sections is changed a "new" individual $\underset{\sim}{\phi}$ must be determined (using N as the "new" number of sections being used).

For the BGAM lumped model

$$V([k+1]\,L/N) = V(kL/N) - j\omega\ell(L/N)\,I(kL/N) \qquad (2\text{-}7a)$$

and

$$I([k+1]\,L/N) = -j\omega c(L/N)V(kL/N) + [1-\omega^2\ell c(L/N)^2]\;I(kL/N) \qquad (2\text{-}7b)$$

or,

$$\underset{\sim}{\phi}_{BGAM} = \begin{bmatrix} 1 & -jZ_c\,2\pi\alpha/N \\ -j2\pi\alpha/(Z_c N) & 1-(2\pi\alpha/N)^2 \end{bmatrix} \qquad (2\text{-}7c)$$

where α is the electrical length (L/λ), Z_c is the characteristic impedance of the line and N is the number of sections of the lumped model being used.

Similarly, it can be shown that

$$\underset{\sim}{\phi}_{FGAM} = \begin{bmatrix} 1 - (2\pi\alpha/N)^2 & -jZ_C\, 2\pi\alpha/N \\ -j2\pi\alpha/(Z_C N) & 1 \end{bmatrix} \qquad (2\text{-}8)$$

$$\underset{\sim}{\phi}_{PI} = \begin{bmatrix} 1 - 2(\pi\alpha/N)^2 & -jZ_C 2\pi\alpha/N \\ j2\pi(\alpha/Z_C)\{(\pi\alpha/N)^2 - 1\} & 1 - 2(\pi\alpha/N)^2 \end{bmatrix} \qquad (2\text{-}9)$$

$$\underset{\sim}{\phi}_{TEE} = \begin{bmatrix} 1 - 2(\pi\alpha/N)^2 & jZ_C 2\pi(\alpha/N)\{(\pi\alpha/N)^2 - 1\} \\ -j2\pi\alpha/(Z_C N) & 1 - 2(\pi\alpha/N)^2 \end{bmatrix} \qquad (2\text{-}10)$$

Figure 2-4 shows a two-conductor transmission line represented as a two-port whose port voltages and currents are related by the overall chain parameter matrix $\underset{\sim}{\phi}_T$. Incorporation of the terminal conditions (equations (2-4)) yields the transfer ratio

$$\frac{V(L)}{V_S} = \frac{z_L \Delta\phi_T}{z_L \phi_{22T} - \phi_{12T}/z_C} \qquad (2\text{-}11a)$$

where $\Delta\phi_T$ is the determinant of $\underset{\sim}{\phi}_T$ ($\Delta\phi_T = \phi_{11T}\phi_{22T} - \phi_{12T}\phi_{21T}$), ϕ_{ijT} is the appropriate element in the overall $\underset{\sim}{\phi}_T$, and z_L is as previously defined (Z_L/Z_C). It can be shown that $\Delta\phi_T = 1$ for the four models under study (see Figure 1-4) for

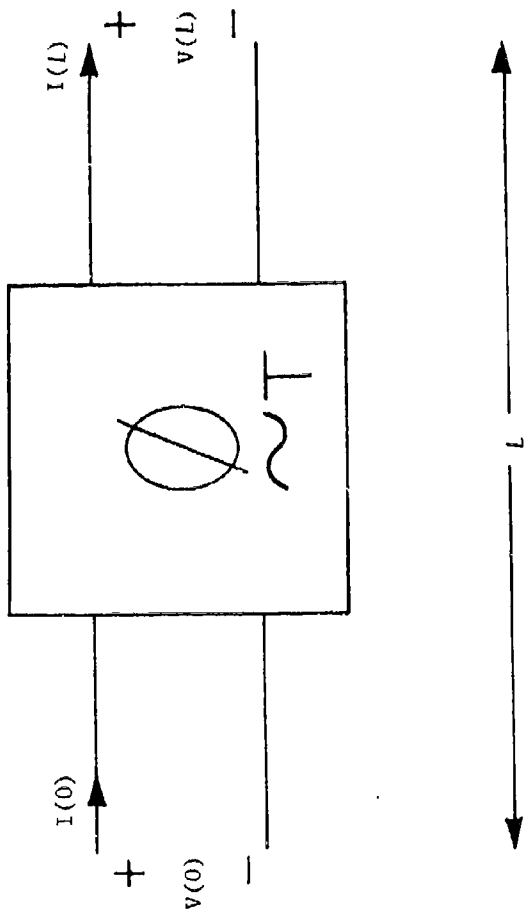

Figure 2-4 Two-Port Representation of a Two-Conductor Transmission Line

any number of sections, so the final result becomes

$$\frac{V(L)}{V_S} = \frac{z_L}{z_L \phi_{22T} - \phi_{12T}/z_C} \qquad (2\text{-}11b)$$

which is identical in form to the transmission line result shown in equation (2-5).

This result was obtained in closed form for easy comparison with the exact transmission line result shown in equation (2-5), but the same numerical results could be obtained by using a circuit analysis code to calculate the "far" end voltage $V(L)$. It can be shown that the voltage transfer ratio in equation (2-11b) is only a function of the impedance ratio z_L for all N. That is, the individual values of Z_L and Z_C have no significance.

For the purpose of comparing the lumped model approximation results to the exact transmission line result, an error function can be defined as

$$\text{Error(dB)} = 20\log_{10}\left[\frac{\left|\frac{V(L)}{V_S}\right|_{\text{Transmission Line}}}{\left|\frac{V(L)}{V_S}\right|_{\text{Lumped Model}}}\right] \qquad (2\text{-}12)$$

Substituting equations (2-5) and (2-11) into equation (2-12) yields

$$\text{Error(dB)} = 20\log_{10}\left[\frac{|z_L \phi_{22T} - \phi_{12T}/z_C|}{|z_L \cos(2\pi\alpha) + j\sin(2\pi\alpha)|}\right] \quad (2\text{-}13)$$

For the BGAM lumped model with N=1, the error becomes

$$\text{Error(dB)} = 20\log_{10}\left[\frac{|z_L\{1 - (2\pi\alpha)^2\} + j2\pi\alpha|}{|z_L \cos(2\pi\alpha) + j\sin(2\pi\alpha)|}\right] . \quad (2\text{-}14)$$

When the line is electrically short, i.e. $2\pi\alpha << 1$, $\cos(2\pi\alpha) \doteq 1$, and $\sin(2\pi\alpha) \doteq 2\pi\alpha$, equation (2-14) further simplifies to

$$\text{Error(dB)} \doteq 20\log_{10}\left[\frac{|z_L + j2\pi\alpha|}{|z_L + j2\pi\alpha|}\right] \quad (2\text{-}15)$$

$$= 0 .$$

It can be shown that the other lumped models depicted in Figure 1-4 yield results that are only slightly different from that shown in equation (2-14), and which are identical to that shown in equation (2-15) (for an electrically short line). These results show that all four of the lumped models are exact as long as the line is electrically short, and that no value of load impedance can be chosen to cause a great change in the error. Thus, it appears that one section of all four lumped models should yield approximately the same prediction accuracy until frequencies are reached where the line is no longer electrically short. It

should be realized that this equivalency was derived only for one section, and that it will not necessarily hold for values of N > 1.

In the next chapter, the transmission line results of equation (2-5) will be compared to the predictions of various sections of the lumped models for z_L's of .01 ($Z_L = .01Z_C$), 1 ($Z_L = Z_C$), and 100 ($Z_L = 100Z_C$).

CHAPTER 3

Two-Conductor Results

In this chapter the predictions of the four lumped models of interest are compared to the exact transmission line results. Various mumbers of sections of the lumped models are used with z_L's .01 (Z_L=.01Z_C), 1 (Z_L=Z_C) and 100 (Z_L=100Z_C). The comparisons are in the form of plots of the voltage transfer ratio magnitudes, and error functions versus the electrical length. These plots are shown in Appendices A an B.

Appendix A contains the comparisons of the exact transmission line voltage transfer ratio to the predictions of various sections of the lumped models, for the three values of z_L discussed previously.

Figures A-1 thru A-3 compare the transmission line result to the predictions of one section of the four lumped models with z_L's of .01, 1, and 100. Figures A-4 thru A-6, A-7 thru A-9, A-10 thru A-12, and A-13 thru A-15 depict the voltage transfer ratio comparisons with N=2, 3, 5, and 10 for three values of z_L discussed previously.

Some interesting, and perhaps surprising, results were obtained, but these are quite easily explained. Figures A-1, A-4, A-7, A-10, and A-13 show that the predictions of the BGAM, FGAM, and PI models are identical (over the range of electrical length shown) for a z_L of .01 (Z_L=.01Z_C), or a "small" load impedance) regardless of the number of sec-

tions used. The reason for this equivalency is readily seen if several sections of the models of interest are cascaded. For example, consider Figure 3-1 in which four sections of the lumped models are cascaded. Since the source impedance is assumed to be zero, the leftmost capacitances in the FGAM and PI lumped models play no part, and the rightmost capacitances in the BGAM and PI lumped models are essentially eliminated by the "small" Z_L, so that all three of these lumped models reduce to the same circuit (see Figure 3-2).

Two interesting results were obtained for $z_L = 100$ ($Z_L = 100 Z_C$) as shown in Figure A-3. First, the FGAM lumped model prediction is unity for the entire range of electrical length shown. This, again, is easily understood if the FGAM lumped model configuration shown in Figure 1-4(b) is recalled. A "large" load impedance effectively eliminates the series inductor, so that the output voltage is identical to the input voltage. The second, perhaps more interesting result is that the PI and TEE lumped model predictions are identical except for the peak amplitudes, and that the BGAM lumped model prediction is simply a frequency shifted version of the PI lumped model prediction. This can also be explained by observing the effects of a "large" load impedance on the appropriate lumped models shown in Figure 1-4. The rightmost inductor in the TEE lumped model is eliminated by the "large" load impedance, and the leftmost capacitor in the PI lumped model has no effect, since

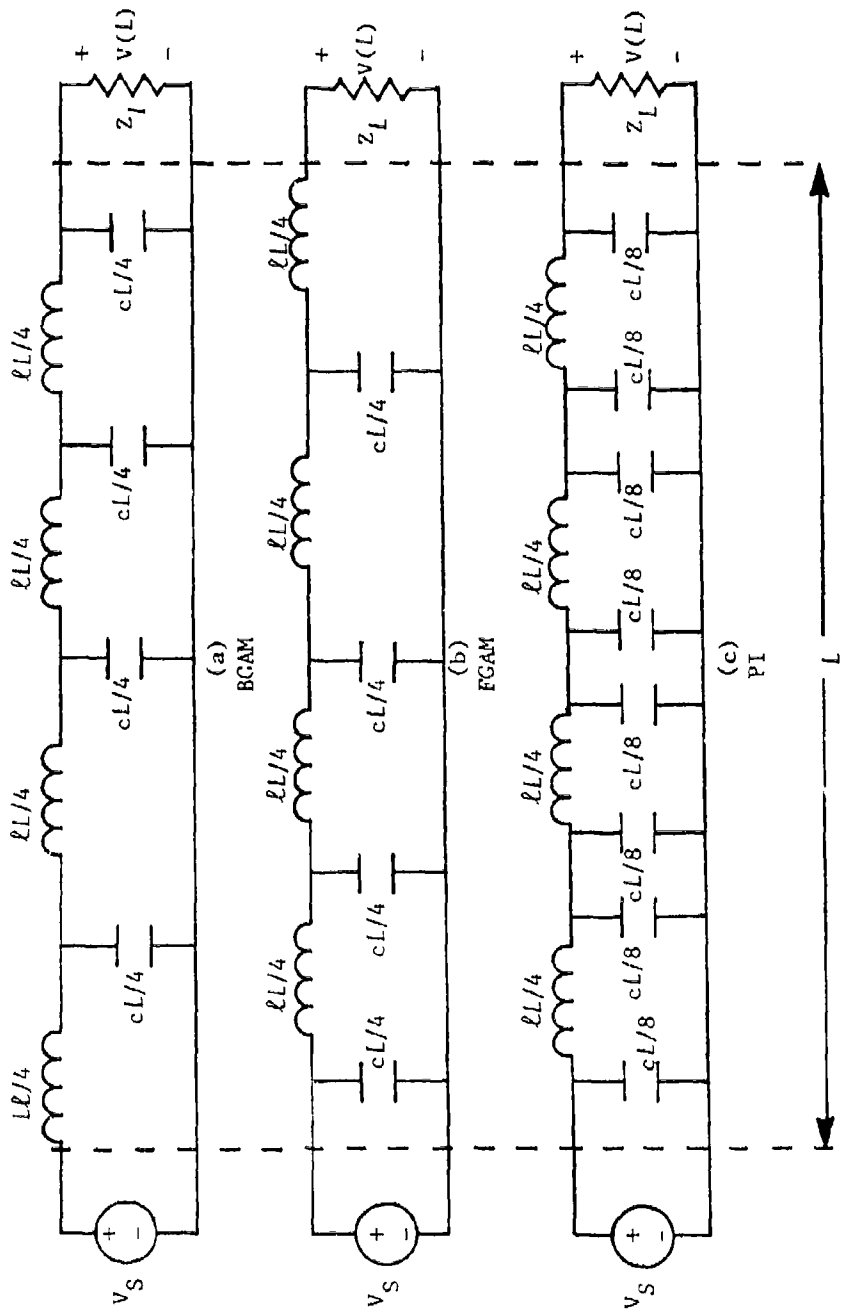

Figure 3-1 Four Sections of the BGAM, FGAM and PI Lumped Models

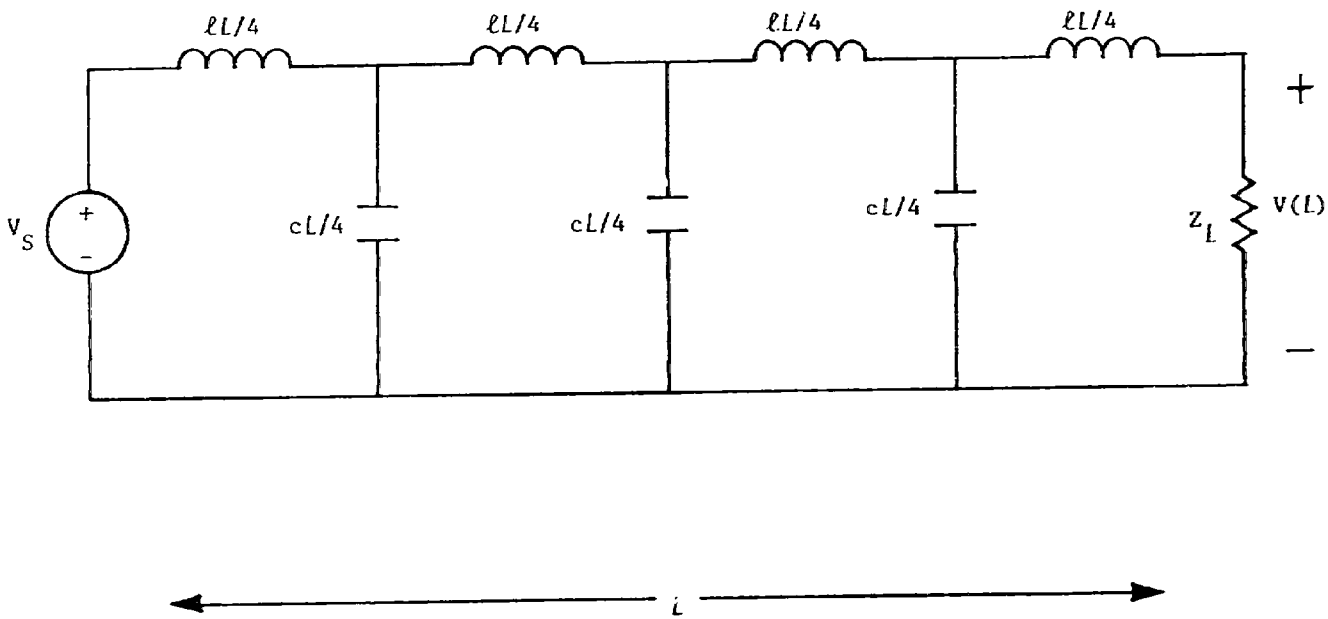

Figure 3-2 Effective "Small" Load Impedance Circuit for the BGAM, FGAM and PI Lumped Models

the source impedance is zero, so that the PI and TEE model are identical except for the values of capacitance and inductance (see Figure 3-3). The resulting frequency responses for the PI and TEE model predictions are identical, and the peak amplitude of the Tee lumped model prediction is larger than that of the PI lumped model. It can be seen that the effective PI lumped model for a "large" load impedance shown in Figure 3-3(a) is the BGAM lumped model with the value of the capacitance halved. Therefore, the BGAM lumped model prediction is the PI lumped model prediction shifted in frequency.

It is also quite obvious that these "large" impedance effects only appear when one section of the lumped models are used. Consider Figure 3-4, which shows the effective "large" load impedance lumped models when two sections of the lumped models are cascaded. It is easily seen that the BGAM, PI, and TEE lumped models are no longer even similar to one another, and that the FGAM lumped model will no longer predict a voltage transfer ratio of unity. These expectations are confirmed in Figures A-6, A-9, A-12 and A-15 ($N > 1$ and $z_L = 100$).

Another important, but expected, result that can be seen from the plots of Appendix A is that the range of accuracy of the lumped models can be increased by adding (cascading) more sections of that lumped model. That is, the prediction error is always reduced by adding another section of a particular lumped model.

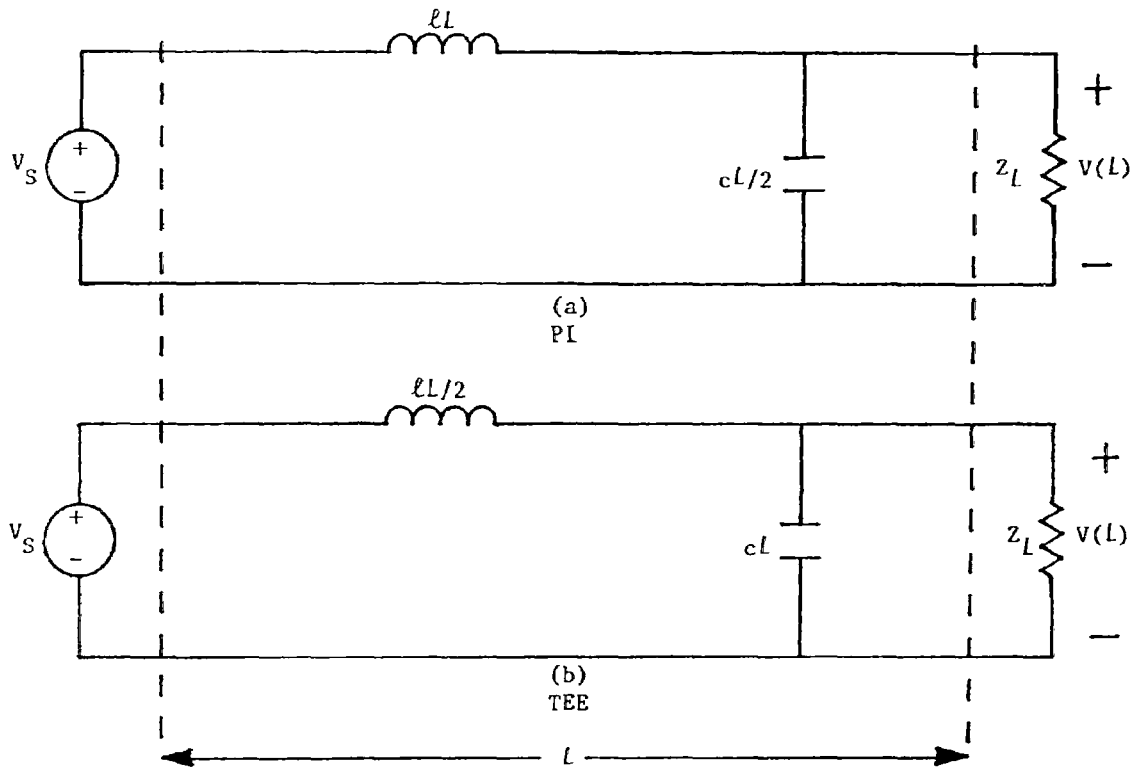

Figure 3-3 Effective "Large" Load Impedance Circuit for the PI and TEE Lumped Models

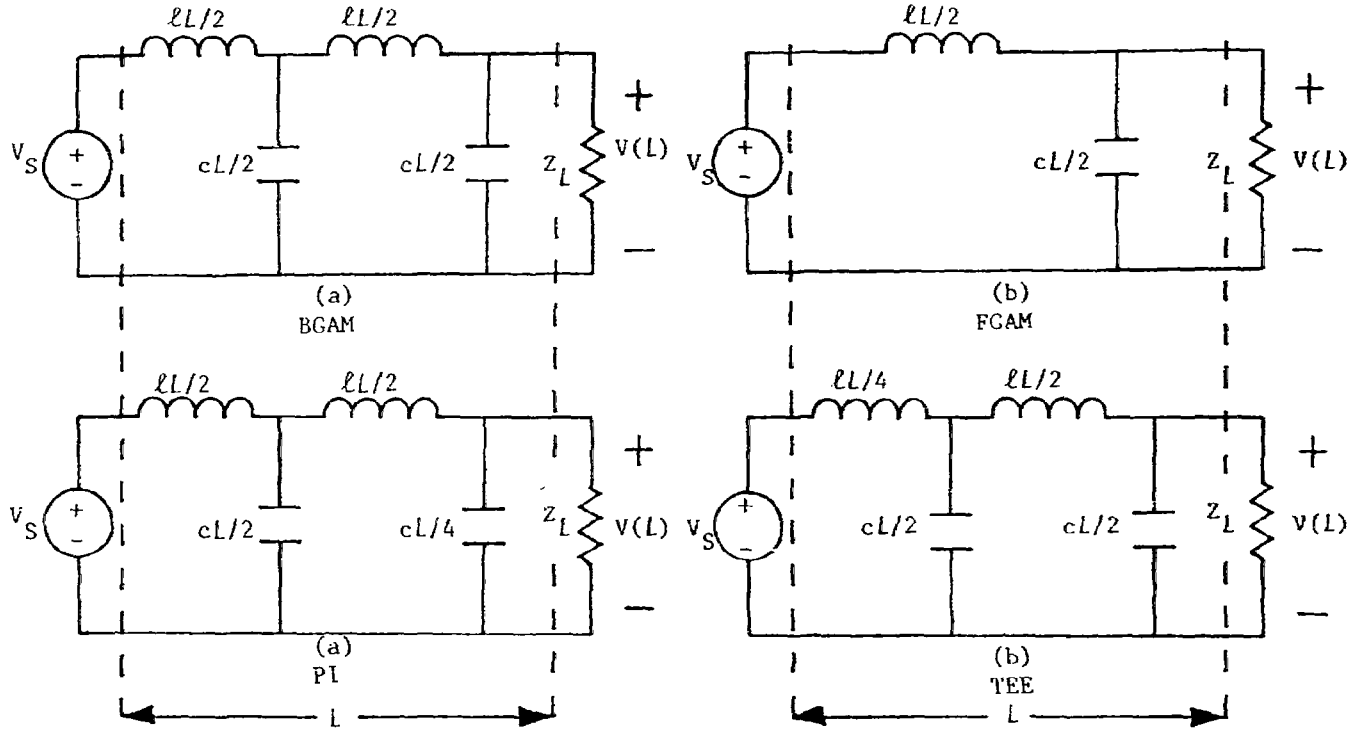

Figure 3-4 Effective "Large" Load Impedance Circuit for 2 Sections of the Four Lumped Models

Appendix B contains the error plots which compare the prediction accuracies of the four lumped models under test using various numbers of sections, and z_L's of .01, 1, and 100. It should be recalled that the error function was defined in equation (2-12) as

$$\text{Error(dB)} = 20\log_{10}\left[\frac{\left|\frac{V(L)}{V_S}\right|_{\text{Transmission Line}}}{\left|\frac{V(L)}{V_S}\right|_{\text{Lumped Model}}}\right] . \quad (3\text{-}1)$$

Figure B-1 shows the prediction error of the BGAM lumped model for 1, 2. 3, 5, and 10 sections with a z_L of .01. Figures B-2, B-3, and B-4 show the prediction error for 1, 2, 3, 5, and 10 sections of the FGAM, PI and TEE lumped models, respectively, with a z_L of .01. Figures B-5 thru B-8, and B-9 thru B-12 show the same lumped models, for the same number of sections, with z_L's of 1 and 100, respectively. From these Figures it is obvious that the range of prediction accuracy does not increase linearly with the addition of more sections. That is, doubling the number of sections will not double the frequency range of accuracy. It is also more obvious from the error plots of Appendix B that the lumped model prediction error is indeed decreased with the addition of more sections of that lumped model.

Table 3-1 depicts the "upper limit" (in terms of electrical length) of the four lumped models for z_L's of .01, 1

and 100. The "upper limit" is defined as the first point where a ±3dB prediction error occurs. From Table 3-1 it can be seen that the value of load impedance has only minimal effect on the prediction accuracy of the lumped models when only one section is used to represent the entire line, and that one section of any of the lumped models yields "good" approximations (within ±3dB of the transmission line results) until frequencies are reached where the line length is approximately 1/10 of a wavelength.

3dB Prediction Error Points (N=1)

Model	z_L = .01	z_L = 1	z_L = 100
BGAM	2.20E-1	2.00E-1	1.05E-1
FGAM	2.20E-1	1.60E-1	1.25E-1
PI	2.20E-1	2.25E-1	2.00E-1
TEE	2.25E-1	2.25E-1	2.00E-1

Table 3-1

The Figures of Appendix B also show that the value of load impedance may cause a significant effect on the prediction accuracy of the lumped models for values of N > 1. For example, consider the PI model with z_L's of .01 and 1 (Figures B-3 and B-7). The effect of the load impedance value on the prediction accuracy for two sections is negligible, but for N ≥ 3 the "upper limit" variation is quite significant. For five sections, for example, the "upper limit" for the PI lumped model with z_L=.01 is approximately .5, but the "upper limit" for a z_L of 1 (matched case) is beyond 1 (past the point where the line length equals a

wavelength).

So, if a transmission line is to be modeled for frequencies where the line length is approximately 1/10 of a wavelength or less, one section of any of the four lumped models shown in Figure 1-4 may be used and the prediction accuracy should be within ±3dB of the actual transmission line result, regardless of the load impedance. If a transmission line model is needed for operating frequencies such that L/λ is greater than 1/10, then more than one section must be used. It is difficult to choose the number of sections that should be used to accurately model the transmission line for these frequencies, because, the range of accuracy is not increased linearly with the addition of more sections. In addition, the load impedance value may then plays a significant role in the prediction accuracy of a particular lumped model.

Nevertheless, some general rules regarding lumped model prediction accuracy can be obtained. For "small" and "matched" load impedances, for example, one may use a FGAM, or BGAM lumped model since they are the simplest (with regard to the number of elements) and yield approximately the same prediction accuracy as the PI and TEE lumped models. For "large" load impedances the PI and TEE lumped models could be used, because their predictions converge to those of the transmission line model result with a fewer number of sections. These general rules of thumb may help decide which lumped model should be used, but there is

still no satisfactory way to estimate how many sections are needed to yield a given accuracy for frequencies where L/λ is greater than approximately 1/10.

The "upper limit" of the lumped model predictions has been defined as the first occurrence of a prediction error of ±3dB. It was defined in this manner so that a maximum electrical length could be noted such that any L/λ less than this value would guarantee a prediction error of less than ±3dB. However, this does not mean that once this value is exceeded, the prediction error will always be above ±3dB. It can be seen in the Figures of Appendix B that this is not the case. The error does increase after the "upper limit" has been reached, but it then decreases to less than ±3dB in some cases. This means that there is another band of frequencies where the lumped model predictions are accurate. In fact, there are some cases where two such bands exist (see Figures B-9 thru B-12, where z_L =100). It appears that locating these prediction error minimums is a problem which should be examined further. They appear to offer a special case solution to the problem of accurately predicting the response of a transmission line operating at frequencies such that L/λ is well in excess of 1/10 with a small number of sections.

However, the "upper limit" of the lumped models is of prime importance, because of the great number of digital circuit applications. In digital circuitry pulses are used instead of single frequency waveforms, so that the wave-

forms may have significant frequency components from DC (0Hz) to frequencies such that the line length is a significant portion of a wavelength. In cases such as this an adequate lumped model would have to predict all (or at least a great majority) of the effects of the significant frequency components. Therefore, the "upper limit" of the lumped model predictions must be matched to the maximum significant frequency component of the input pulse waveform to yield accurate prediction results.

For the convenience of the reader the major points of this chapter are restated below.

It was shown that:

1. The range of accuracy of the four lumped models under test can be increased (the prediction error decreased) by adding more sections of that lumped model. But this range of accuracy does not increase in a linear fashion.

2. One section of any of the four lumped models of interest will yield accurate prediction results (within $\pm$3dB of the exact transmission line result) for frequencies such that L/λ is approximately 1/10, or less, regardless of the load impedance value.

3. Load impedance values may significantly effect the prediction accuracy of a lumped model when more than one section of that lumped model must be used.

4. When more than one section of a lumped model must be used there is no satisfactory method to estimate the

number of sections required to yield accurate prediction results.

5. There appear to be some general rules that could help in the selection of a lumped model:

A. For "small" and "matched" loads the BGAM, or FGAM lumped models should yield predictions as accurate as the PI or TEE lumped models, but the effort of solution should be reduced, because of their architectural simplicity.

B. For "large" impedance loads a PI or TEE lumped model should be used, because their prediction accuracy is increased by a significantly smaller number of sections.

6. There are "high frequency" bands of low prediction error (high prediction accuracy) which may be well above the "upper limit" of the particular lumped model being used.

In the next chapter the methods shown in Chapter 2 will be extended to a more useful and interesting case, namely crosstalk on a three-conductor transmission line.

CHAPTER 4

Three-Conductor Crosstalk Analytical Development

Figure 4-1 shows a Δx section of a lossless, uniform, three-conductor transmission line in a homogeneous medium. Again, since the TEM mode of propagation is assumed, this Δx section of line can be modeled exactly, as shown in Figure 4-2. The subscripts R and G refer to the receptor and generator lines, respectively, and the per-unit-length inductance and capacitance, are denoted by ℓ and c, respectively. It should also be noted that a subscript of m refers to either the mutual per-unit-length inductance or capacitance of the line. For example, ℓ_R refers to the per-unit-length self-inductance of the receptor line, while c_m refers to the per-unit-length mutual capacitance between the lines. Again, since the line is assumed to be lossless, the per-unit-length resistance, r, is zero, and the per-unit-conductance, g, is zero.

The transmission line equations can be derived from the model of a Δx section shown in Figure 4-2, and the sinusoidal steady-state version of these equations become, in the limit as $\Delta x \to 0$ [10]

$$\frac{dV_G(x)}{dx} = -j\omega\ell_G I_G(x) - j\omega\ell_m I_R(x) \qquad (4\text{-}1a)$$

$$\frac{dV_R(x)}{dx} = -j\omega\ell_m I_G(x) - j\omega\ell_R I_R(x) \qquad (4\text{-}1b)$$

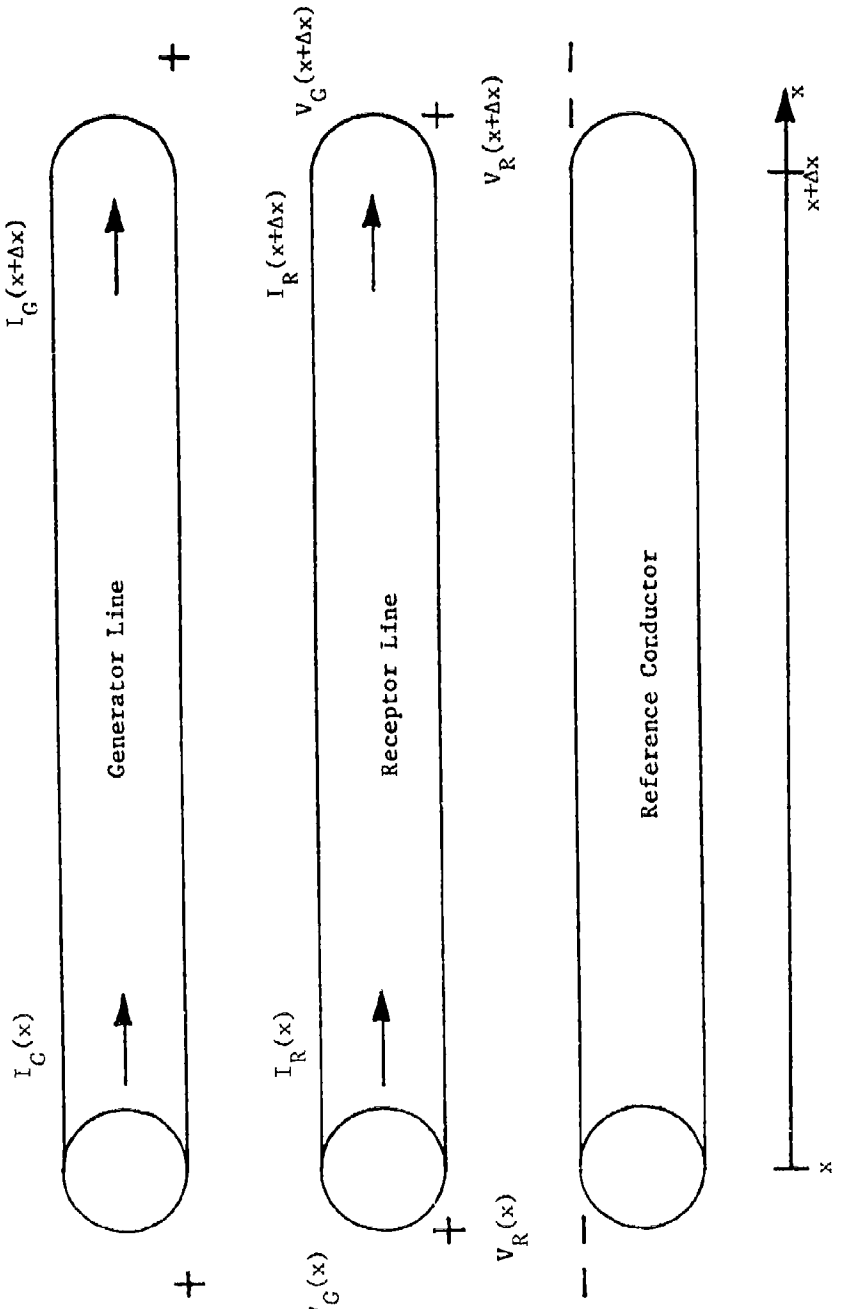

Figure 4-1 Δx Section of a 3-Conductor Transmission Line

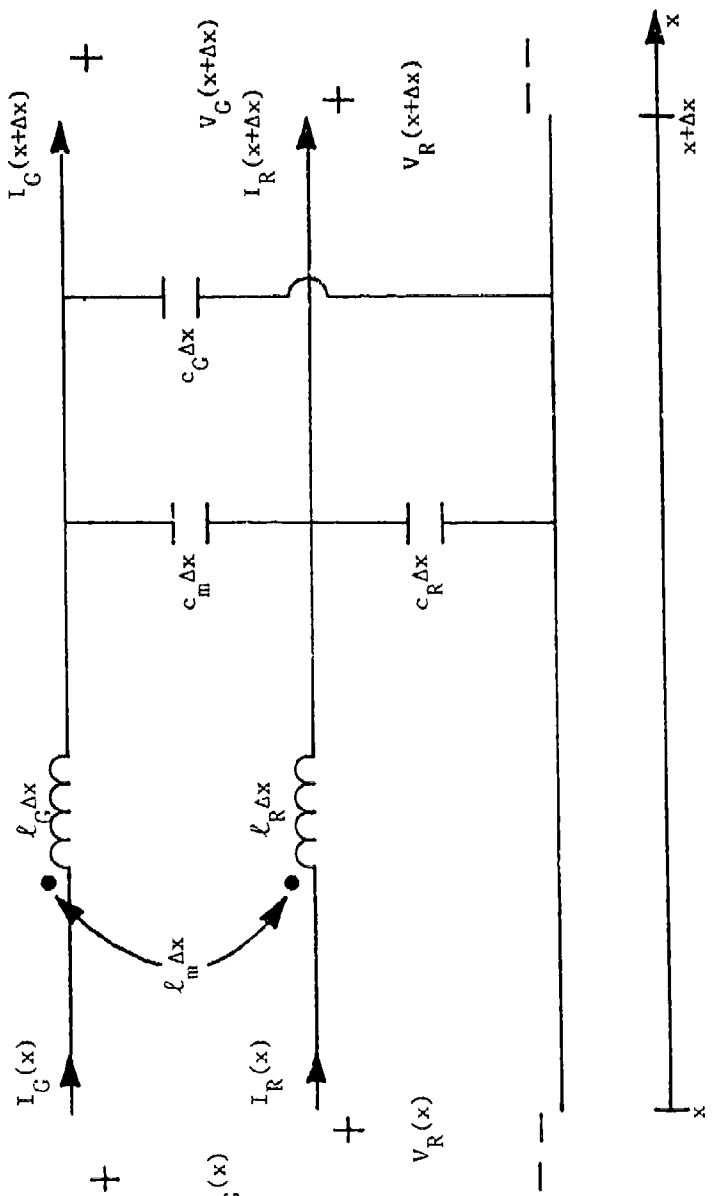

Figure 4-2 3-Conductor Transmission Line Model

$$\frac{dI_G(x)}{dx} = -j\omega(c_G + c_m)V_G(x) + j\omega c_m V_R(x) \qquad (4\text{-}1c)$$

$$\frac{dI_R(x)}{dx} = j\omega c_m V_G(x) - j\omega(c_R + c_m)V_R(x). \qquad (4\text{-}1d)$$

The solution of these equations can be written in terms of the chain parameter matrix, as

$$\begin{bmatrix} \underset{\sim}{V}(L) \\ \underset{\sim}{I}(L) \end{bmatrix} = \underset{\sim}{\Phi}_{TLINE} \begin{bmatrix} \underset{\sim}{V}(0) \\ \underset{\sim}{I}(0) \end{bmatrix} \qquad (4\text{-}2)$$

where

$$\underset{\sim}{V}(L) = \begin{bmatrix} V_G(L) \\ V_R(L) \end{bmatrix}, \quad \underset{\sim}{I}(L) = \begin{bmatrix} I_G(L) \\ I_R(L) \end{bmatrix},$$
$$\underset{\sim}{V}(0) = \begin{bmatrix} V_G(0) \\ V_R(0) \end{bmatrix}, \quad \underset{\sim}{I}(0) = \begin{bmatrix} I_G(0) \\ I_R(0) \end{bmatrix}, \qquad (4\text{-}3a)$$

and

$$\underset{\sim}{\Phi}_{TLINE} = \begin{bmatrix} \mathrm{Cos}(\beta L)\underset{\sim}{I} & -jv\mathrm{Sin}(\beta L)\underset{\sim}{L} \\ -jv\mathrm{Sin}(\beta L)\underset{\sim}{C} & \mathrm{Cos}(\beta L)\underset{\sim}{I} \end{bmatrix}. \qquad (4\text{-}3b)$$

$\underset{\sim}{I}$ is the identity matrix,

$$\underset{\sim}{I} = \begin{bmatrix} 1 & 0 \\ 0 & 1 \end{bmatrix} \qquad (4\text{-}4a)$$

$\underset{\sim}{L}$ and $\underset{\sim}{C}$ are the per-unit-length inductance and capacitance matrices, respectively,

$$\underset{\sim}{L} = \begin{bmatrix} \ell_G & \ell_m \\ \ell_m & \ell_R \end{bmatrix} \tag{4-4b}$$

$$\underset{\sim}{C} = \begin{bmatrix} c_G + c_m & -c_m \\ -c_m & c_R + c_m \end{bmatrix} \tag{4-4c}$$

and β, ℓ, and v are as previously defined [10]. It should also be noted, that since a homogeneous medium is assumed $\underset{\sim}{L}$ and $\underset{\sim}{C}$ are related by [1]

$$\underset{\sim}{LC} = \mu\varepsilon\underset{\sim}{I} = \underset{\sim}{I}/v^2 \tag{4-5}$$

Figure 4-3 shows a terminated three-conductor transmission line, with the generator line being driven by an ideal, sinusoidal voltage source, V_S. The terminal conditions are

$$\underline{V}(0) = \underline{V}_0 - \underset{\sim}{Z}_0\underline{I}(0) \tag{4-6a}$$

and

$$\underline{V}(\ell) = \underset{\sim}{Z}_\ell\underline{I}(\ell) \tag{4-6b}$$

where

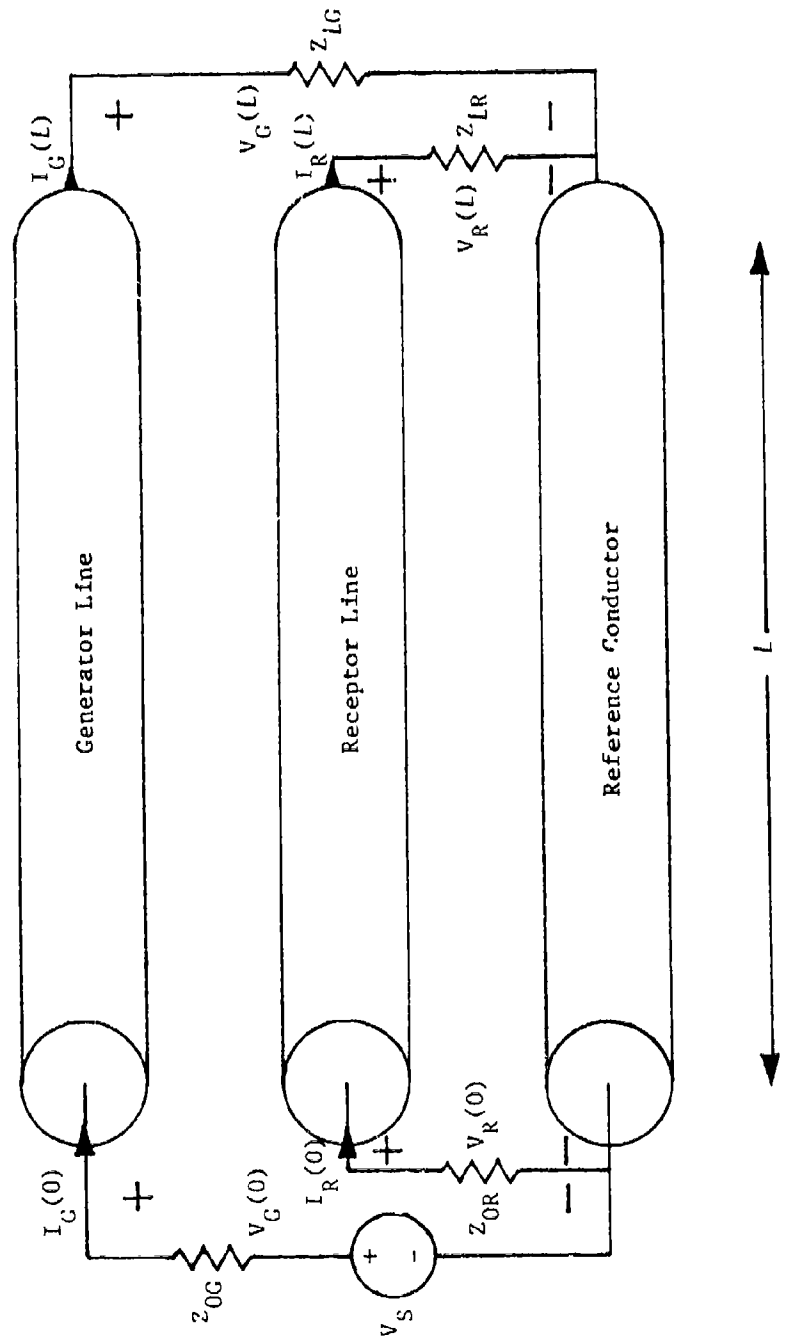

Figure 4-3 Terminated 3-Conductor Transmission Line

$$\underline{V}_0 = \begin{bmatrix} 1 \\ 0 \end{bmatrix} V_S \qquad (4\text{-}7a)$$

$$\underline{Z}_0 = \begin{bmatrix} Z_{0G} & 0 \\ 0 & Z_{0R} \end{bmatrix} \qquad (7\text{-}7b)$$

$$\underline{Z}_L = \begin{bmatrix} Z_{LG} & 0 \\ 0 & Z_{LR} \end{bmatrix} . \qquad (4\text{-}7c)$$

The subscripts 0 and L in equations (4-7) denote the near and far end of the line, respectively, while the G and R denote the line of interest, as previously defined. i.e. Z_{OR} is the impedance terminating the "near" end of the receptor line. Incorporation of these terminal conditions into equations (4-2) and (4-3), and solving for the crosstalk voltage transfer ratios yields [10]

$$\frac{V_R(0)}{V_S} = \frac{jSin(2\pi\alpha)X_{M0}\{Cos(2\pi\alpha) + jFSin(2\pi\alpha)\}}{D_{EN}} \qquad (4\text{-}8a)$$

$$\frac{V_R(L)}{V_S} = \frac{jSin(2\pi\alpha)X_{ML}}{D_{EN}} , \qquad (4\text{-}8b)$$

where

$$F = \alpha_{LG} + \alpha_{LR} / \{(1 + \alpha_{LG}\alpha_{LR})F_{AC}\} , \qquad (4\text{-}9a)$$

$$X_{MO} = kZ_{OR}(1 + \alpha_{LG}\alpha_{LR})/(F_{AC} D_Z A_{RP} A_{GP}), \qquad (4\text{-}9b)$$

$$X_{ML} = -kZ_{LR}(1 - \alpha_{OR}\alpha_{LG})/(F_{AC} D_Z A_{RP} A_{GP}), \qquad (4\text{-}9c)$$

$$D_{EN} = \cos^2(2\pi\alpha) - B\sin^2(2\pi\alpha) + Aj\{\cos(2\pi\alpha) + \sin(2\pi\alpha)\} \qquad (4\text{-}9d)$$

and α is again defined as, L/λ.

Equations (4-8) are a modified version of the results given in [10], and are written in this form to yield an easily computed value of the crosstalk between cables in a three-conductor transmission line, while at the same time attempting to minimize the amount of input data. As one might expect, this results in a large number of new variables that must must now be defined to yield a complete understanding of the three-conductor results shown in equations (4-8).

First, Z_{CG} and Z_{CR} are the characteristic impedance of the generator line in the presence of the receptor line, and the characteristic impedance of the receptor line in the presence of the generator line, respectively, and are defined by the following relations:

$$Z_{CG} = \sqrt{\ell_G/(c_G + c_m)} \qquad (4\text{-}10a)$$

and

$$Z_{CR} = \sqrt{\ell_R/(c_R + c_m)} \qquad (4\text{-}10b)$$

τ_R and τ_G are the time constants of the receptor and generator circuits, respectively, and are defined as

$$\tau_R = \frac{\ell_R L}{Z_{OR} + Z_{LR}} + (c_R + c_m) L \frac{Z_{OR} Z_{LR}}{Z_{OR} + Z_{LR}} \qquad (4\text{-}11a)$$

and

$$\tau_G = \frac{\ell_G L}{Z_{OG} + Z_{LG}} + (c_G + c_m) L \frac{Z_{OG} Z_{LG}}{Z_{OG} + Z_{LG}} \; . \qquad (4\text{-}11b)$$

To simplify these two equations somewhat, it is useful to define the quantities

$$\alpha_{OR} = Z_{OR}/Z_{CR}, \qquad \alpha_{LR} = Z_{LR}/Z_{CR}, \qquad (4\text{-}12)$$

$$\alpha_{OG} = Z_{OG}/Z_{CG}, \qquad \alpha_{LG} = Z_{LG}/Z_{CG} .$$

This results in

$$\tau_R = \frac{\ell_R L (1 + \alpha_{OR}\alpha_{LR})}{Z_{OR} + Z_{LR}} , \qquad (4\text{-}13a)$$

and

$$\tau_G = \frac{\ell_G L (1 + \alpha_{OG}\alpha_{LG})}{Z_{OG} + Z_{LG}} \; . \qquad (4\text{-}13b)$$

The coupling coeficient between the receptor and generator lines is denoted as k, and is defined as

$$k = \ell_m / \sqrt{\ell_G \ell_R} = c_m / \sqrt{(c_G + c_m)(c_R + c_m)} . \qquad (4\text{-}14)$$

Two equations further relating the self inductance of the

respective lines to their characteristic impedances can be denoted as

$$Z_{CG} = v\ell_G\sqrt{1-k^2} \tag{4-15a}$$

and

$$Z_{CR} = v\ell_R\sqrt{1-k^2}. \tag{4-15b}$$

Some further simplifying quantities can be defined as

$$F_{AC} = \sqrt{1-k^2}, \tag{4-16}$$

$$D_Z = \sqrt{Z_{CG}Z_{CR}}, \tag{4-17}$$

$$A_{RP} = \alpha_{OR} + \alpha_{LR}, \tag{4-18}$$

$$A_{RP2} = 1 + \alpha_{OR}\alpha_{LR}, \tag{4-19}$$

$$A_{GP} = \alpha_{OG} + \alpha_{LG}, \tag{4-20}$$

$$A_{GP2} = 1 + \alpha_{OG}\alpha_{LG}, \tag{4-21}$$

$$A = \tau_R + \tau_G, \tag{4-22}$$

$$\psi = \frac{k^2(1 - \alpha_{OG}\alpha_{LR})(1 - \alpha_{LG}\alpha_{OR})}{A_{GP2}\,A_{RP2}} \tag{4-23}$$

and

$$B = \tau_R\tau_G(1 - \psi). \tag{4-24}$$

Now equations (4-8) are completely defined.

It should be noted that if $Z_{OG}=Z_{OR}=Z_{LG}=Z_{LR}=Z$, and $Z_{CG}=Z_{CR}=Z_C$, then the three-conductor results shown in equations (4-8) become a function of the ratio of Z/Z_C, and do not depend on the individual values of Z and Z_C. It should be pointed out that this is not true in general; e.g., if the characteristic impedances of both lines are not identical, and/or the load impedances are not equal.

Now that the exact three-conductor result has been obtained, the lumped model results must be found. Since we are interested in calculating results for several different numbers of sections we will, again, calculate the chain parameter matrix for one section of each lumped model, and simply perform N matrix multiplications to obtain the overall chain parameter matrix (for N identical sections of that lumped model). But, due to the large number of equations, incorporation of the terminal conditions is much more involved than it was for the two-conductor case, so that a closed form solution for the crosstalk voltage transfer functions will not be obtained for the lumped model representations.

Figure 4-4 shows the three-conductor versions of the four lumped models that we have been analyzing. The chain parameter matrices can be derived from these circuits and, for the BGAM lumped model

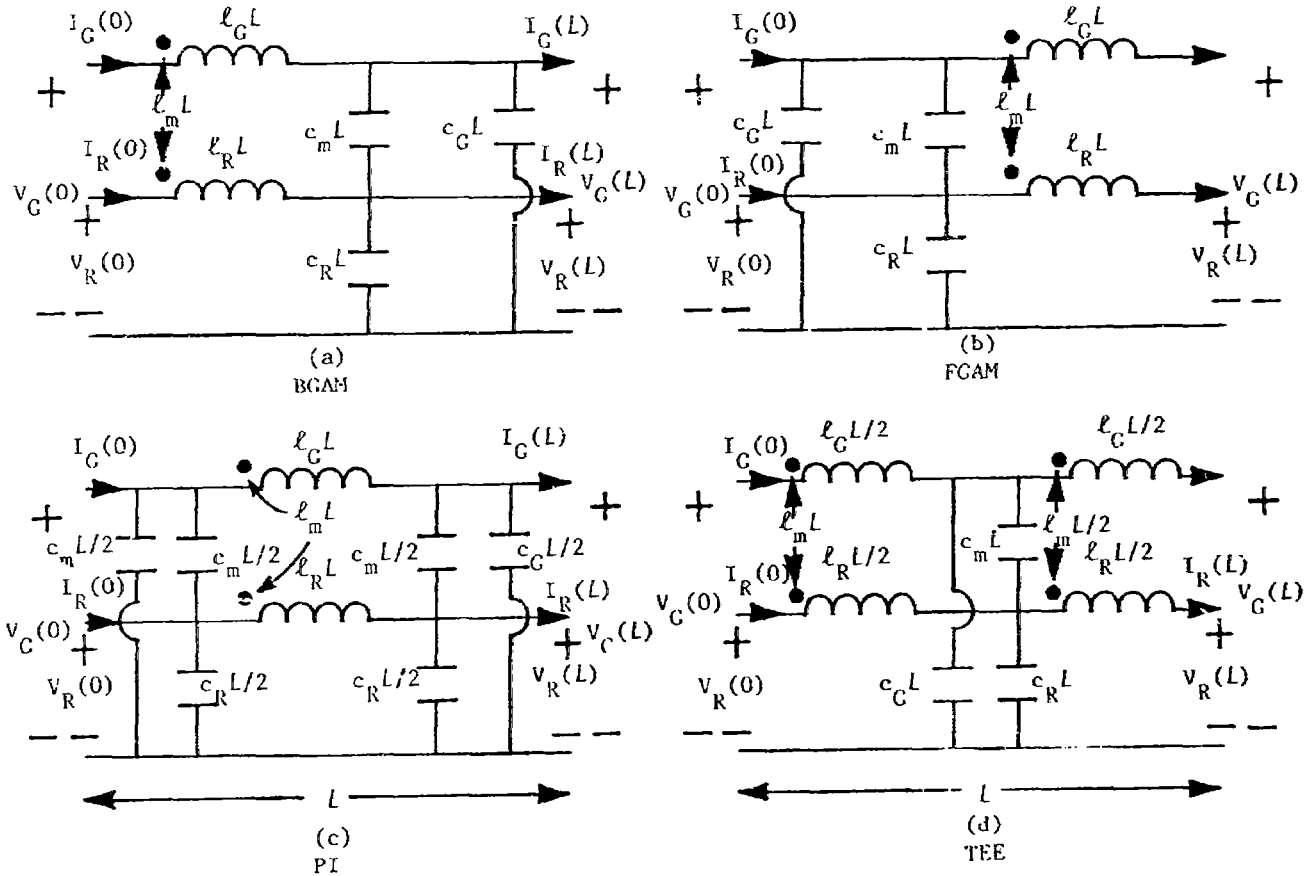

Figure 4-4 Lumped Models for the 3-Conductor Case

$$\begin{bmatrix} V_G(L) \\ V_R(L) \end{bmatrix} = \begin{bmatrix} V_G(0) \\ V_R(0) \end{bmatrix} - j\omega(L/N)\underset{\sim}{L}\begin{bmatrix} I_G(0) \\ I_R(0) \end{bmatrix} \quad (4\text{-}25a)$$

and

$$\begin{bmatrix} I_G(L) \\ I_R(L) \end{bmatrix} = -j\omega(L/N)\underset{\sim}{C}\begin{bmatrix} V_G(0) \\ V_R(0) \end{bmatrix} + \{1-\omega^2L^2/(vN)^2\}\begin{bmatrix} I_G(0) \\ I_R(0) \end{bmatrix} \quad (4\text{-}25b)$$

or,

$$\underset{\sim}{\phi}_{BGAM} = \begin{bmatrix} \underset{\sim}{I} & -j\omega(L/N)\underset{\sim}{L} \\ -j\omega(L/N)\underset{\sim}{C} & \{1-\omega^2L^2/(vN)^2\}\underset{\sim}{I} \end{bmatrix} \quad (4\text{-}25c)$$

Since $\omega L = 2\pi v\alpha$, and $\underset{\sim}{C} = \underset{\sim}{L}^{-1}/v^2$ the chain parameter matrix for one section of the BGAM lumped model becomes

$$\underset{\sim}{\phi}_{BGAM} = \begin{bmatrix} \underset{\sim}{I} & -j2\pi v(\alpha/N)\underset{\sim}{L} \\ -j2\pi(\alpha/Nv)\underset{\sim}{L}^{-1} & \{1-4\pi^2(\alpha/N)^2\}\underset{\sim}{I} \end{bmatrix} \quad (4\text{-}26)$$

Similarly,

$$\underset{\sim}{\phi}_{FGAM} = \begin{bmatrix} \{1-4\pi^2(\alpha/N)^2\}\underset{\sim}{I} & -j2\pi v(\alpha/N)\underset{\sim}{L} \\ -j2\pi(\alpha/vN)\underset{\sim}{L}^{-1} & \underset{\sim}{I} \end{bmatrix} \quad (4\text{-}27)$$

$$\underset{\sim}{\phi}_{PI} = \begin{bmatrix} \{1-2\pi^2(\alpha/N)^2\}\underset{\sim}{I} & -j2\pi v(\alpha/N)\underset{\sim}{L} \\ -j2\pi(\alpha/vN)(1-\pi^2(\alpha/N)^2\underset{\sim}{L}^{-1} & \{1-2\pi^2(\alpha/N)^2\}\underset{\sim}{I} \end{bmatrix} \quad (4\text{-}28)$$

$$\underset{\sim}{\Phi}_{TEE} = \begin{bmatrix} \{1-2\pi^2(\alpha/N)^2\}\underset{\sim}{I} & -j2\pi v(\alpha/N)(1-\pi^2(\alpha/N)^2\underset{\sim}{L} \\ -j2\pi(\alpha/vN)\underset{\sim}{L}^{-1} & \{1-2\pi^2(\alpha/N)^2\}\underset{\sim}{I} \end{bmatrix} \quad (4\text{-}29)$$

Figure 4-5 shows a three-conductor transmission line represented by an overall chain parameter matrix, $\underset{\sim}{\Phi}_T$. Recall that the terminal conditions are

$$\underline{V}(L) = \underset{\sim}{Z}_L \underline{I}(L) \quad (4\text{-}30a)$$

and

$$\underline{V}(0) = \underline{V}_0 - \underset{\sim}{Z}_0 \underline{I}(0), \quad (4\text{-}30b)$$

and, from the definition of the overall chain parameter matrix,

$$\underline{V}(L) = \underset{\sim}{\Phi}_{11}\underline{V}(0) + \underset{\sim}{\Phi}_{12}\underline{I}(0) \quad (4\text{-}30c)$$

and

$$\underline{I}(L) = \underset{\sim}{\Phi}_{21}\underline{V}(0) + \underset{\sim}{\Phi}_{22}\underline{I}(0). \quad (4\text{-}30d)$$

The lumped model crosstalk predictions can be obtained by solving these four equations (equations (4-30)).

Since it can be shown explicitly that the transmission line result is a function of Z/Z_C for the special case of $Z_{CR}=Z_{CG}=Z_C$, and $Z_{0G}=Z_{LG}=Z_{0R}=Z_{LR}=Z$, all that needs to be shown to prove that the lumped model results are a function of Z/Z_C for the same special case, is to show that the chain parameter matrix of each of the lumped models for any

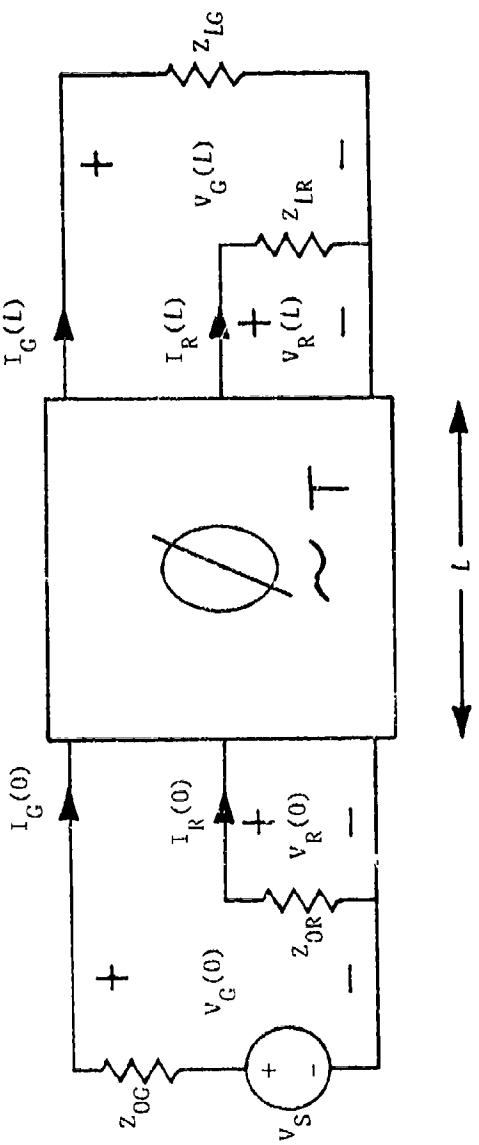

Figure 4-5 Three-Port Representation of a 3-Conductor Line

value of N has the same form as the chain parameter matrix of the transmission line model (see equation (4-3b)).

If it is remembered that $\underset{\sim}{C}=\underset{\sim}{L}^{-1}/v^2$, for the case of interest, it is easily seen that the lumped model $\underset{\sim}{\phi}$'s shown in equations (4-26) thru (4-29) are of the same form as the transmission line $\underset{\sim}{\phi}$, for N = 1. It can also be shown that the lumped model $\underset{\sim}{\phi}$'s have this same general form for all N. Therefore, for the special case previously discussed, the lumped model results are a function of Z/Z_C. That is, the individual values of Z and Z_C have no significance.

Once again, an error function can be defined as

$$\text{Error(dB)} = 20\log_{10}\left[\frac{\left|\frac{V(X)}{V_S}\right|_{\text{Transmission Line}}}{\left|\frac{V(X)}{V_S}\right|_{\text{Lumped Model}}}\right] \qquad (4\text{-}31)$$

for the purpose of comparing prediction accuracies of the lumped models. Here, X represents the "near" (0) or the "far" (ℓ) end crostalk, respectively.

The next chapter will investigate the prediction accuracy of the three-conductor lumped models of interest, discuss the advantages and disadvantages of the different lumped models, and show the effects of the value of load impedance on the accuracy of the lumped model predictions.

CHAPTER 5

Three-Conductor Results

In this chapter the crosstalk predictions of the four lumped models are compared to the exact crosstalk results for the three-conductor case. The results are plots, which are of the same general form as the two-conductor results described in Chapter 3, and are shown in Appendices C, D, E, and F. These results were obtained using a coupling coefficient, k, of .1753, a characteristic impedance, Z_C, of 271.1, and assuming the special case of $Z_{CG} = Z_{CR} = Z_C$, and $Z_{OG} = Z_{LG} = Z_{OR} = Z_{LR} = Z$, so that the resulting transfer ratios are a function of Z/Z_C. It should be noted that the values of k and Z_C specified above correspond to two #20 guage wires 2cm above a ground plane with the wires separated by 2cm. Toward the end of the chapter, a general example ($Z_{OG} \neq Z_{LG} \neq Z_{OR} \neq Z_{LR}$) will be shown. It will also be shown that this general example yielded approximately the same qualitative results as the special case mentioned above.

Appendix C contains the comparison of the exact three-conductor line "near" end crosstalk voltage transfer ratio to the predicted crosstalk voltage transfer ratios of several sections (N=1, 2, 3, 5, and 10) of the four lumped models for values of Z/Z_C of .01 ($Z=.01Z_C$), 1 ($Z=Z_C$) and 100 ($Z=100Z_C$). For example, Figure C-1 compares the exact transmission line result to the predictions of one section

of the four lumped models with a Z/Z_C of .01.

Appendix D contains the comparisons of the "far" end crosstalk for the same values of N as above, with values of Z/Z_C of .01 and 100. For example, Figure D-2 compares the exact transmission line result to the predictions of one section of the four lumped models with a Z/Z_C of 100. The comparisons for one section of the four lumped models with a Z/Z_C of 1 are shown in Figures 5-1 (BGAM and FGAM predictions), and 5-2 (PI and TEE predictions). These two figures were included for the sake of completeness, since the exact "far" end crosstalk for the matched case ($Z/Z_C=1$) is identically zero. It can be seen from these two figures that the BGAM and FGAM lumped model predictions are much more accurate than the PI or TEE lumped model predictions.

Appendix E contains the "near" end crosstalk error plots for N=1, 2, 3, 5, and 10 with values of Z/Z_C of .01, 1, and 100. It should be remembered that the "near" end error function is defined as

$$\text{Error(dB)} = 20\log_{10}\left[\frac{\left|\frac{V(0)}{V_S}\right|_{\text{Transmission Line}}}{\left|\frac{V(0)}{V_S}\right|_{\text{Lumped Model}}}\right] \qquad (5\text{-}1)$$

For instance, Figure E-3 is a plot of the PI lumped model prediction error for N=1, 2, 3, 5, and 10 with a Z/Z_C of .01.

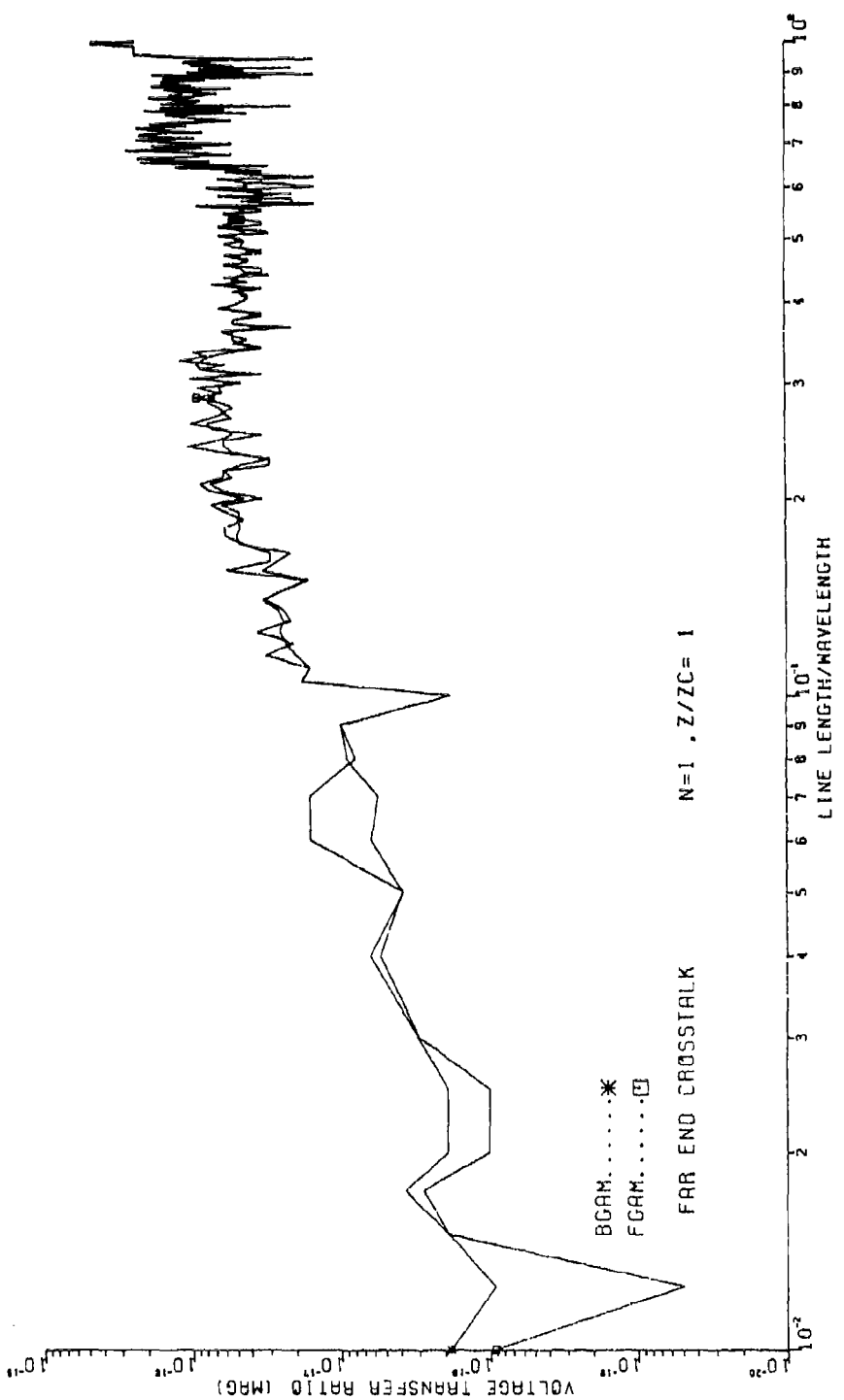

Figure 5-1 "Far" End BGAM and FGAM Lumped Model Predictions for the Matched Case

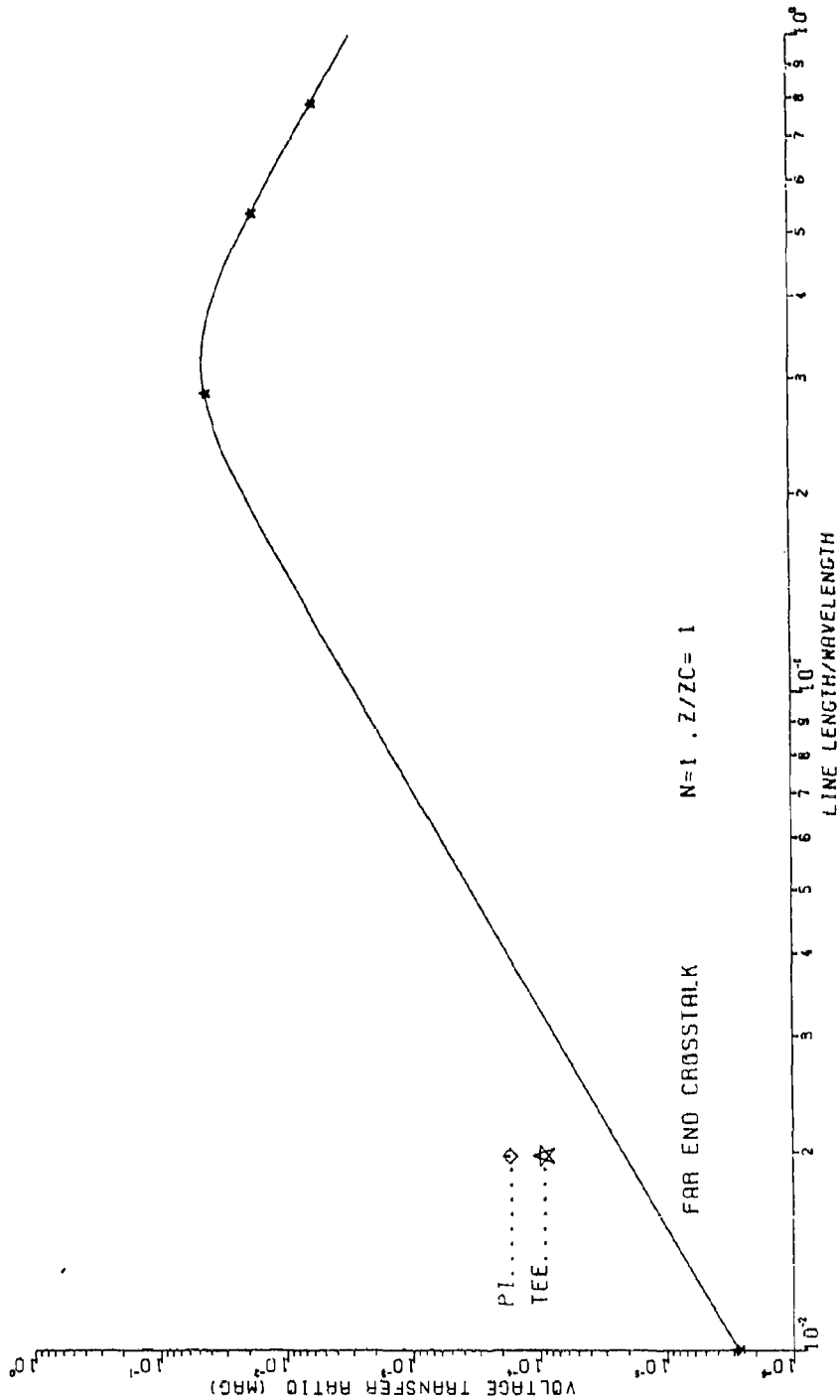

Figure 5-2 "Far" End PI and TEE Lumped Model Predictions for the Matched Case

Appendix F contains the plots of the corresponding "far" end error function,

$$\text{Error(dB)} = 20\log_{10}\left[\frac{\left|\frac{V(L)}{V_S}\right|_{\text{Transmission Line}}}{\left|\frac{V(L)}{V_S}\right|_{\text{Lumped Model}}}\right] \qquad (5\text{-}2)$$

for N=1, 2, 3, 5, and 10 with values of Z/Z_C of .01 and 100 (the error function is undefined for the matched case, because the exact transmission line result is identically zero). For example Figure F-6 shows the FGAM lumped model prediction error for N=1, 2, 3, 5, and 10 with a Z/Z_C of 100.

Some interesting results can be seen in Appendices C-F, but since the three-conductor line lumped model circuits are much more complicated than was the case for the two-conductor line, these "interesting" results will merely be pointed out. No attempt will be made to explain the causes for these "interesting" results. Tables 5-1 and 5-2 show the cases of interest along with the figures in which they are displayed. It should be noted that an equal sign implies equality only over the range of L/λ shown in the accompanying figures.

Figures	Near End Crosstalk Models
E-4 and E-11	TEE(Z/Z_C=.01) ≈ PI(Z/Z_C=100)
E-1 and E-10	BGAM(Z/Z_C=.01) ≈ FGAM(Z/Z_C=100)
E-2 and E-4	FGAM(Z/Z_C=.01) ≈ BGAM(Z/Z_C=100)
E-5 and E-6	BGAM(Z/Z_C=1) ≈ FGAM(Z/Z_C=1)
E-7 and E-8	PI(Z/Z_C=1) ≈ TEE(Z/Z_C=1)
E-3 and E-12	PI(Z/Z_C=.01) ≈ TEE(Z/Z_C=100)

Table 5-1

Figure	Far End Crosstalk Models
F-4 and F-7	$TEE(Z/Z_C=.01) = PI(Z/Z_C=100)$
F-1,2,3 and F-5,6,8	$BGAM=FGAM=PI(Z/Z_C=.01) = BGAM=FGAM=TEE(Z/Z_C=100)$

Table 5-2

Again, a ±3dB error point can be defined as the "upper limit" of the lumped model predictions. That is, the value of L/λ which results in the first occurrence of a ±3dB error is defined as the "upper limit" of that particular lumped model. Table 5-3 shows the "upper limit" for one section of the four lumped models for values of Z/Z_C of .01, 1, and 100. From Table 5-3 it can be seen that the value of Z/Z_C has little effect on the "upper limit" of the "near" end lumped model predictions, and very nearly no effect on the "far" end prediction accuracy. It can also be seen that one section of any of the four lumped models will yield predictions that are within ±3dB of the exact three-conductor transmission line result for frequencies such that L/λ is 1/10 or less, regardless of the value of Z/Z_C. From the figures shown in Appendices C-F it can be seen that the lumped model prediction accuracy is increased nonlinearly with the addition of more sections of that lumped model. That is, the error is always reduced when another section of the lumped model is added, but the range of accuracy is not increased linearly, i.e. if one section is accurate up to L/λ =1/10, then two sections will not be accurate up to L/λ =1/5. These qualitative results are the

same as the results obtained for the two-conductor line (Chapter 3). But, the general rules for choosing a lumped model for operating frequencies such that L/λ is larger than 1/10 seem to be somewhat different. For a "small" or "large" load impedance it seems that the PI and TEE lumped models yield the best overall results ("near" and "far" end crosstalk predictions), while the BGAM and FGAM lumped models yield much more accurate predictions for the matched case.

3dB Error Point (N=1)

	Near End			Far End	
Model	Z/Z_C=.01	Z/Z_C=1	Z/Z_C=100	Z/Z_C=.01	Z/Z_C=100
BGAM	1.40E-1	4.25E-1	1.00E-1	2.20E-1	2.20E-1
FGAM	1.00E-1	4.25E-1	1.40E-1	2.20E-1	2.20E-1
PI	1.75E-1	2.65E-1	2.10E-1	2.20E-1	2.20E-1
TEE	2.10E-1	2.65E-1	1.75E-1	2.20E-1	2.20E-1

Table 5-3

What has been shown for the three-conductor case applies only to the special case of $Z_{OG}=Z_{LG}=Z_{OR}=Z_{LR}=Z$. Figure 5-3 and 5-4 show the voltage transfer ratio results for the general case of $Z_{OG}=0\Omega$, $Z_{LG}=100k\Omega$, $Z_{OR}=50\Omega$, and $Z_{LR}=1\Omega$ (the coupling coefficient, k, is .1753 and the characteristic impedance of the lines, Z_{CG} and Z_{CR}, are 271.1). These values were chosen, because the model used in [11] had an "upper limit" of approximately $L/\lambda=1/1000$ when they were used. It can be seen in Figures 5-3 and 5-4, that the "upper limit" of one section of any of the four lumped models is only slightly less than $L/\lambda=1/10$. This leads one to believe that the special case results obtained

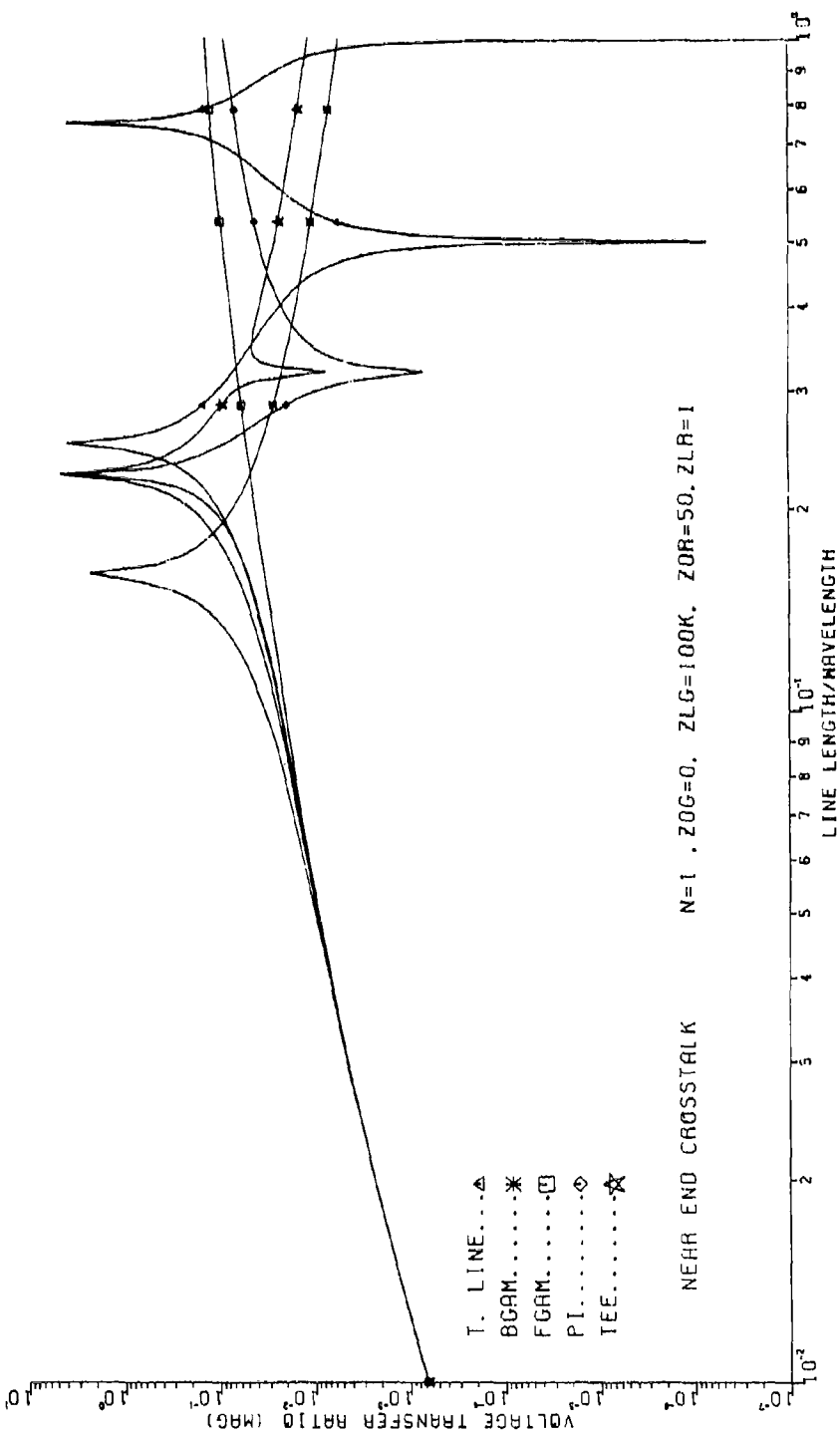

Figure 5-3 General "Near" End Crosstalk Result

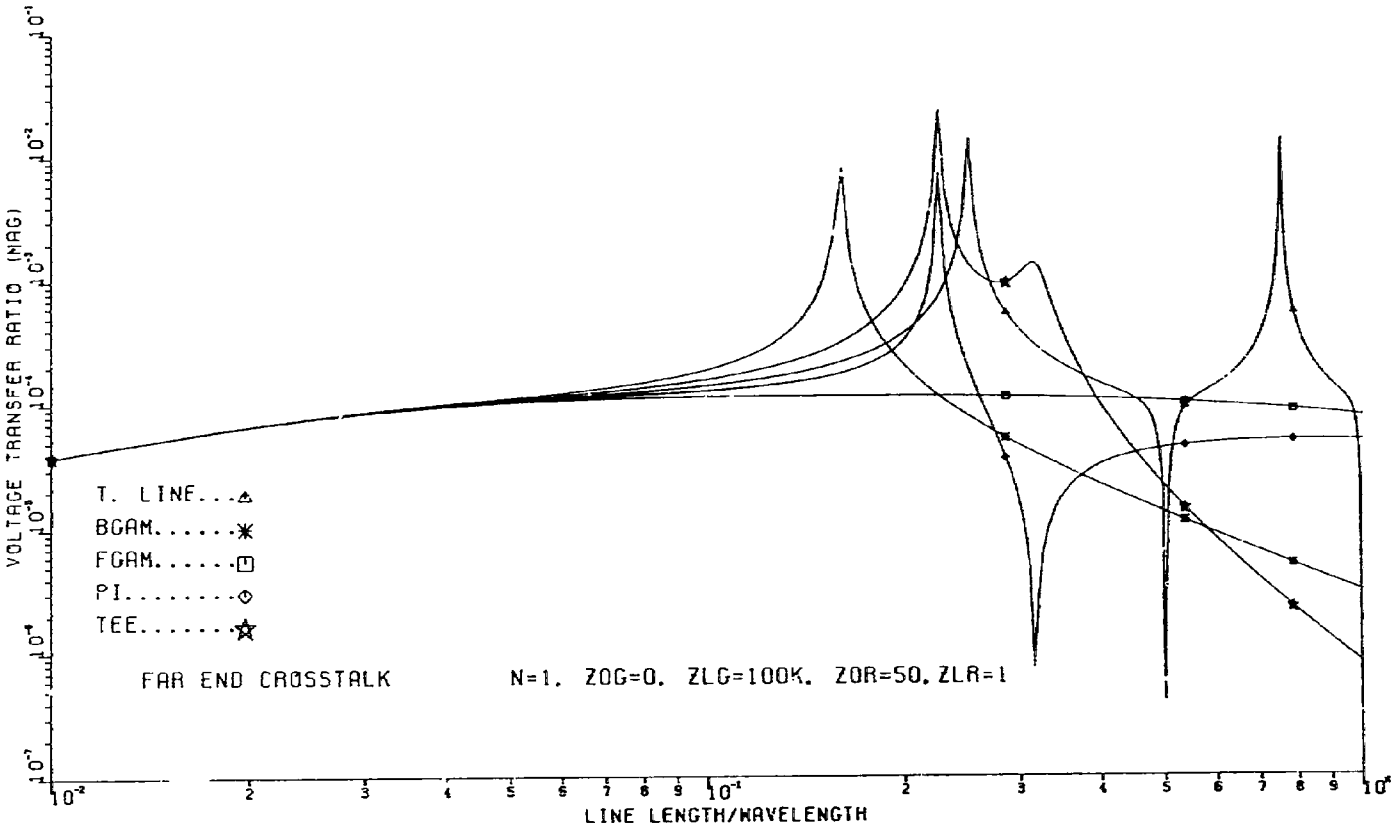

Figure 5-4 General "Far" End Crosstalk Result

from the plots shown in Appendices C-F may apply to the more general cases, i.e., $Z_{0G} \neq Z_{LG} \neq Z_{0R} \neq Z_{LR}$.

So, it appears that the general results obtained for the two-conductor lumped models also apply to the general three-conductor lumped models. That is, one section of any of the four lumped models yield accurate results until frequencies are reached where L/λ is approximately 1/10 or less, and that the prediction error of the lumped models is reduced with the addition of more sections of that lumped model, but at the same time, the range of prediction accuracy is not increased in a linear fashion.

Chapter 6

Summary and Conclusions

In this report the voltage transfer ratio predictions of the BGAM, FGAM, PI, and TEE lumped iterative models were compared to the exact, transmission line equation results, for various values of load impedances, and several different numbers of sections, for the two and three-conductor cases. The lines were assumed to be uniform, lossless, and immersed in a homogeneous medium.

It was found that, for both cases, one section of any of the four lumped models mentioned above will yield prediction accuracies within $\pm$3dB of the exact transmission line result for an L/λ of approximately 1/10 or less, regardless of the load impedance value. It was also shown that the lumped models prediction error was reduced with the addition of more sections of a particular lumped model. But, the range of accurate predictions (in terms of electrical length) did not increase in a linear fashion. It was also found that the value of load impedance may significantly effect the lumped models prediction accuracies when L/λ is $> 1/10$ (where more than one section of a lumped model must be used to yield accurate prediction results).

Since the relation between the number of sections of a particular lumped model, and the resulting prediction accuracy (in terms of electrical length) is a nonlinear one it is difficult to find a satisfactory method of predicting

the number of sections that must be used to yield a desired prediction accuracy (when the operating frequency is such, that L/λ is $> 1/10$). This problem is made even more complex by the fact that the load impedance value may play a significant role in the lumped models prediction accuracy.

However, it was found that there were some general rules that should help in the selection of the "best" lumped model, depending on the value of load impedance present. For the two-conductor case the "wise" choices appear to be the BGAM or FGAM lumped models for a "small" or "matched" load impedance (when compared to the characteristic impedance of the line), and the PI or TEE lumped models for a "large" load impedance. For the three-conductor case, which is of much more interest, the "wise" choices appear to be the PI or TEE lumped models for a "large" or "small" load impedance and the BGAM or FGAM lumped models for the "matched" case.

These general rules and the fact that one section of any of the lumped models will yield accurate predictions for frequencies such that L/λ is 1/10 or less will undoubtedly prove somewhat useful in the prediction of crosstalk (interference) problems, but they are somewhat limited in scope. So, further work still needs to be performed in this area A reasonable method for estimating the number of sections, of a particular lumped model, needed to yield a given prediction accuracy must be found for lumped itera-

tive transmission line modeling to be truly effective. The multifrequency (pulse) input waveform case also needs to be examined further. This report briefly discussed the more obvious problems involved when a pulse input wave form (such as a trapazoidal pulse used in digital applications) is used. But. the general properties discussed previously, were found only for the single frequency case, and may not prove to be very useful for the multifrequency case. Because the relationship between the frequency domain and the time domain is not at all clear.

Therefore, this paper should only be considered as a first step in the investigation of lumped model approximations of transmission lines.

APPENDIX A

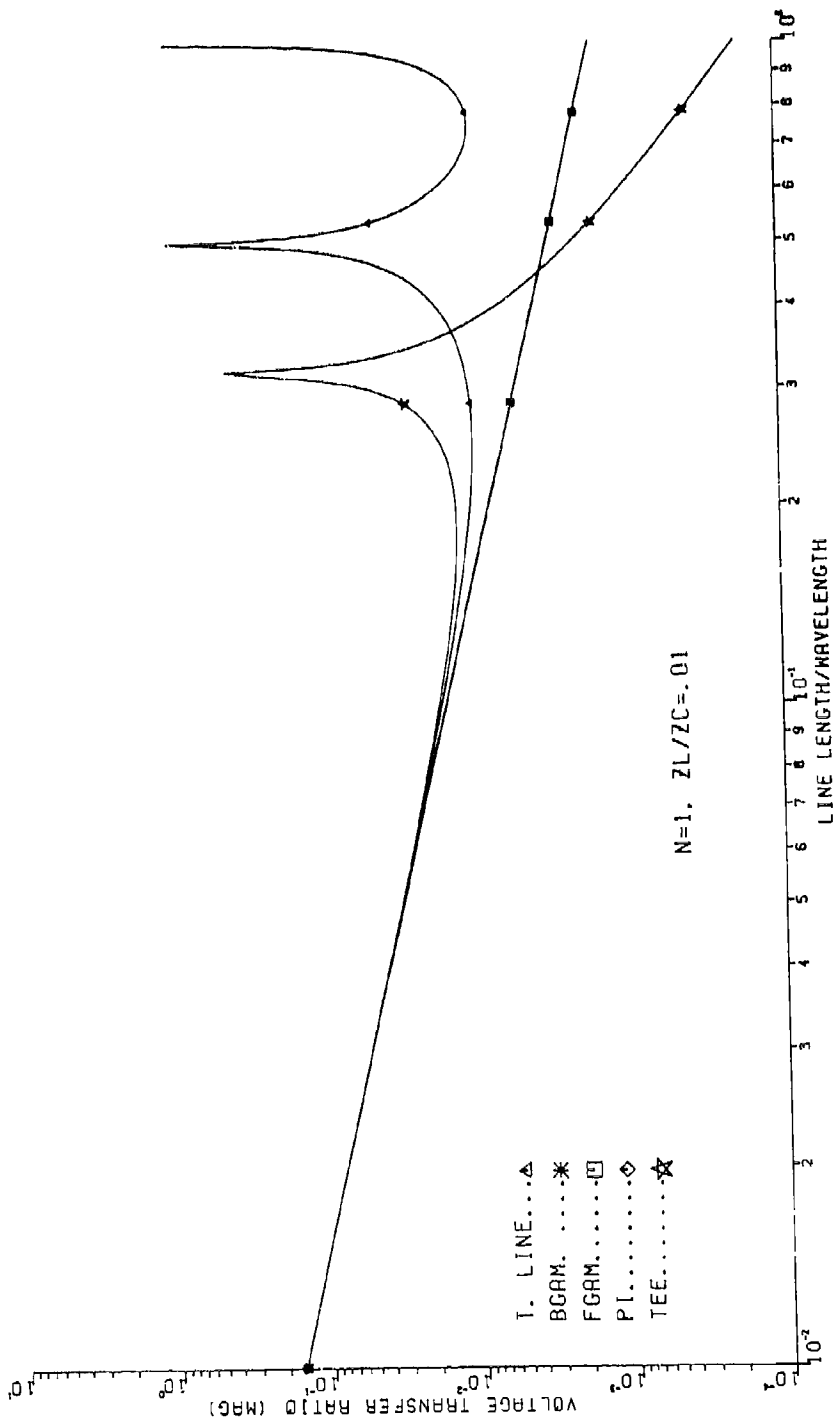

Figure A-1

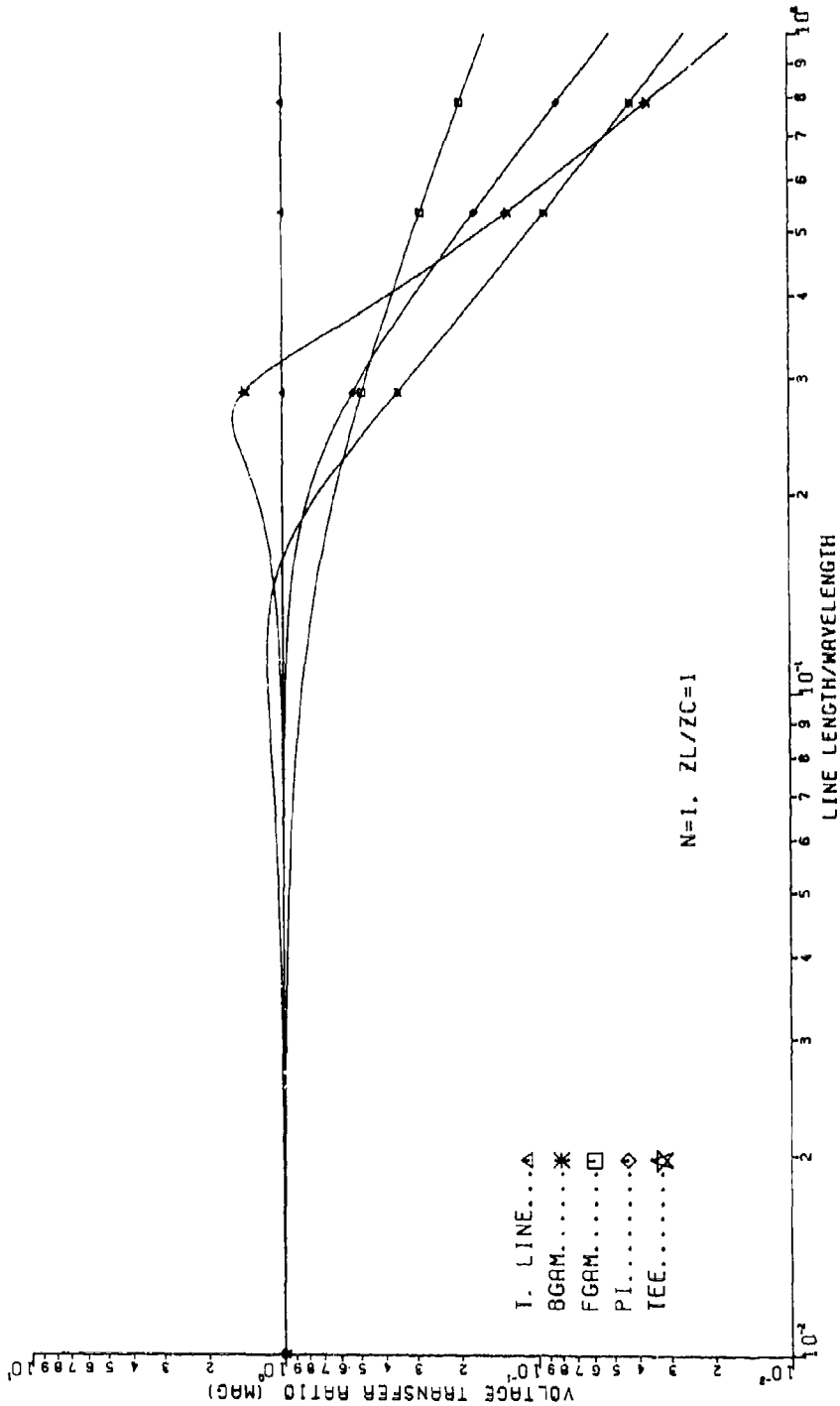
VOLTAGE TRANSFER RATIO (MAG)
LINE LENGTH/WAVELENGTH
N=1. ZL/ZC=1
T. LINE...
BGAM.....
FGAM.....
PI.....
TEE.....

Figure A-2

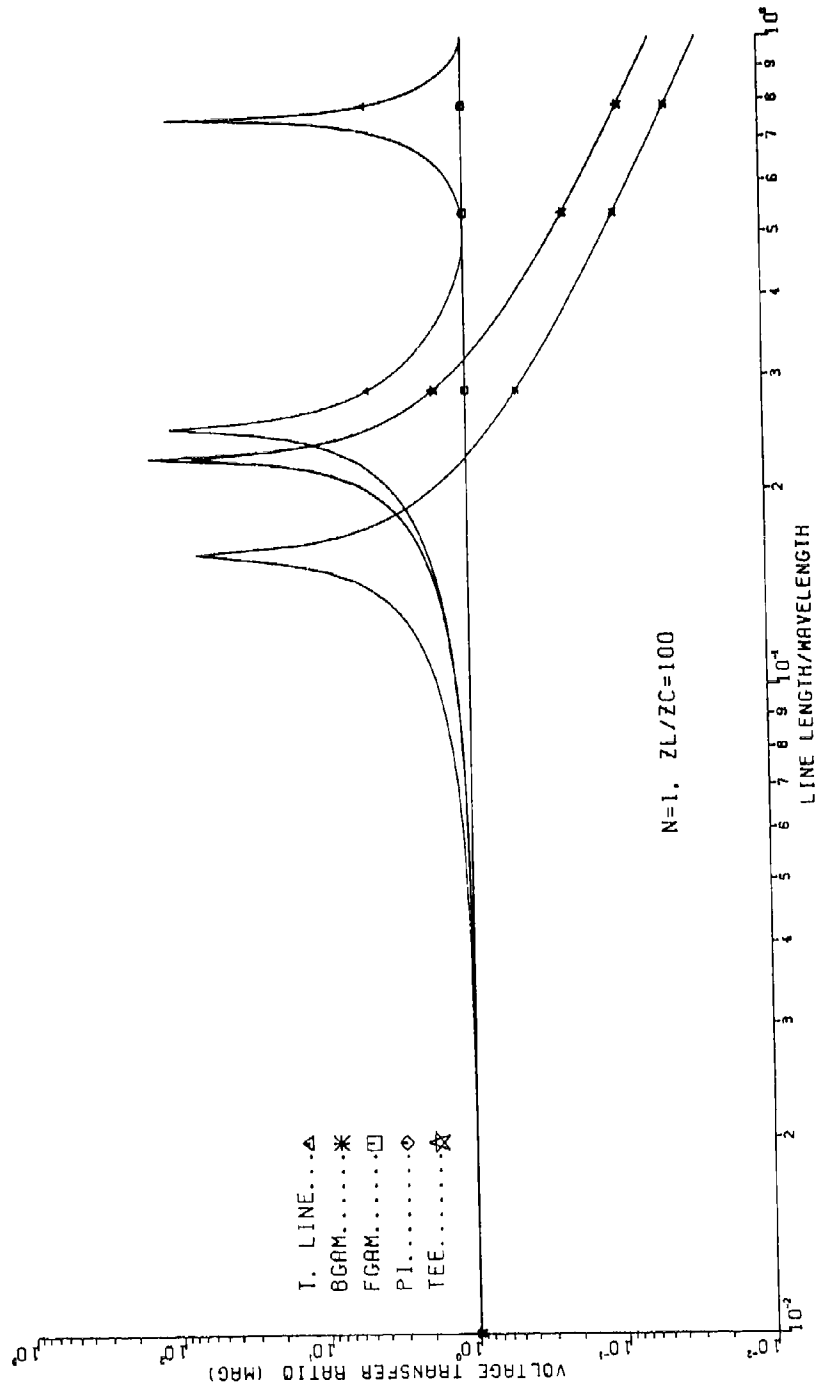
T. LINE...
BGAM.....
FGAM.....
PI.....
TEE.....
N=1, ZL/ZC=100
VOLTAGE TRANSFER RATIO (MAG)
LINE LENGTH/WAVELENGTH

Figure A-3

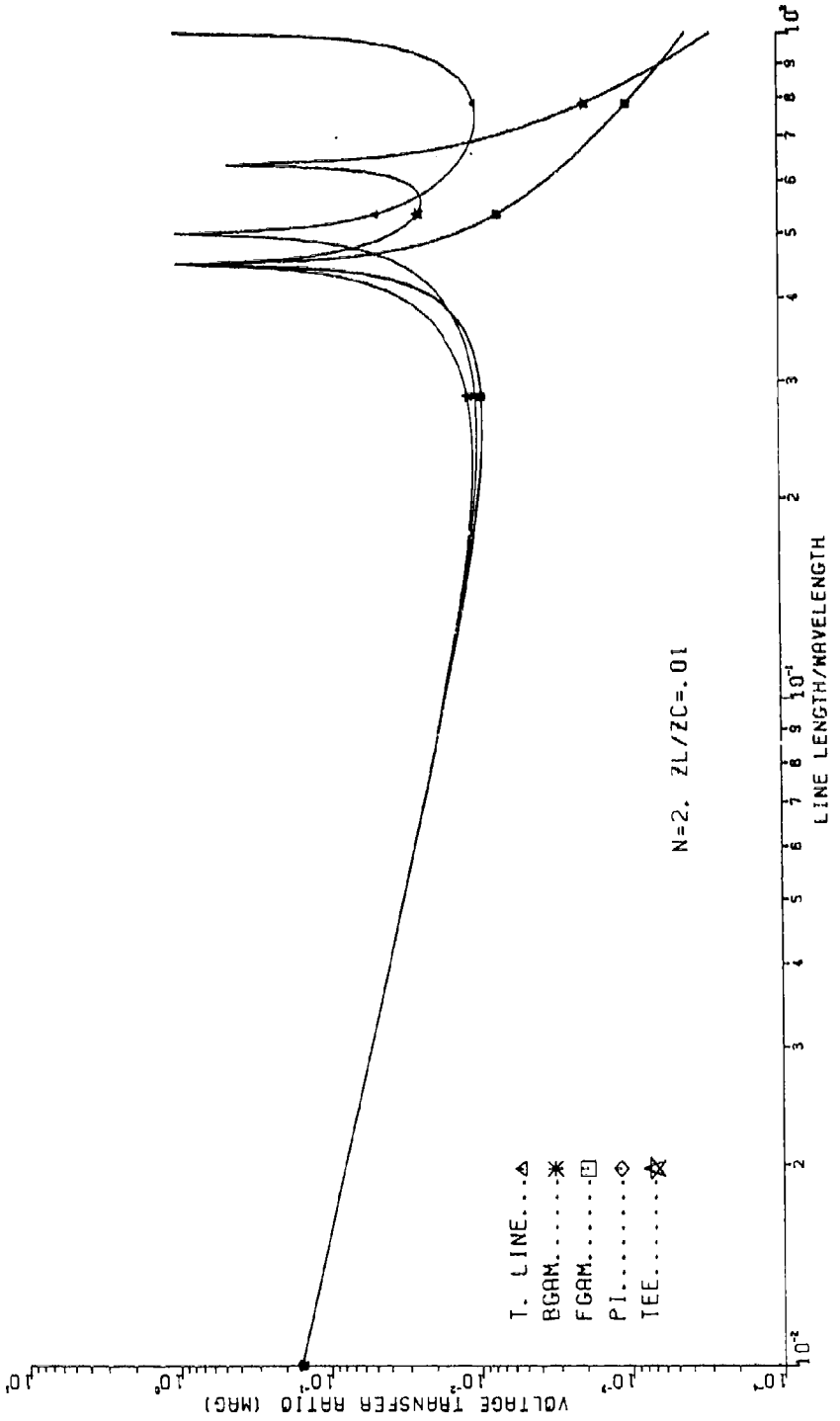
VOLTAGE TRANSFER RATIO (MAG)
LINE LENGTH/WAVELENGTH
N=2. ZL/ZC=.01
T. LINE...
BGAM.....
FGAM.....
PI.....
TEE.....

Figure A-4

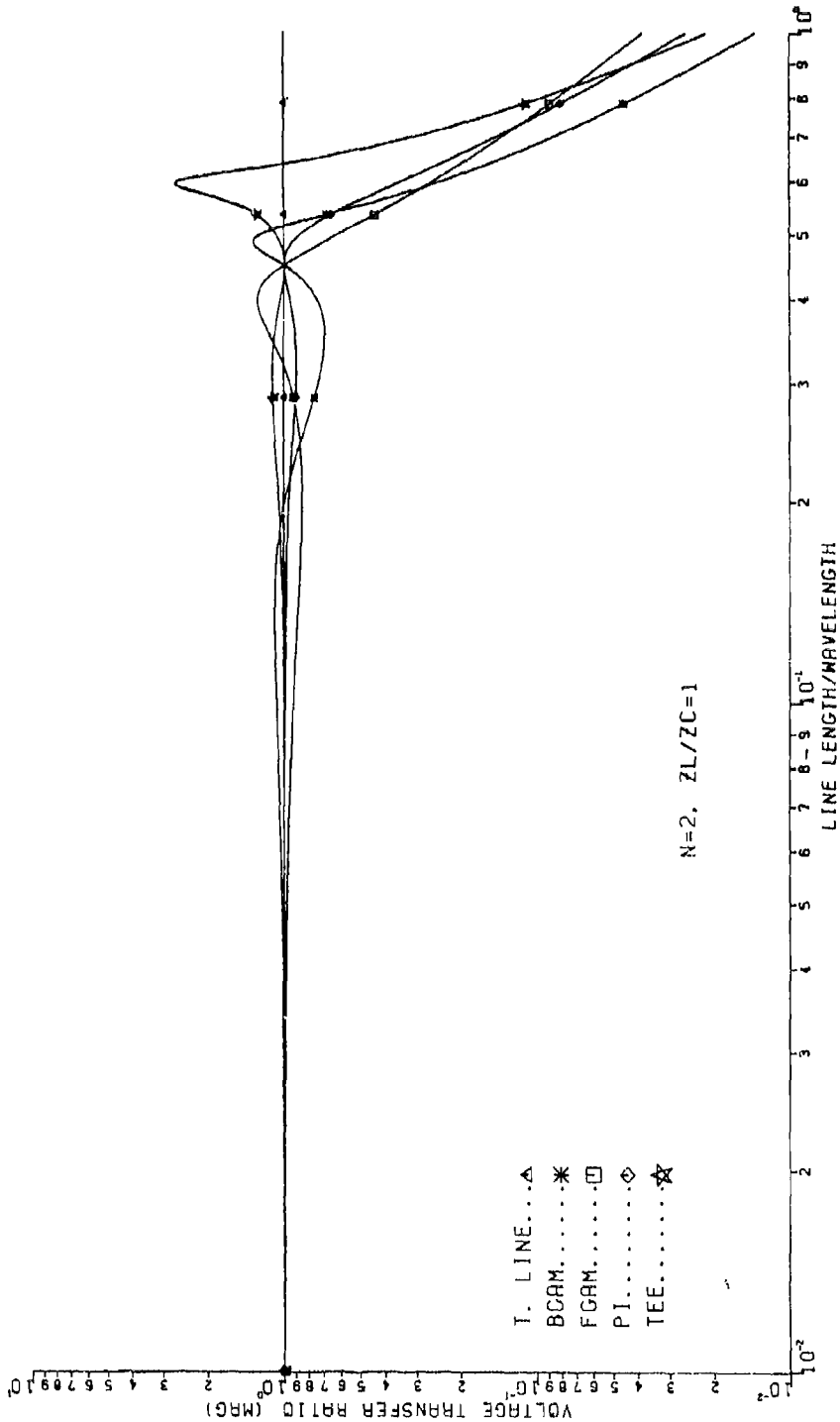
VOLTAGE TRANSFER RATIO (MAG)
LINE LENGTH/WAVELENGTH
N=2, ZL/ZC=1
T. LINE...
BCAM.....
FCAM.....
PI.....
TEE.....

Figure A-5

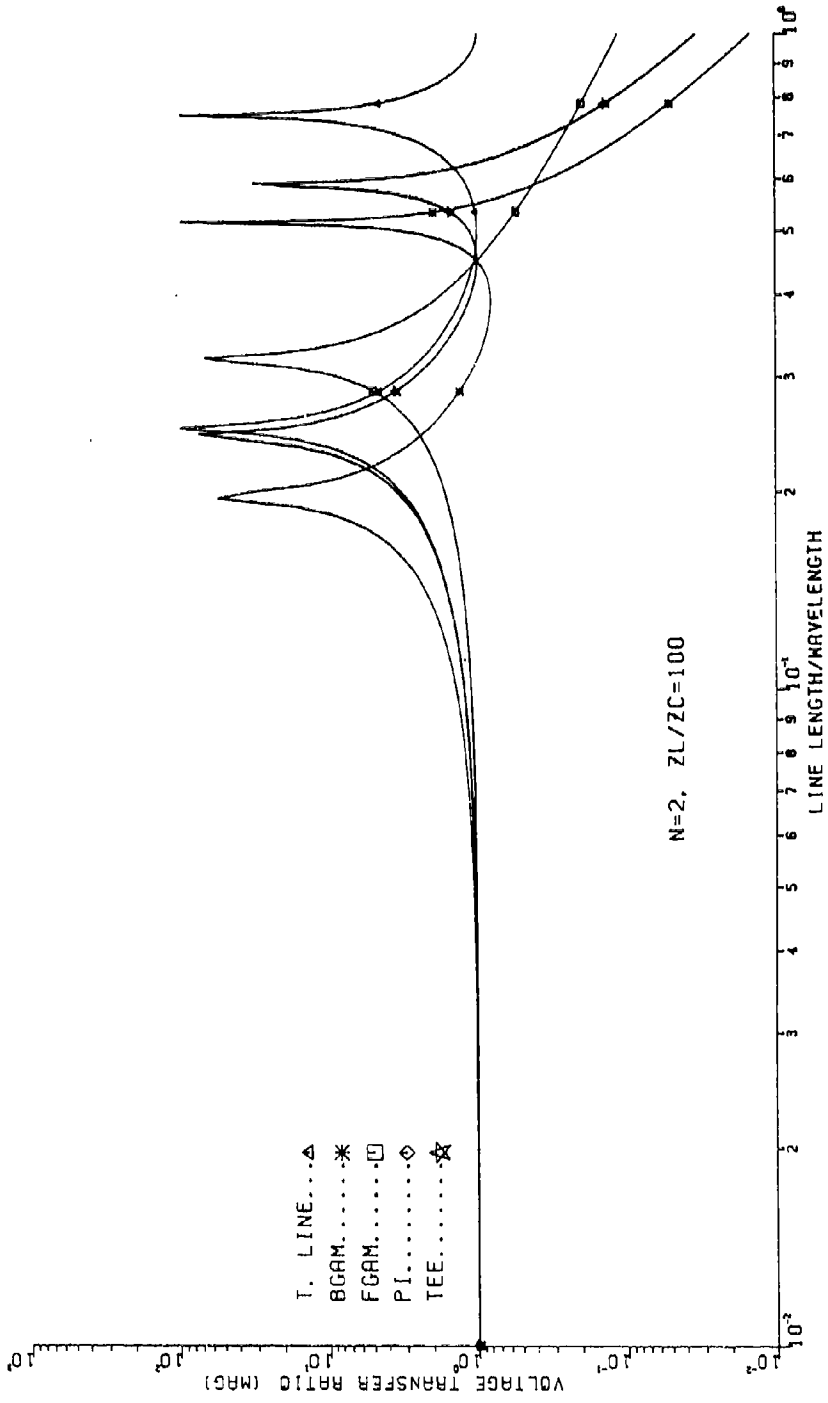
T. LINE
BGAM
FGAM
PI
TEE
N=2, ZL/ZC=100
VOLTAGE TRANSFER RATIO (MAG)
LINE LENGTH/WAVELENGTH

Figure A-6

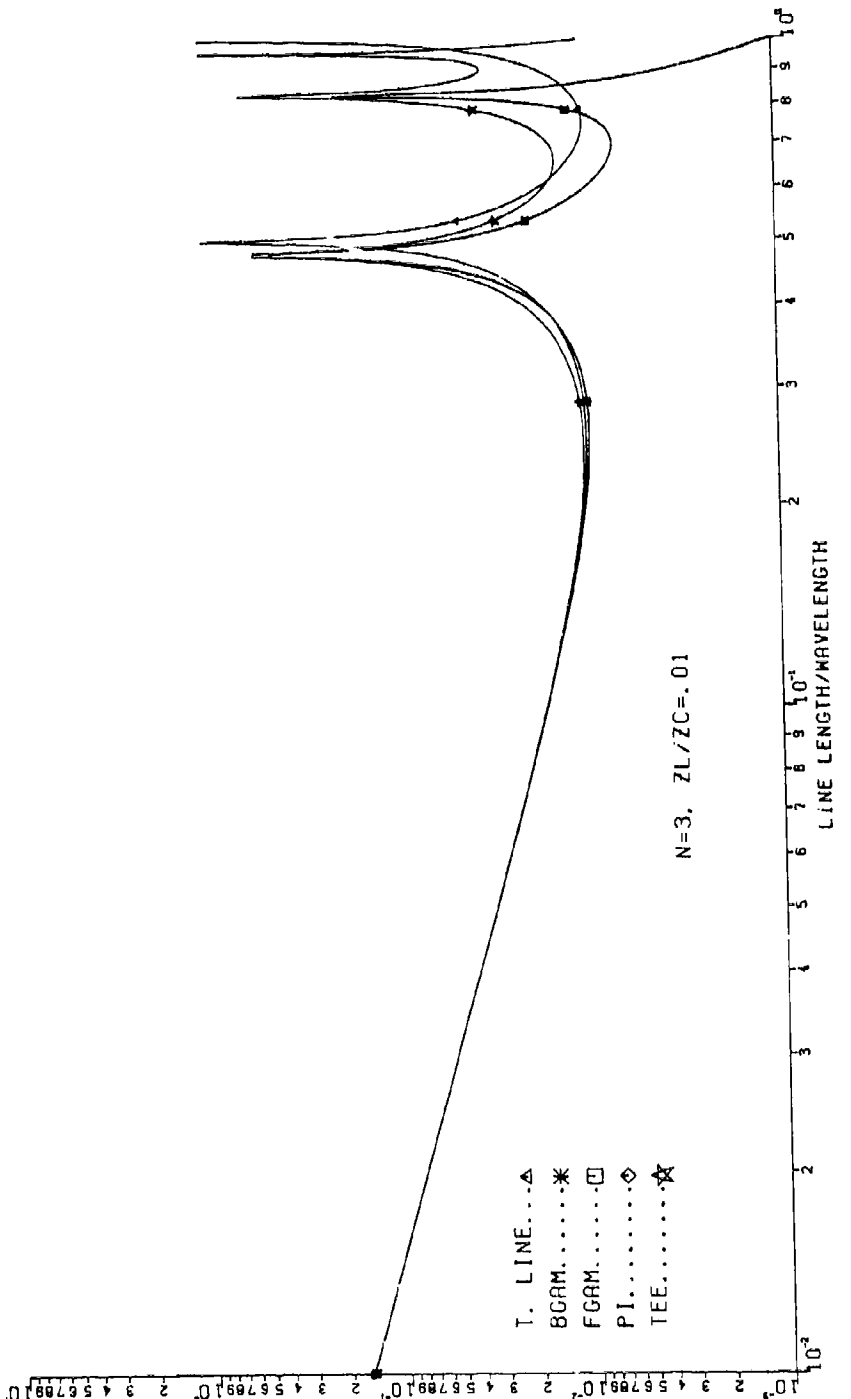
VOLTAGE TRANSFER RATIO (MAG)
LINE LENGTH/WAVELENGTH
N=3, ZL/ZC=.01
T. LINE...
BGAM.....
FGAM.....
PI.....
TEE.....

Figure A-7

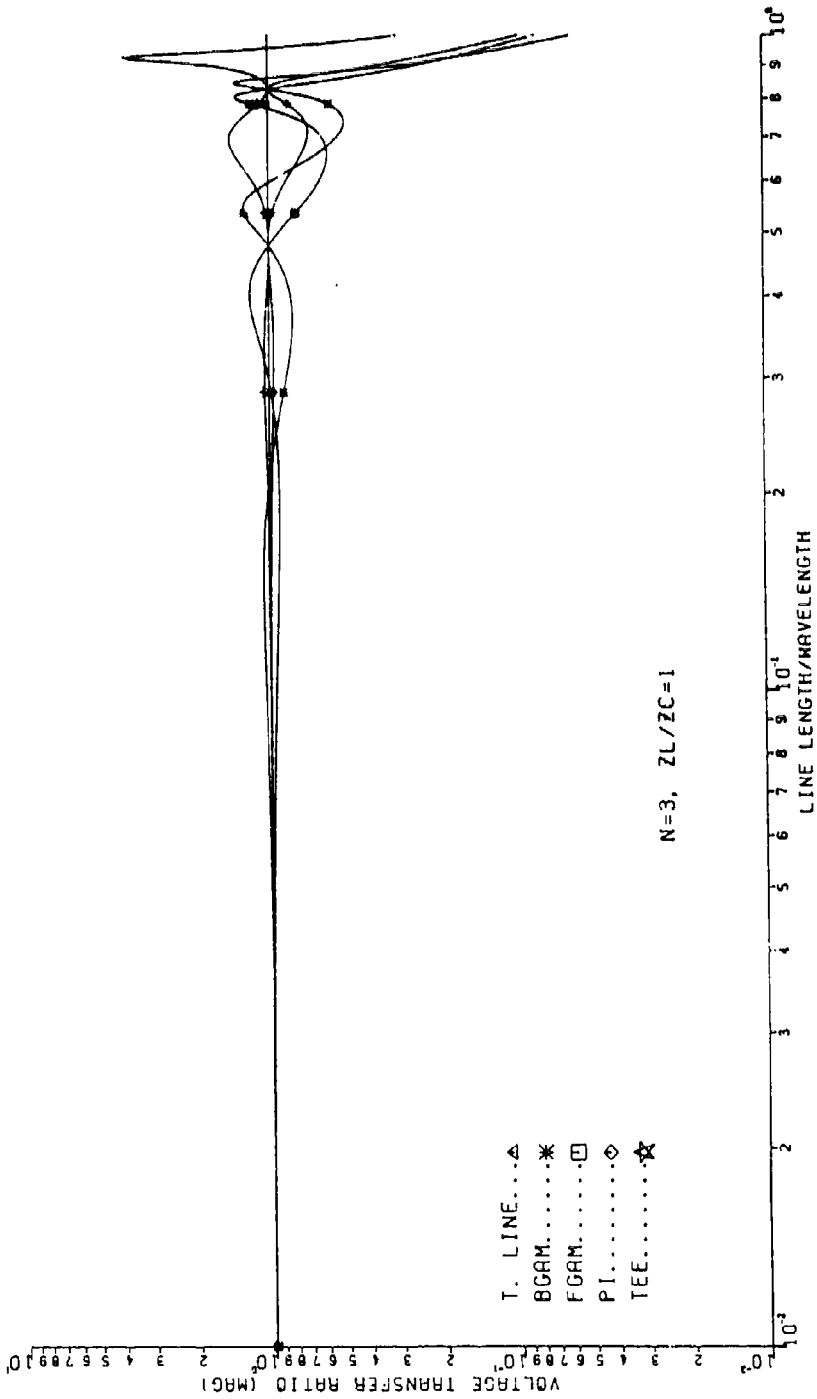
VOLTAGE TRANSFER RATIO (MAG)
LINE LENGTH/WAVELENGTH
N=3, ZL/ZC=1
T. LINE...
BGAM.....
FGAM.....
PI.....
TEE.....

Figure A-8

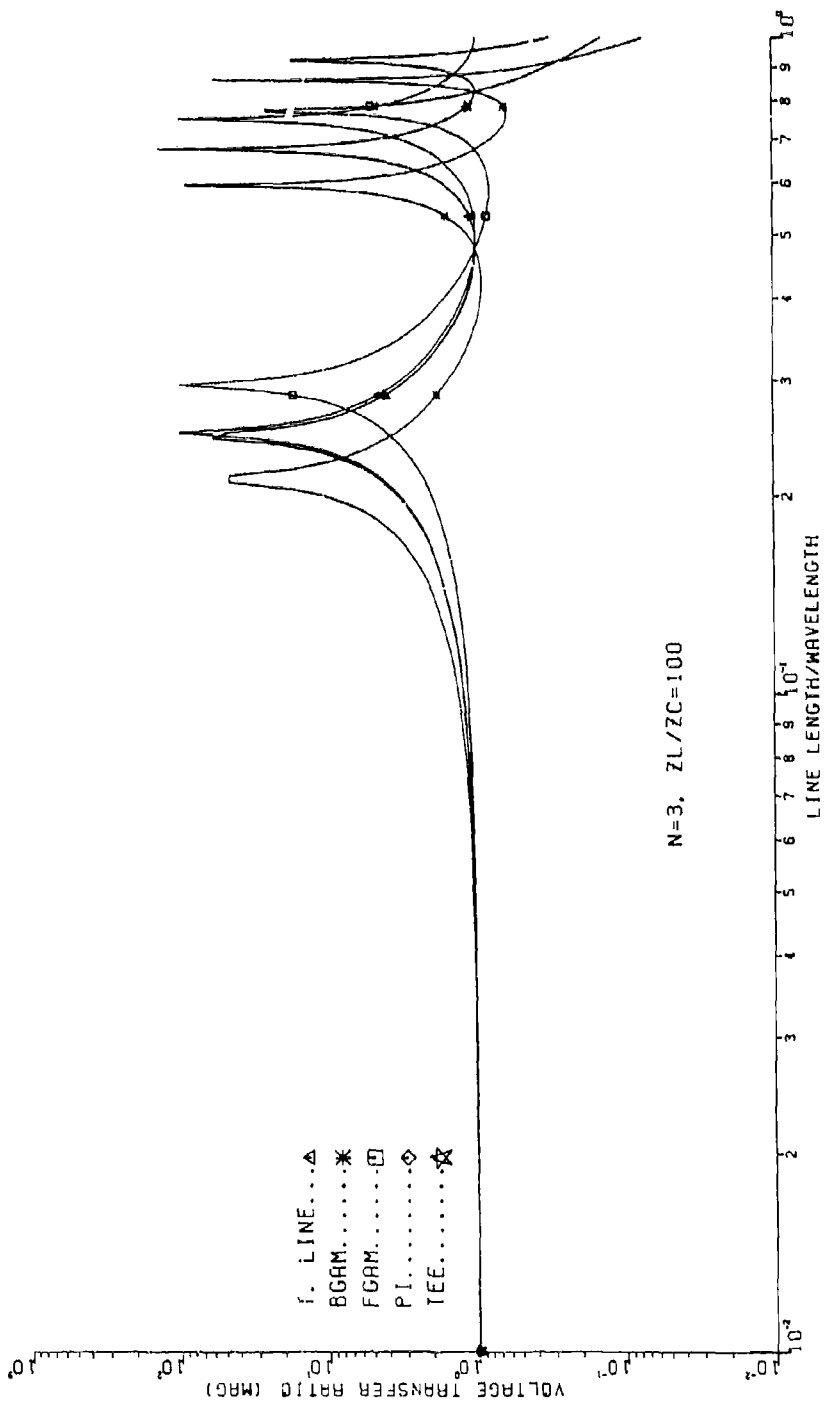
VOLTAGE TRANSFER RATIO (MAG)
LINE LENGTH/WAVELENGTH
N=3, ZL/ZC=100
F. LINE
BGAM
FGAM
PI
TEE

Figure A-9

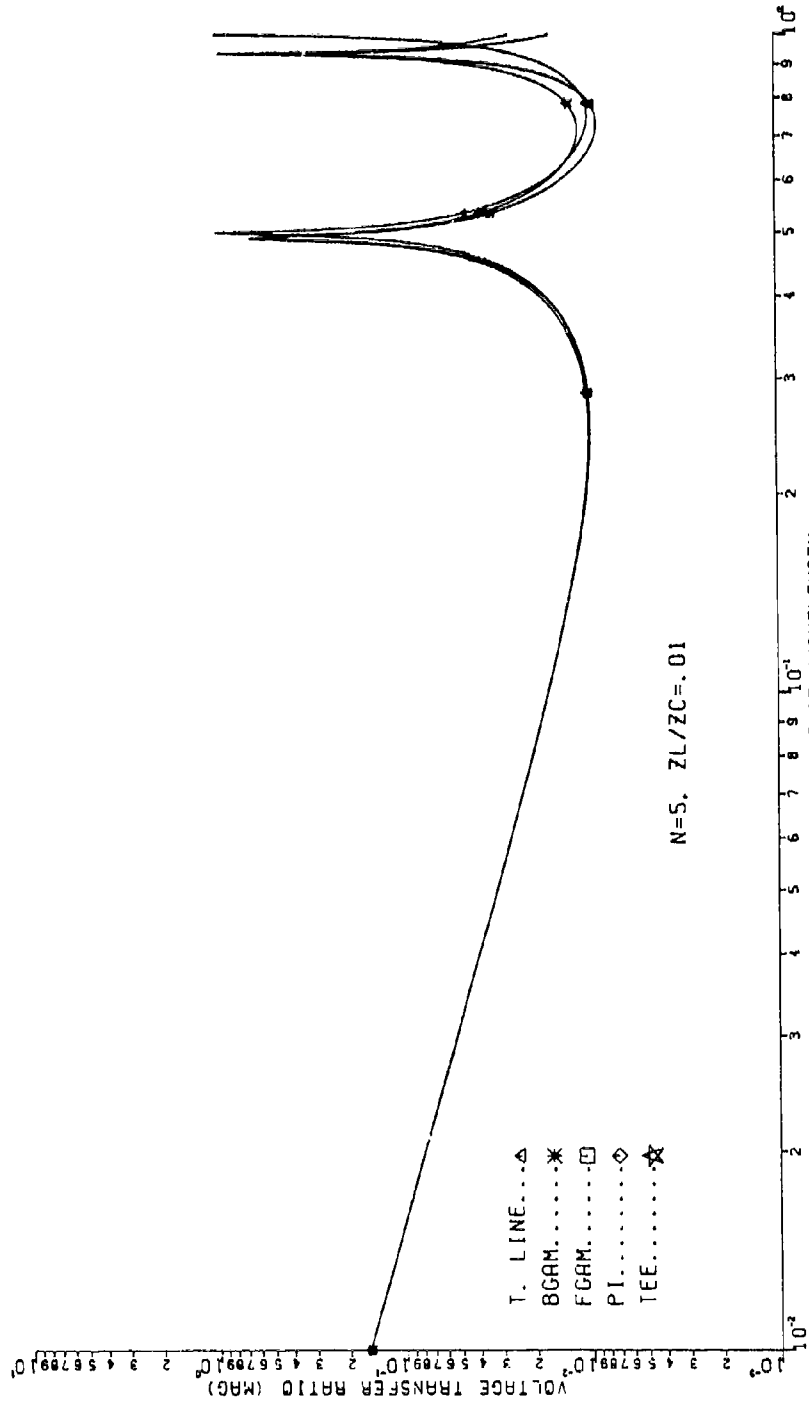
VOLTAGE TRANSFER RATIO (MAG)
LINE LENGTH/WAVELENGTH
N=5. ZL/ZC=.01
T. LINE
BGAM
FGAM
PI
TEE

Figure A-10

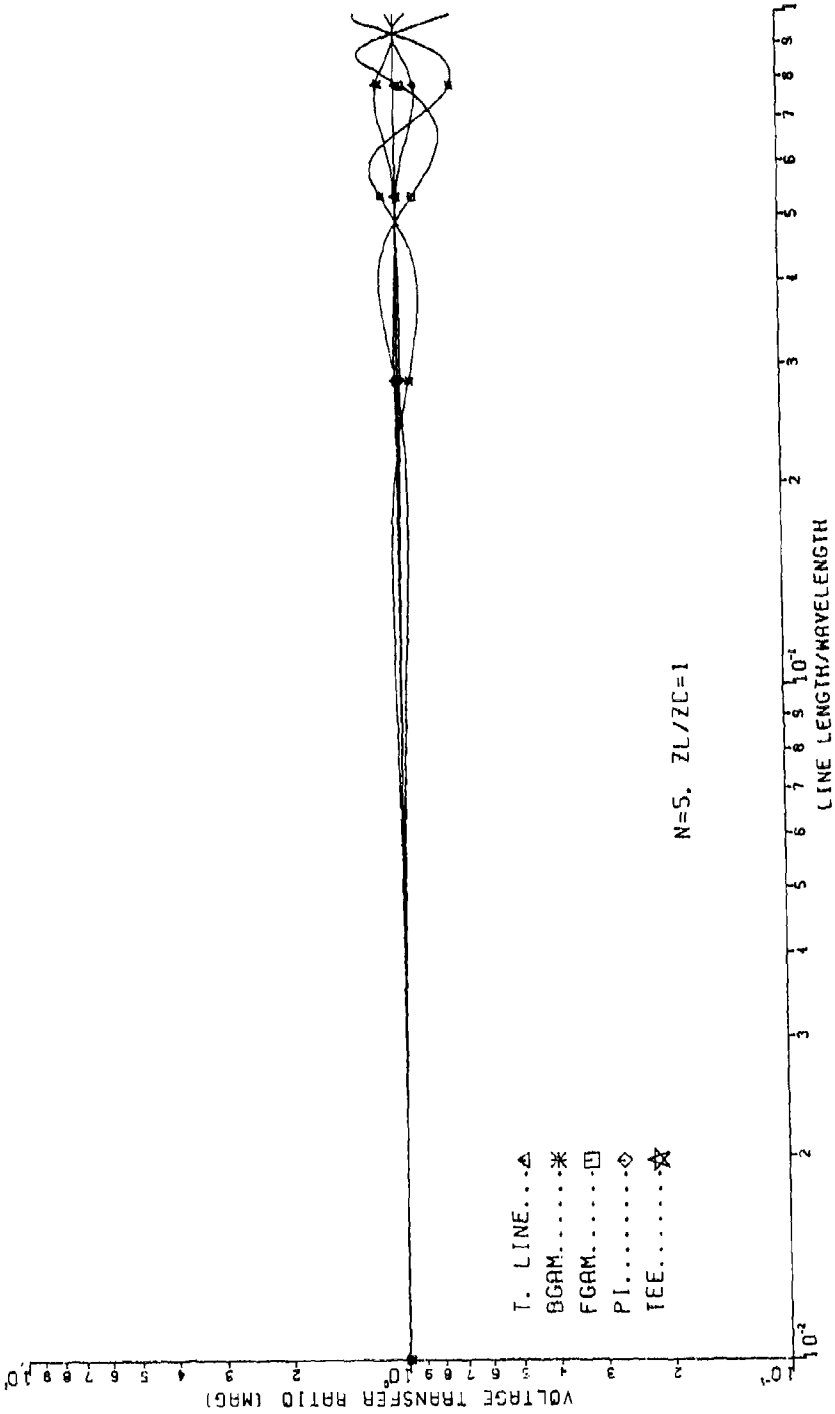
VOLTAGE TRANSFER RATIO (MAG)
LINE LENGTH/WAVELENGTH
N=5. ZL/ZC=1
T. LINE
BGAM
FGAM
PI
TEE

Figure A-11

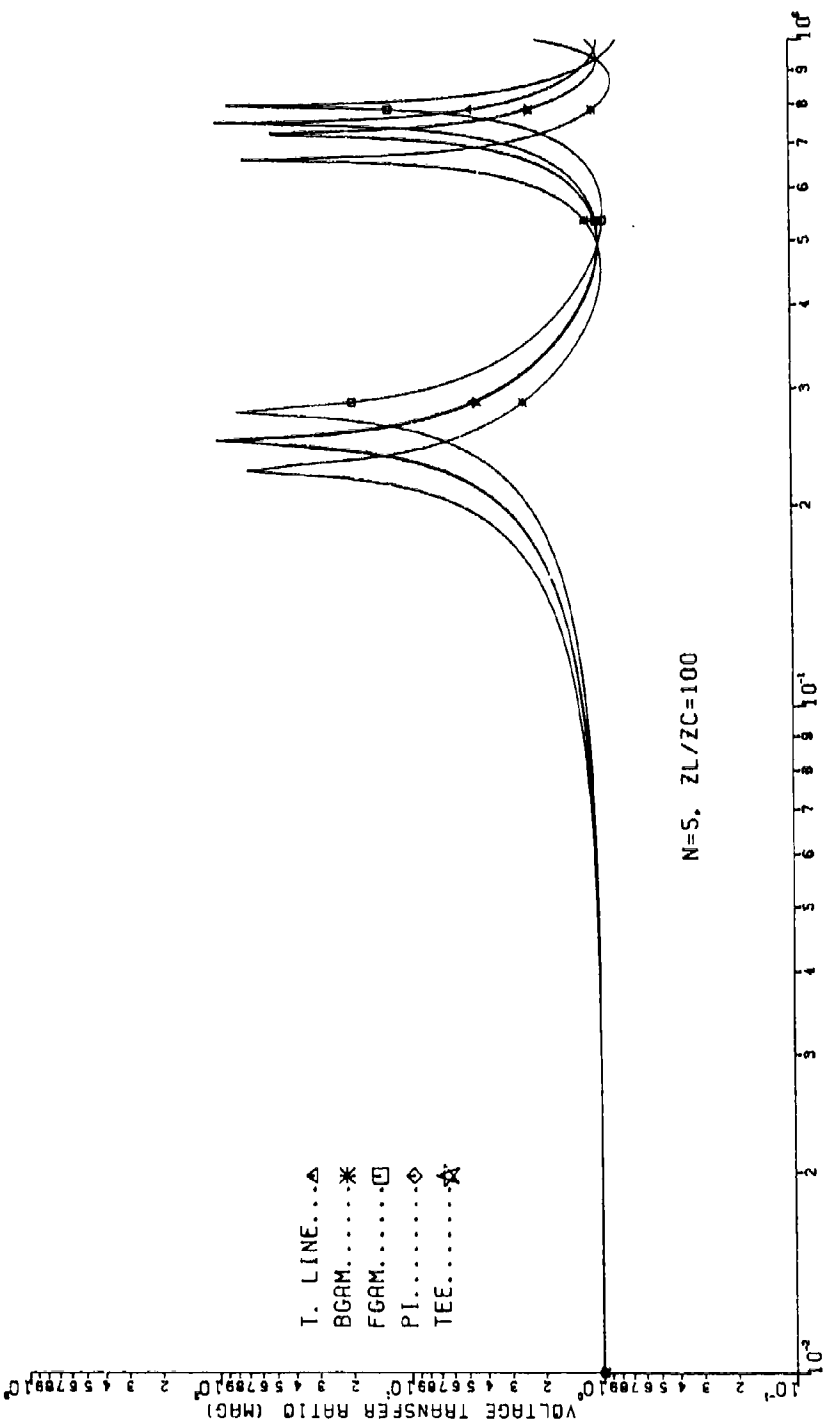
T. LINE...
BGAM.....
FGAM.....
PI.....
TEE.....
N=5, ZL/ZC=100
VOLTAGE TRANSFER RATIO (MAG)
LINE LENGTH/WAVELENGTH

Figure A-12

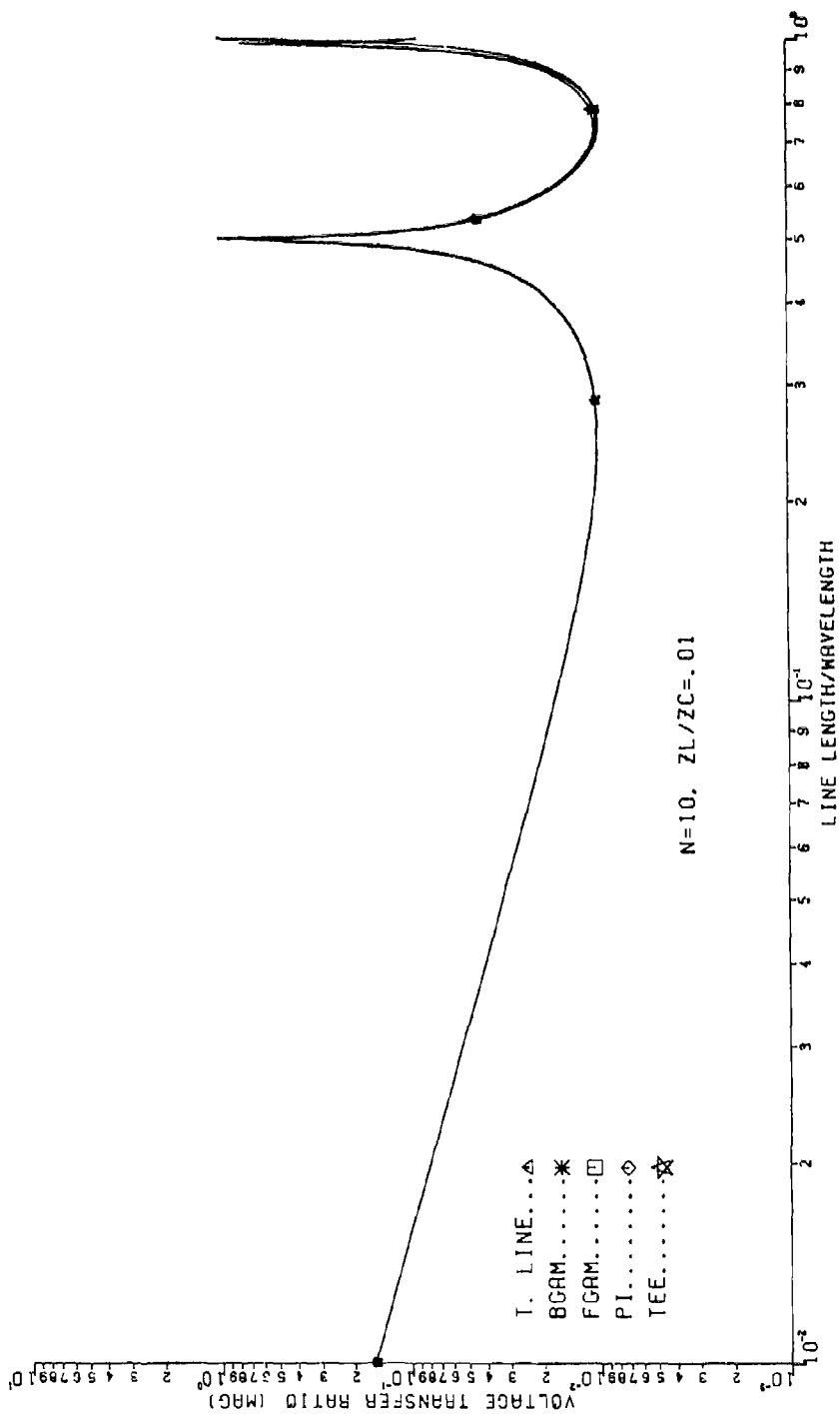
T. LINE...
BGAM.....
FGAM.....
PI.....
TEE.....
N=10. ZL/ZC=.01
VOLTAGE TRANSFER RATIO (MAG)
LINE LENGTH/WAVELENGTH

Figure A-13

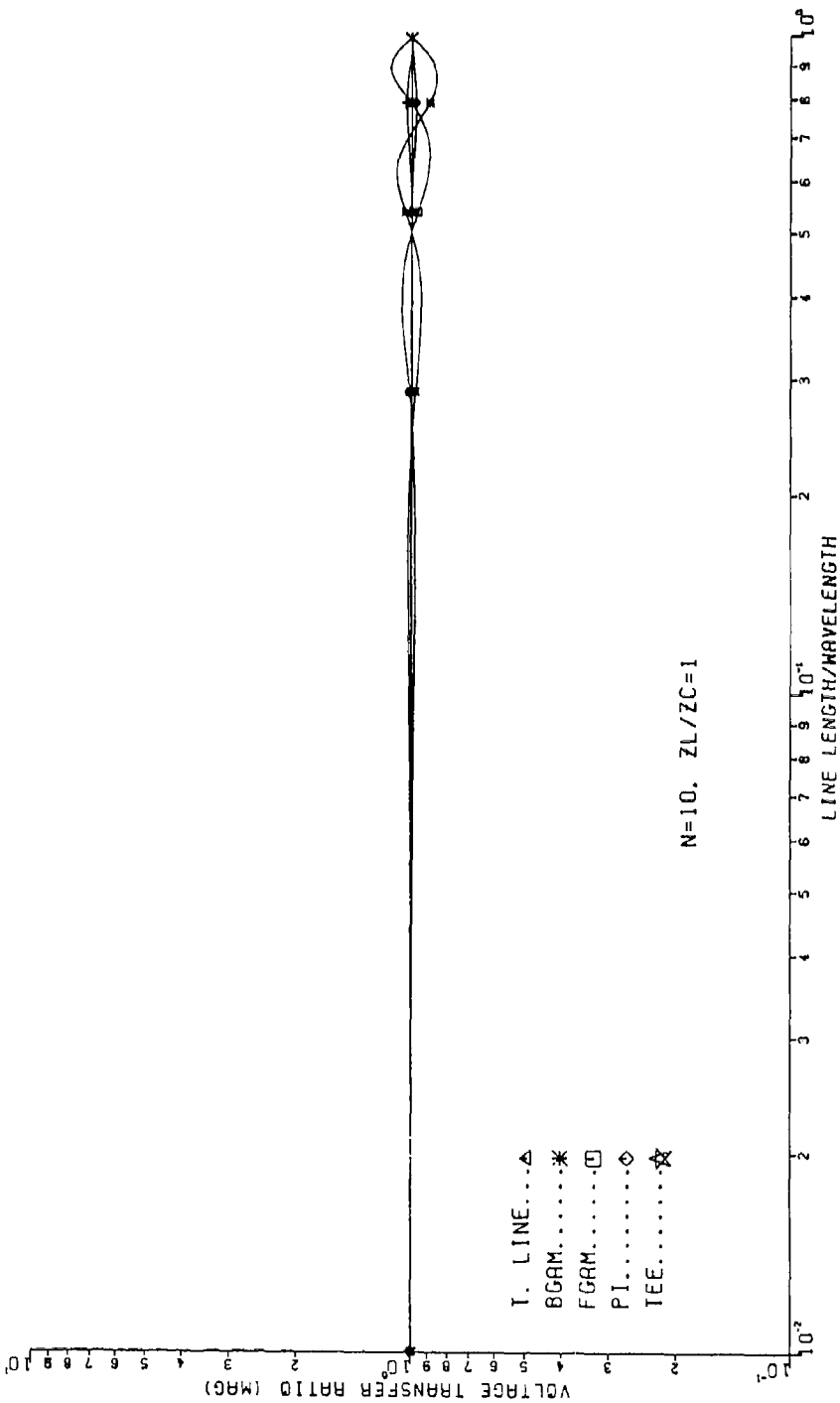
VOLTAGE TRANSFER RATIO (MAG)
LINE LENGTH/WAVELENGTH
N=10. ZL/ZC=1
T. LINE
BGAM
FGAM
PI
TEE

Figure A-14

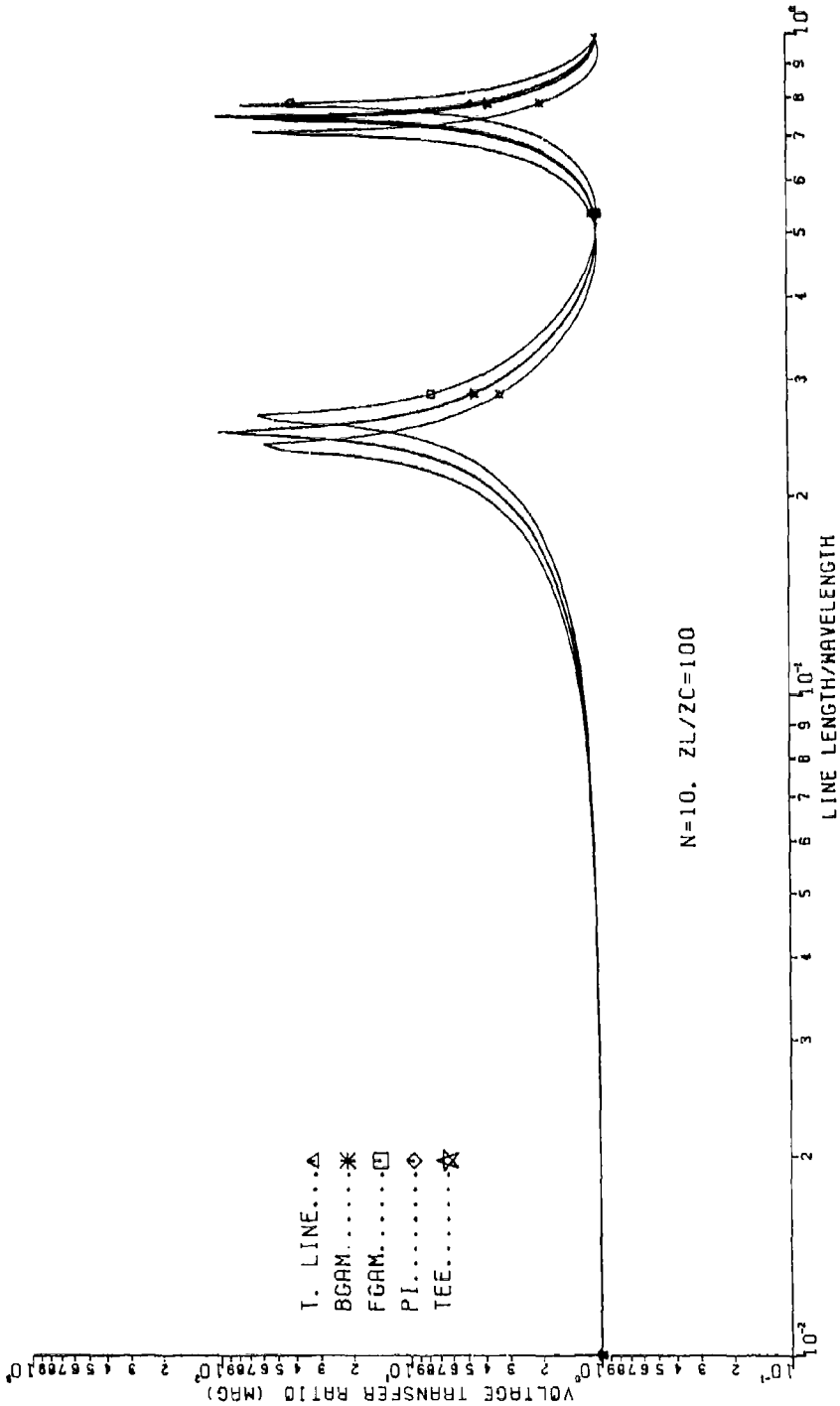
T. LINE...
BGAM.....
FGAM.....
PI.....
TEE.....
VOLTAGE TRANSFER RATIO (MAG)
N=10. ZL/ZC=100
LINE LENGTH/WAVELENGTH

Figure A-15

APPENDIX B

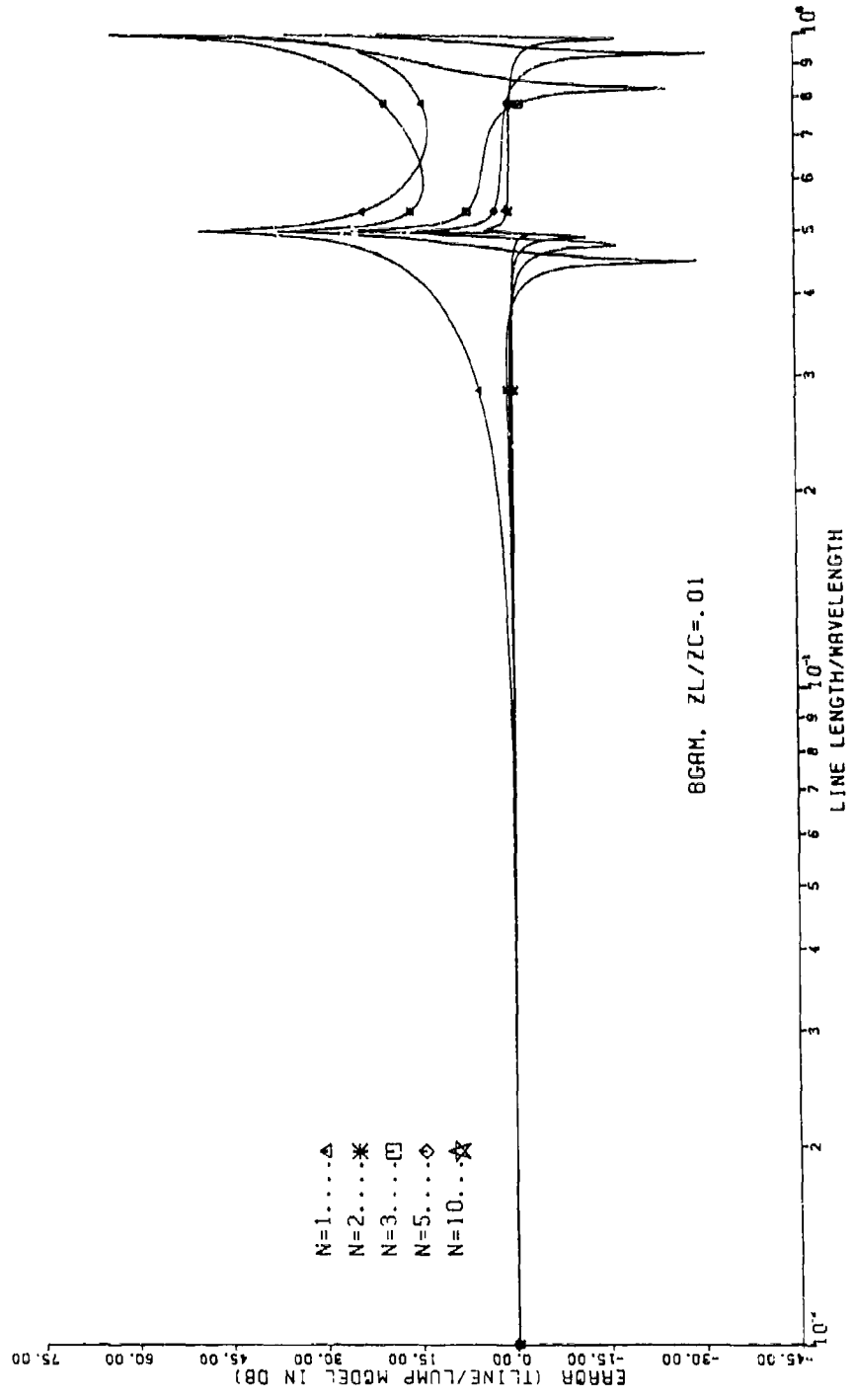

Figure B-1

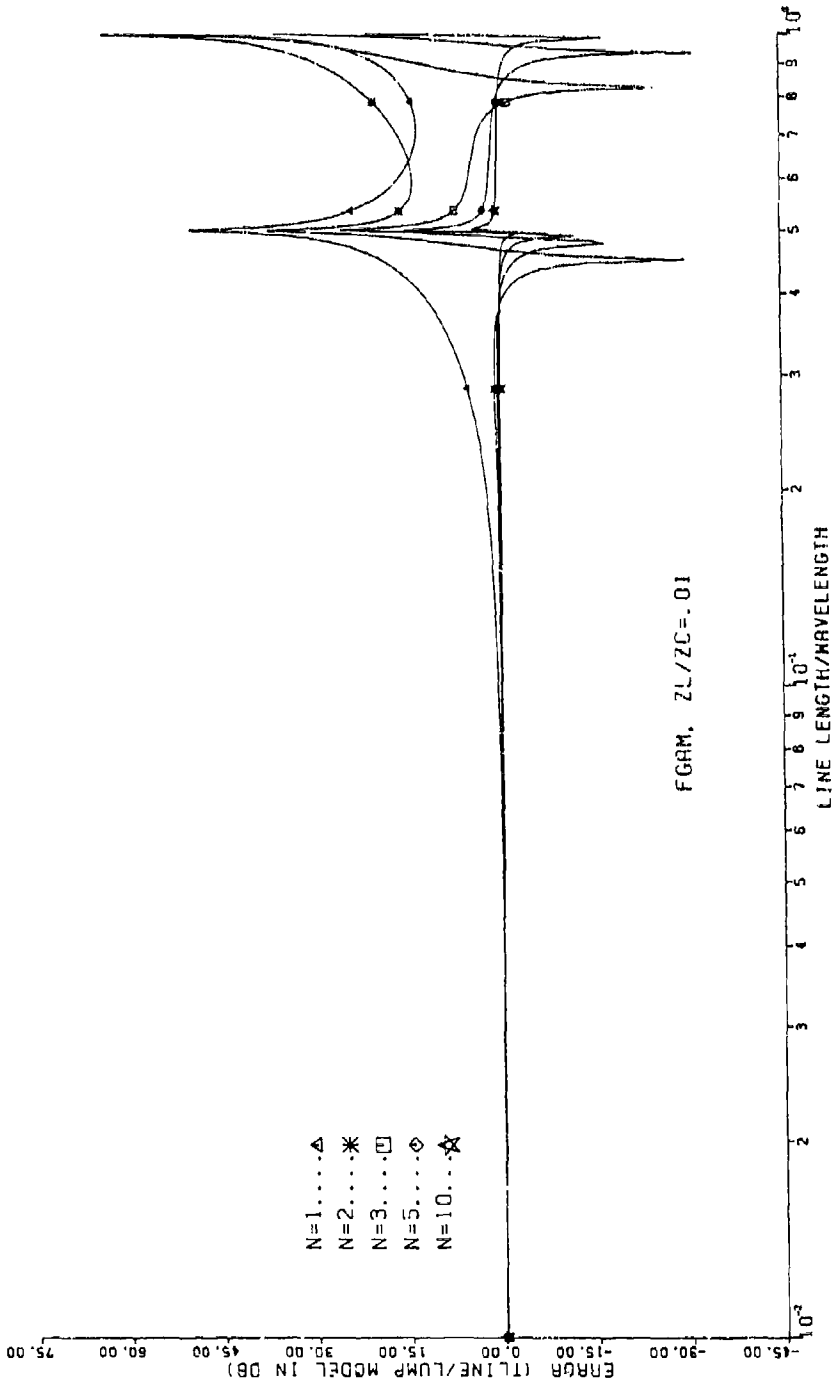
ERROR (TLINE/LUMP MODEL IN DB)
75.00
60.00
45.00
30.00
15.00
0.00
-15.00
-30.00
-45.00
N=1.....
N=2.....
N=3.....
N=5.....
N=10....
FGAM, ZL/ZC=.01
LINE LENGTH/WAVELENGTH

Figure B-2

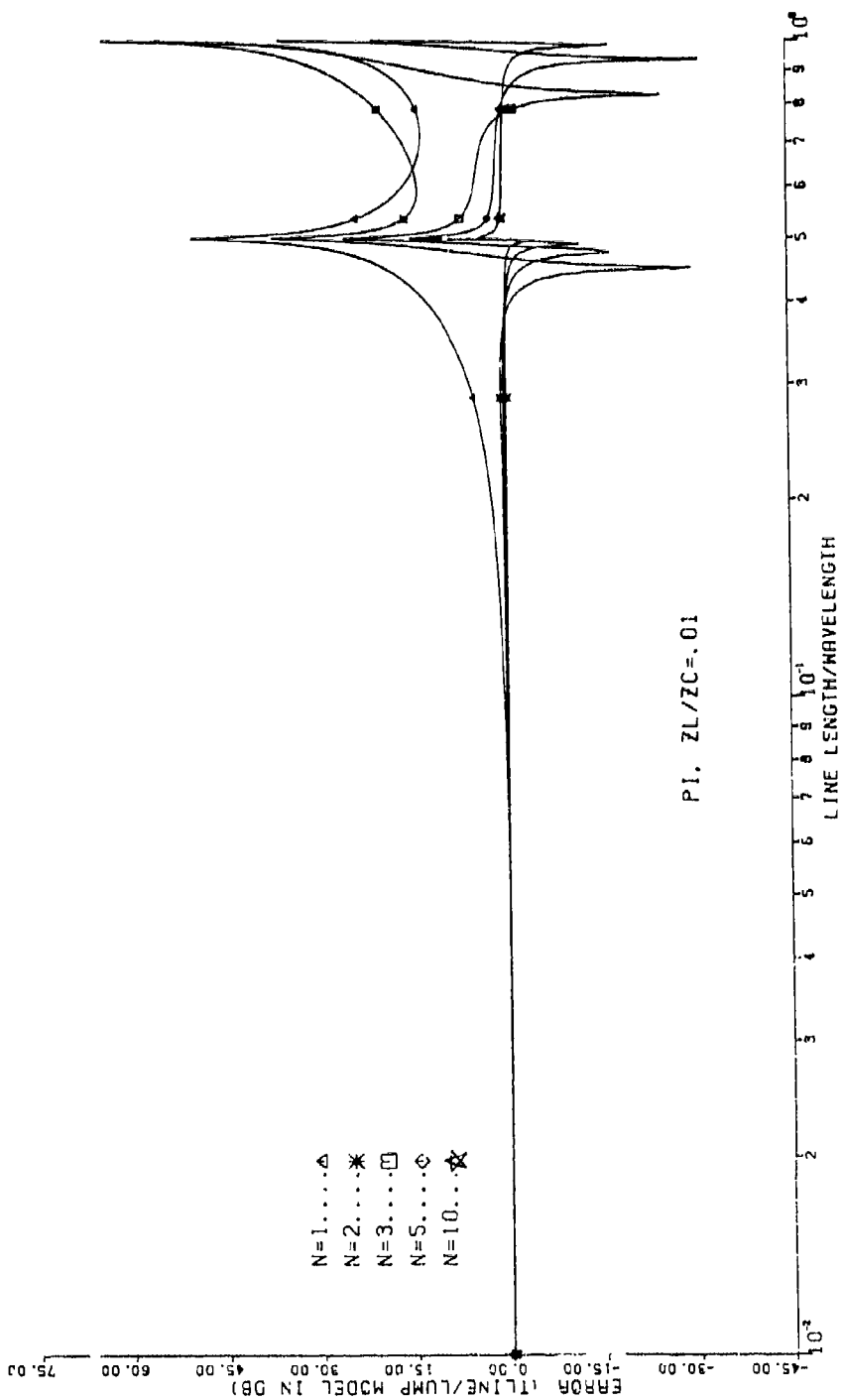
ERROR (LINE/LUMP MODEL IN DB)
75.00
60.00
45.00
30.00
15.00
0.00
-15.00
-30.00
-45.00
LINE LENGTH/WAVELENGTH
10^{-2}
10^{-1}
10^{0}
N=1....
N=2....
N=3....
N=5....
N=10...
PI, ZL/ZC=.01

Figure B-3

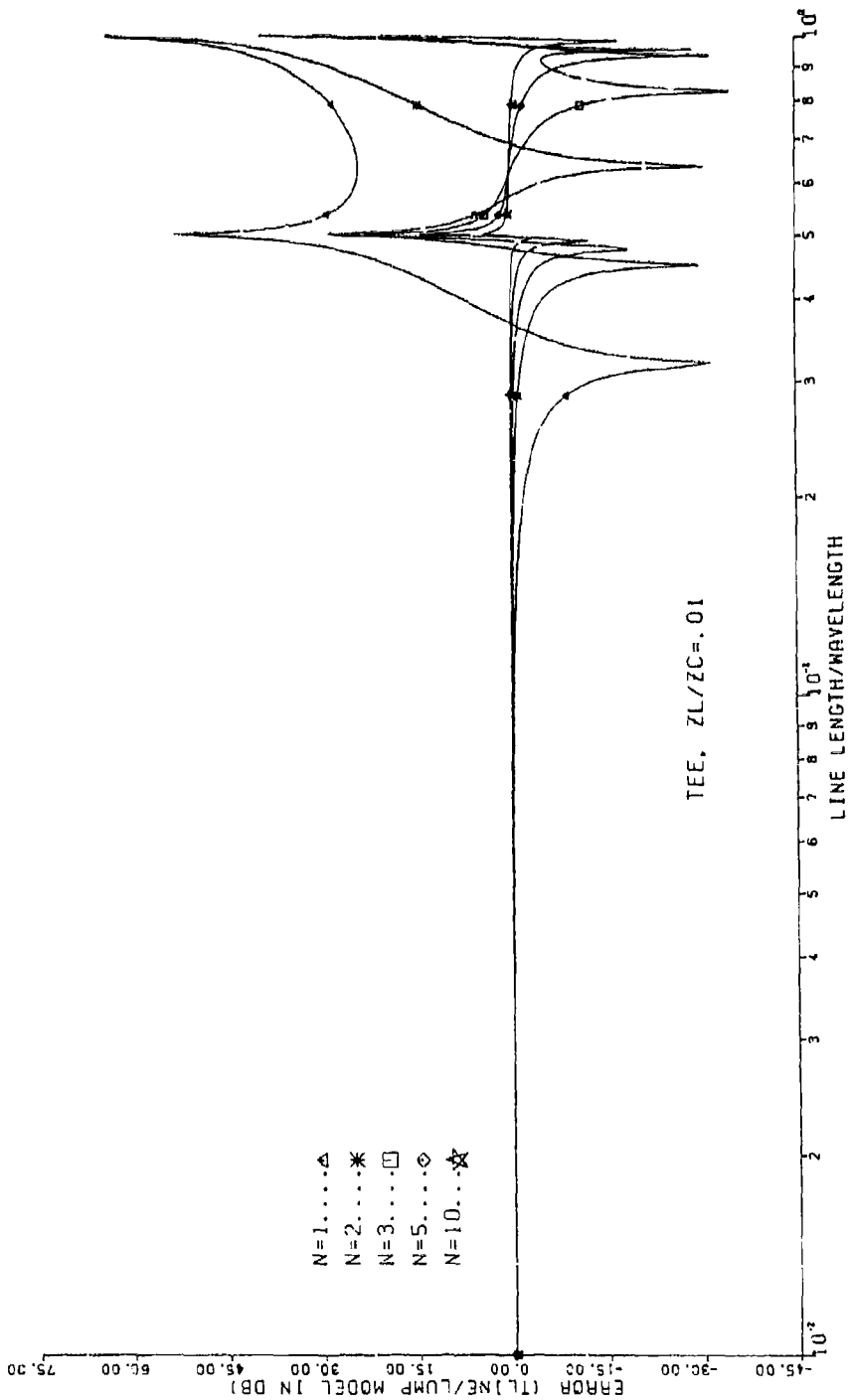
ERROR (TL)NE/LUMP MODEL IN DB)
-45.00
-30.00
-15.00
0.00
15.00
30.00
45.00
60.00
75.00
LINE LENGTH/WAVELENGTH
TEE, ZL/ZC=.01
N=1
N=2
N=3
N=5
N=10

Figure B-4

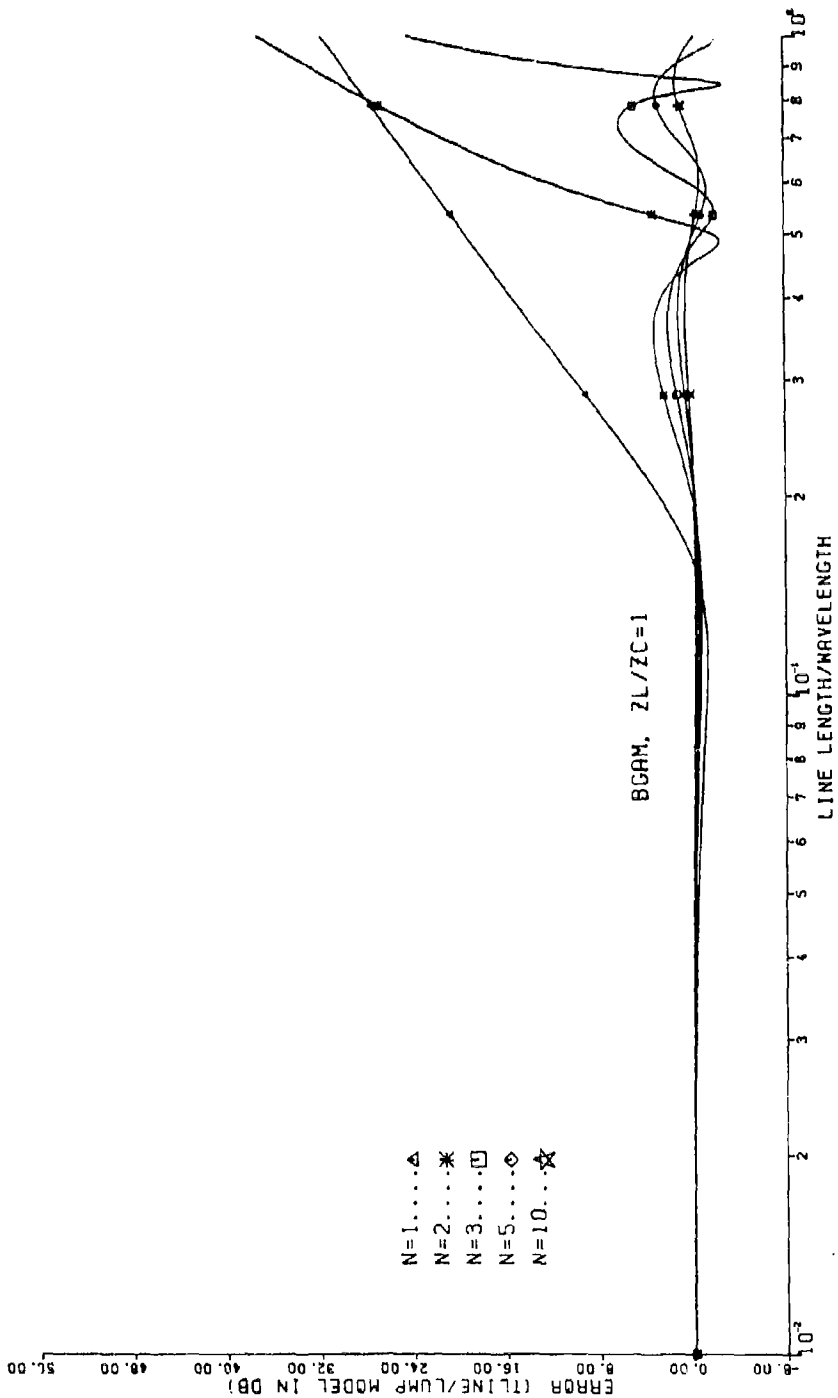
BGAM, ZL/ZC=1
N=1.....
N=2.....
N=3.....
N=5.....
N=10.....
ERROR (LINE/LUMP MODEL IN DB)
LINE LENGTH/WAVELENGTH

Figure B-5

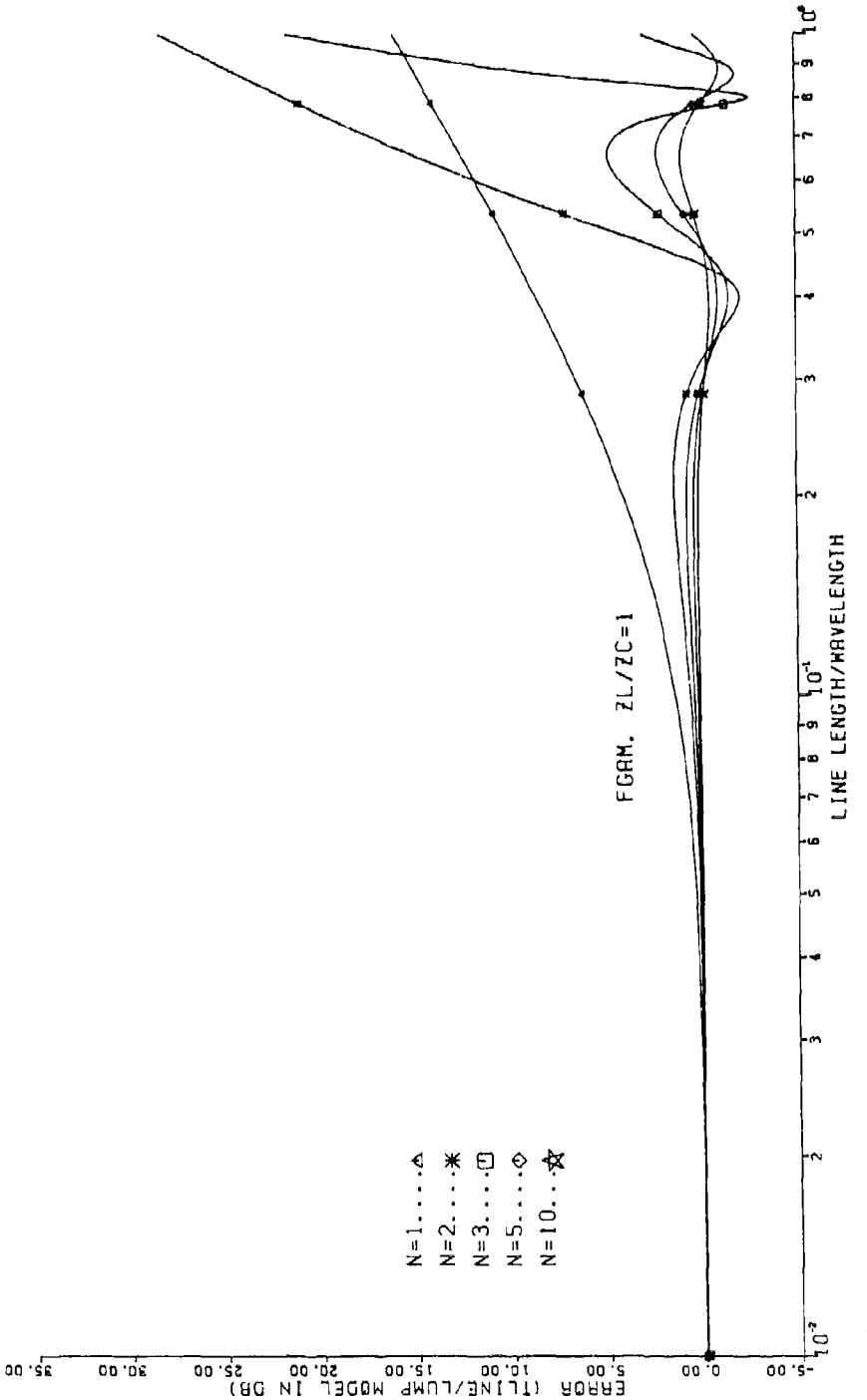
ERROR (TLINE/LUMP MODEL IN DB)
35.00
30.00
25.00
20.00
15.00
10.00
5.00
0.00
-5.00
10^{-2}
2
3
4
5
6
7
8
9
10^{-1}
2
3
4
5
6
7
8
9
10^{0}
LINE LENGTH/WAVELENGTH
FGAM. ZL/ZC=1
N=1....△
N=2....✳
N=3....□
N=5....◇
N=10...☆

Figure B-6

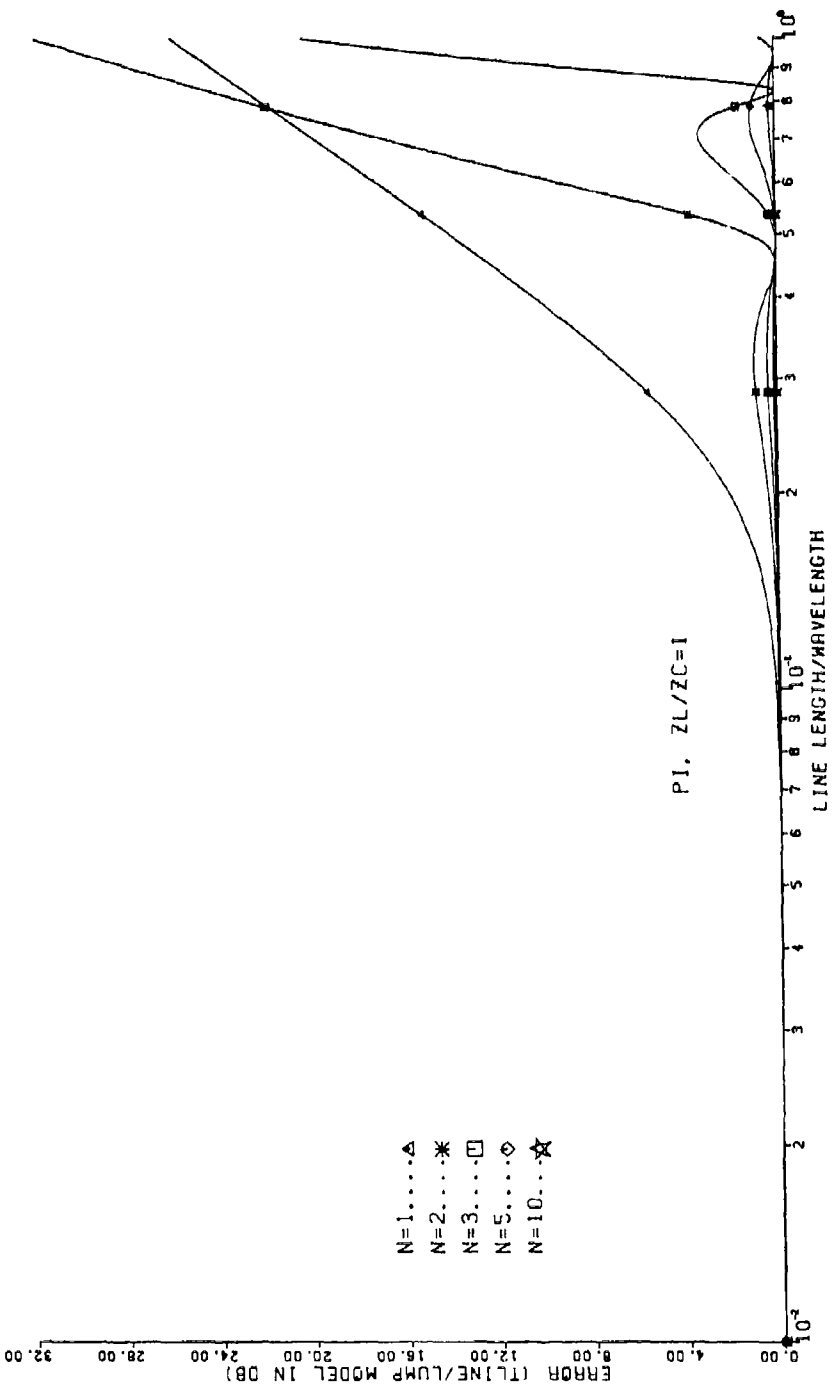
ERROR (LINE/LUMP MODEL IN DB)
0.00
4.00
8.00
12.00
16.00
20.00
24.00
28.00
32.00
LINE LENGTH/WAVELENGTH
PI, ZL/ZC=1
N=1
N=2
N=3
N=5
N=10

Figure B-7

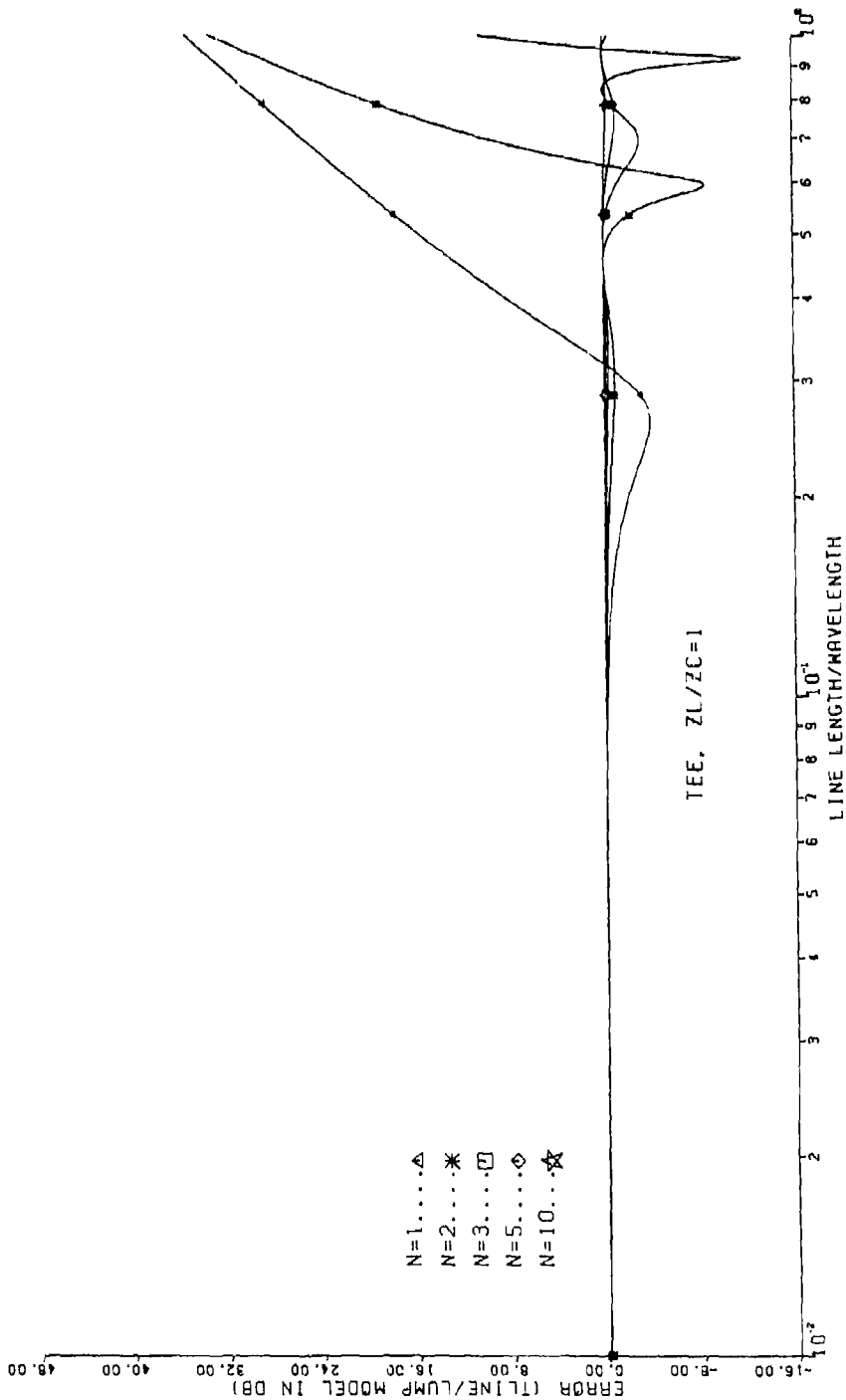
ERROR (TLINE/LUMP MODEL IN DB)
48.00
40.00
32.00
24.00
16.00
8.00
0.00
-8.00
-16.00
LINE LENGTH/WAVELENGTH
10^{-2}
10^{-1}
10^{0}
TEE, ZL/ZC=1
N=1
N=2
N=3
N=5
N=10

Figure B-8

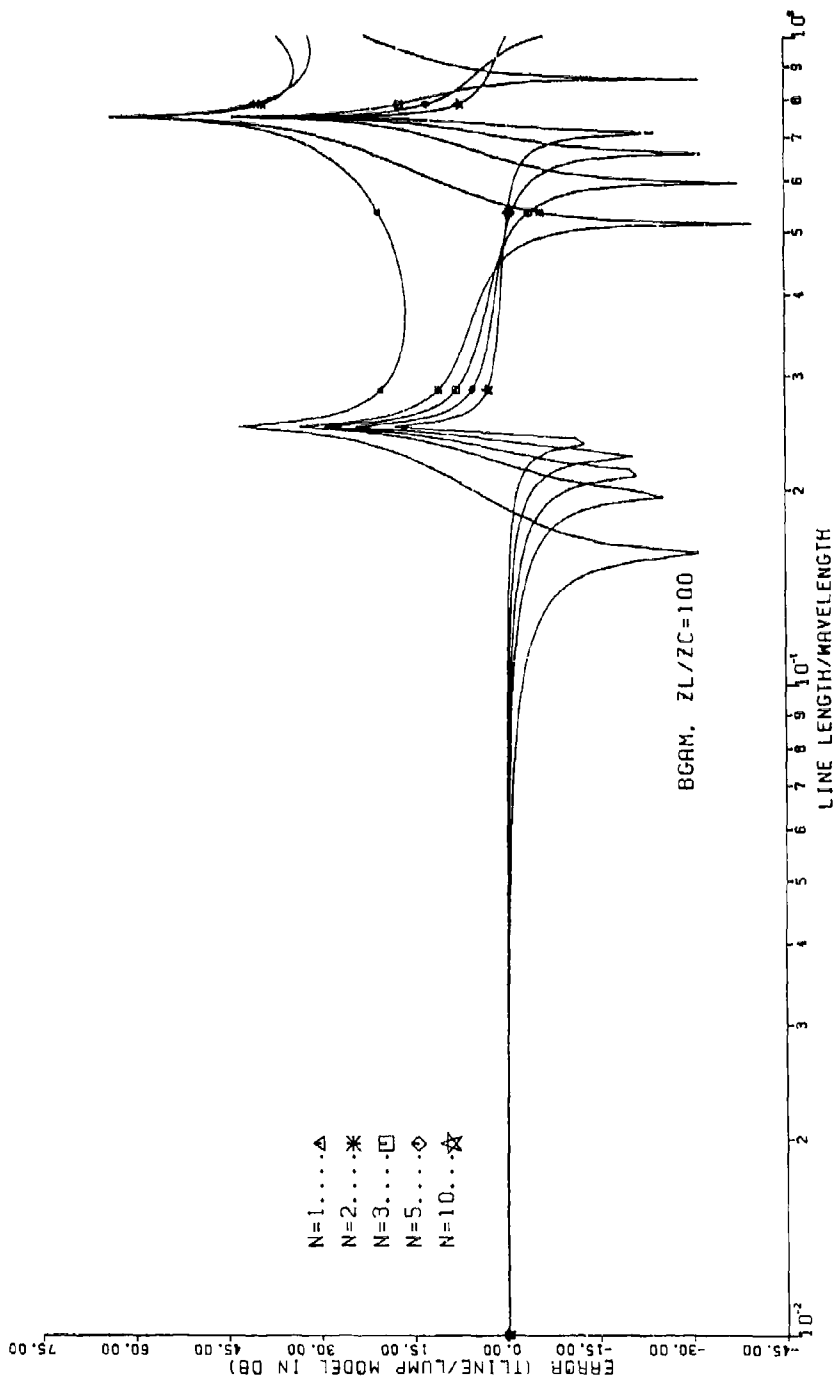
ERROR (TLINE/LUMP MODEL IN DB)
75.00
60.00
45.00
30.00
15.00
0.00
-15.00
-30.00
-45.00
10^{-2}
2
3
4
5
6
7
8
9
10^{-1}
2
3
4
5
6
7
8
9
10^{0}
LINE LENGTH/WAVELENGTH
BEAM, ZL/ZC=100
N=1....
N=2....
N=3....
N=5....
N=10...

Figure B-9

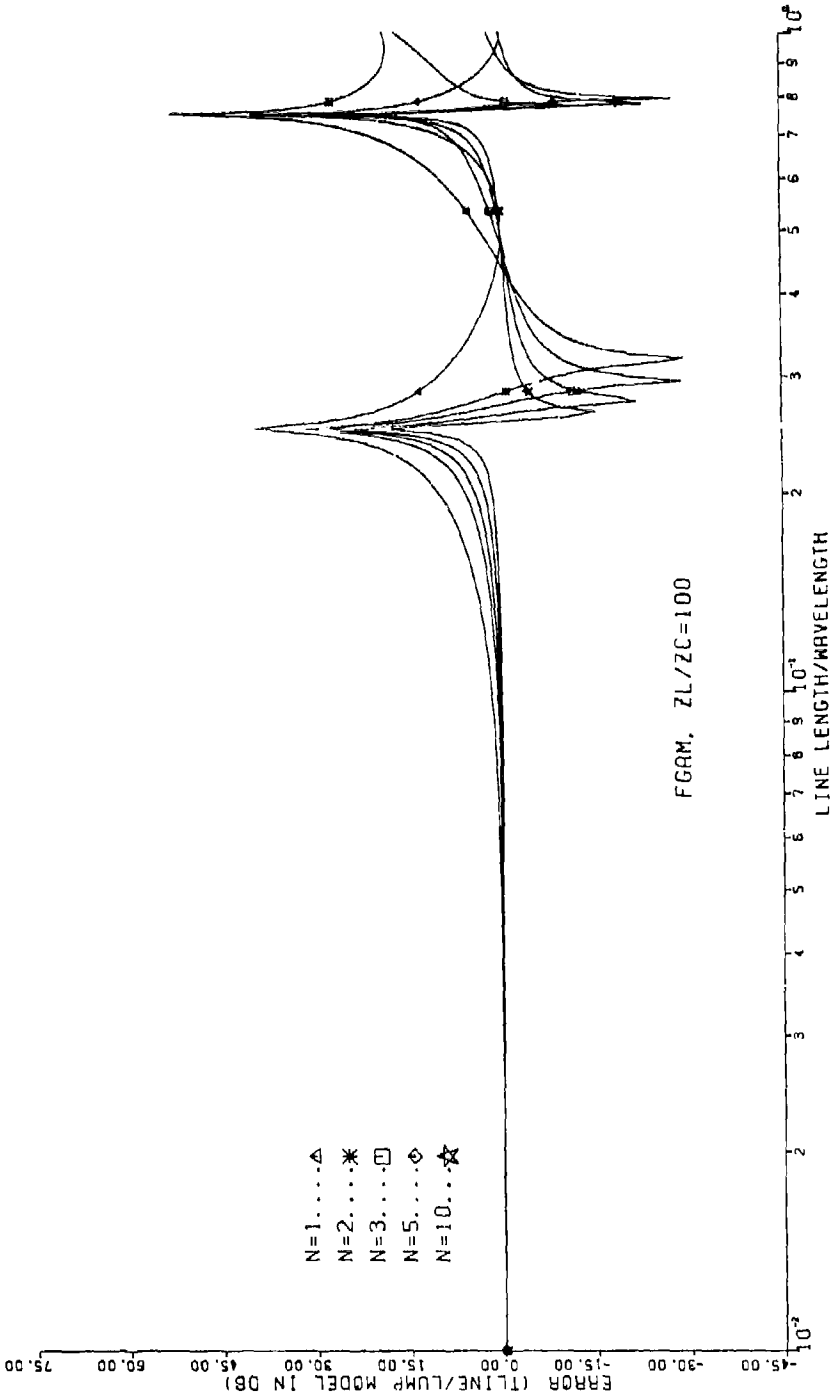
ERROR (TLINE/LUMP MODEL IN DB)
75.00
60.00
45.00
30.00
15.00
0.00
-15.00
-30.00
-45.00
10^{-2}
10^{-1}
10^{0}
LINE LENGTH/WAVELENGTH
N=1....
N=2....
N=3....
N=5....
N=10...
FGAM, ZL/ZC=100

Figure 8-10

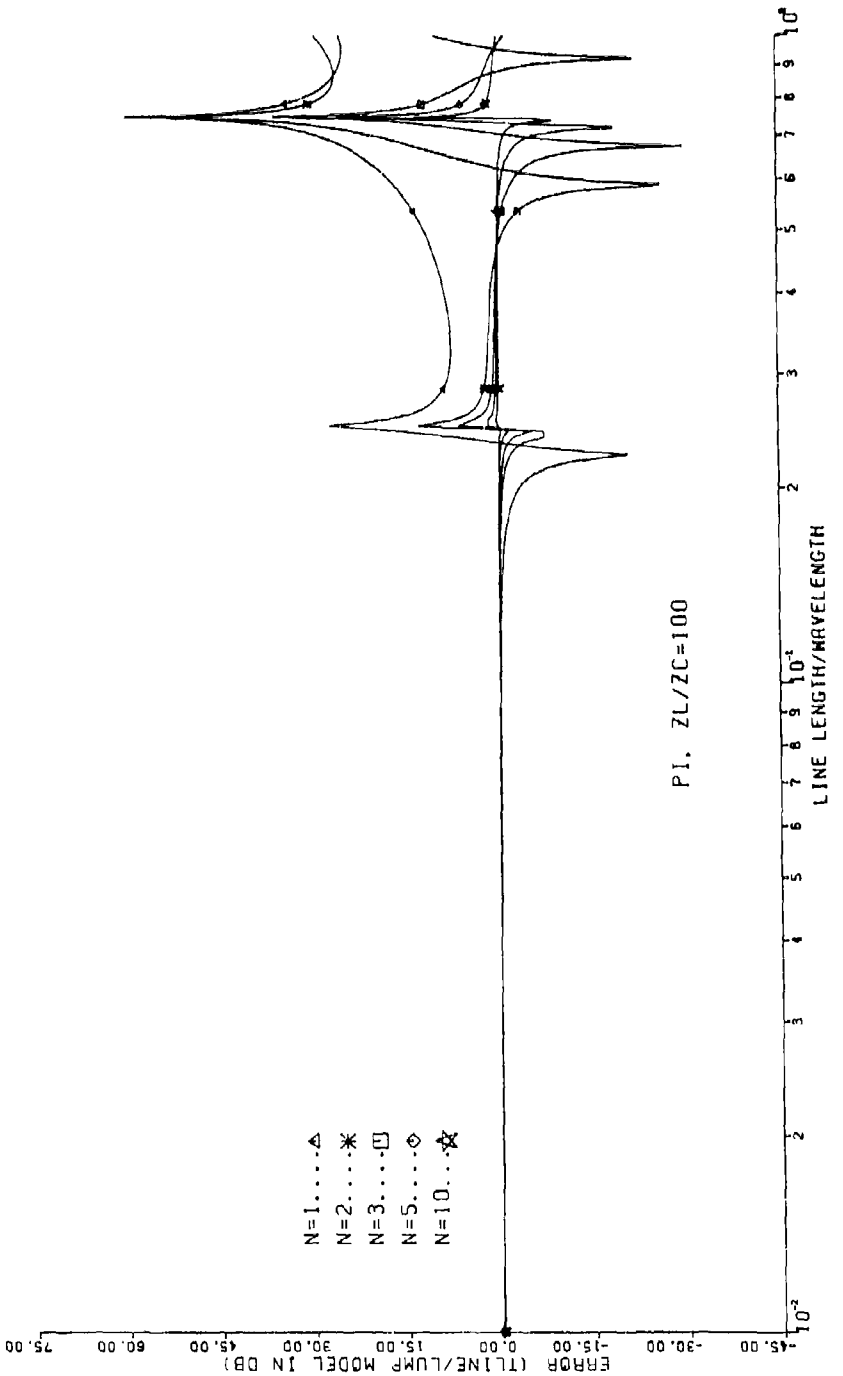
ERROR (TLINE/LUMP MODEL IN DB)
75.00
60.00
45.00
30.00
15.00
0.00
-15.00
-30.00
-45.00
N=1....
N=2....
N=3....
N=5....
N=10...
LINE LENGTH/WAVELENGTH
PI, ZL/ZC=100

Figure B-11

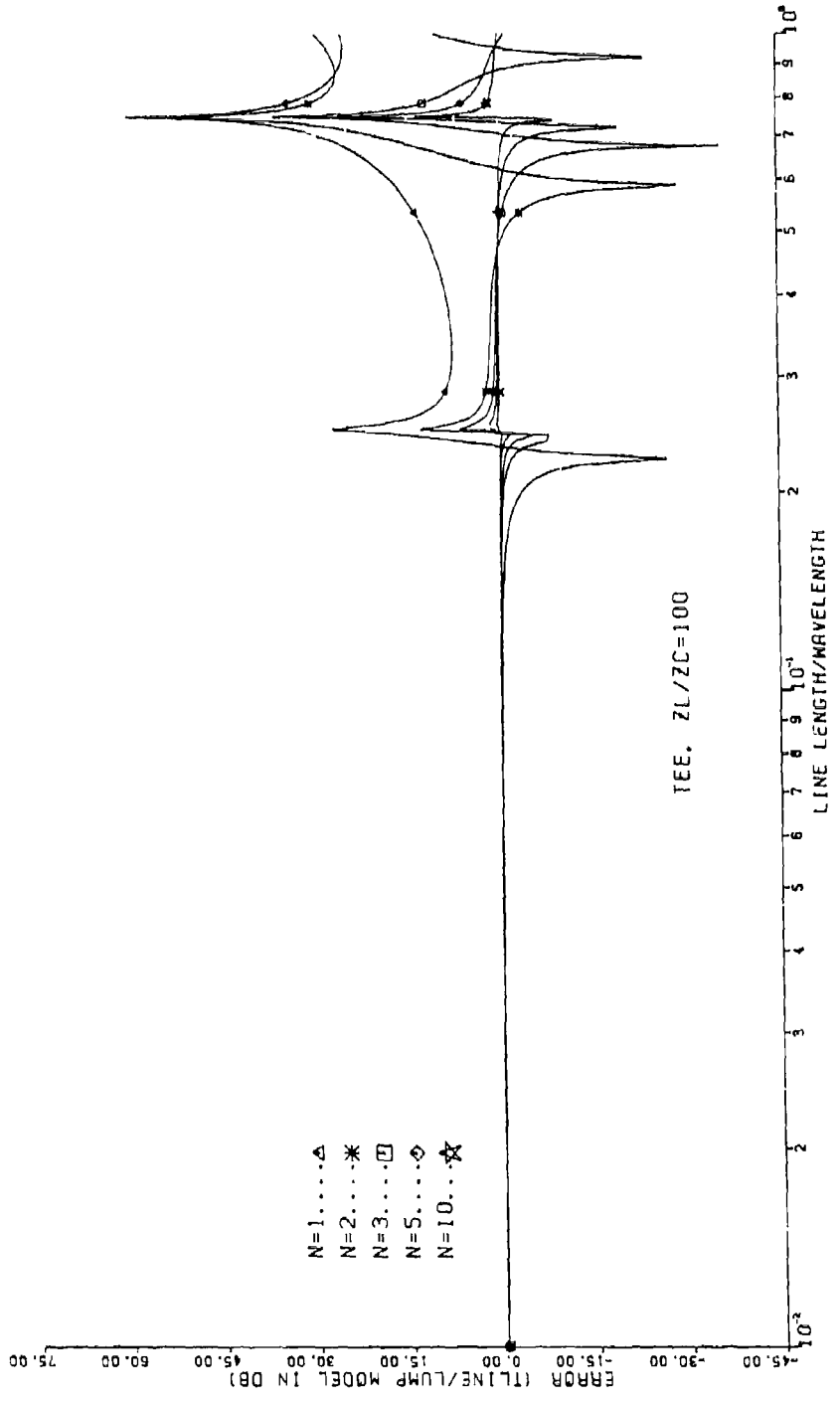
ERROR (TLINE/LUMP MODEL IN DB)
75.00
60.00
45.00
30.00
15.00
0.00
-15.00
-30.00
-45.00
10^{-2}
10^{-1}
10^{0}
LINE LENGTH/WAVELENGTH
TEE, ZL/ZC=100
N=1.
N=2.
N=3.
N=5.
N=10.

Figure B-12

APPENDIX C

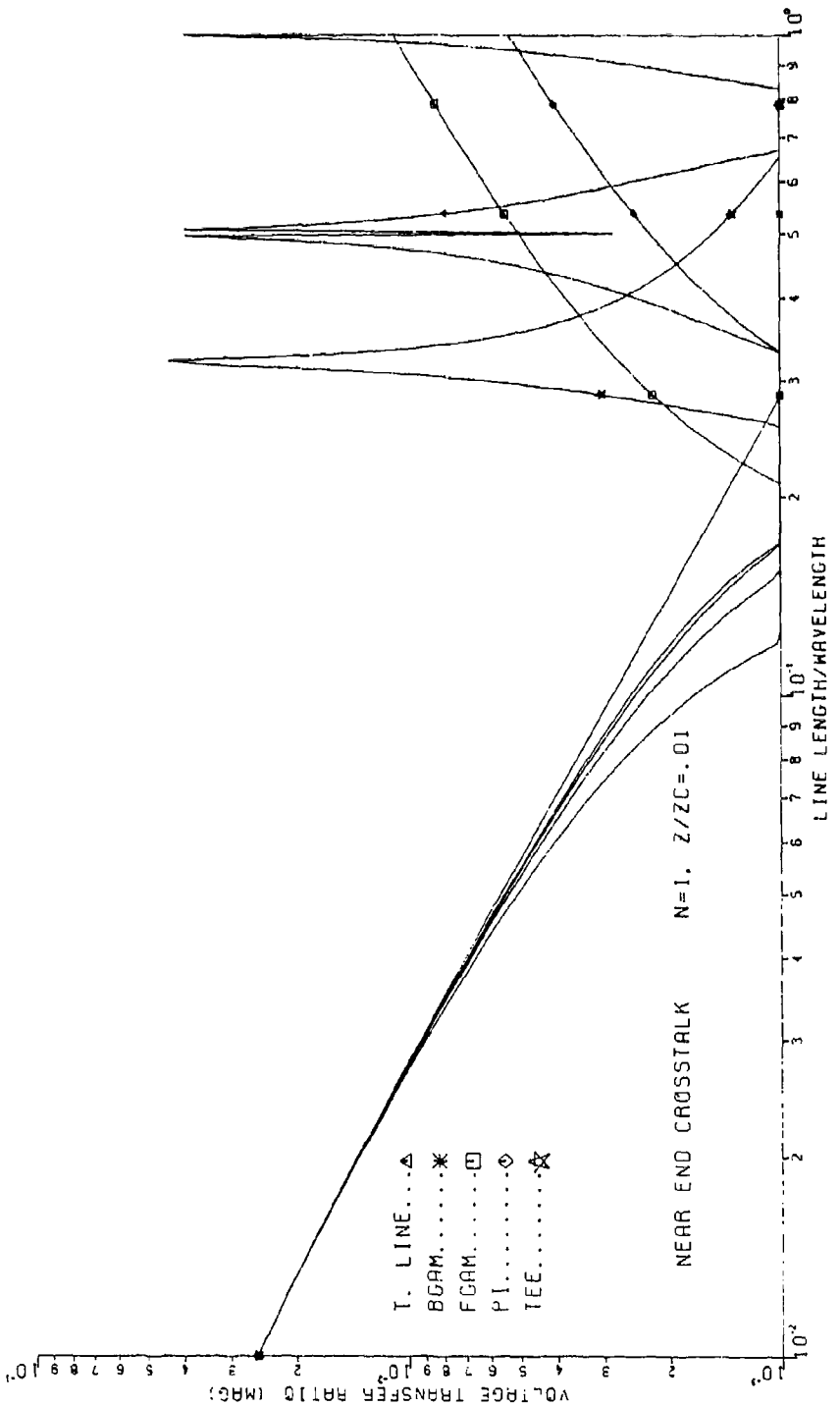

Figure C-1

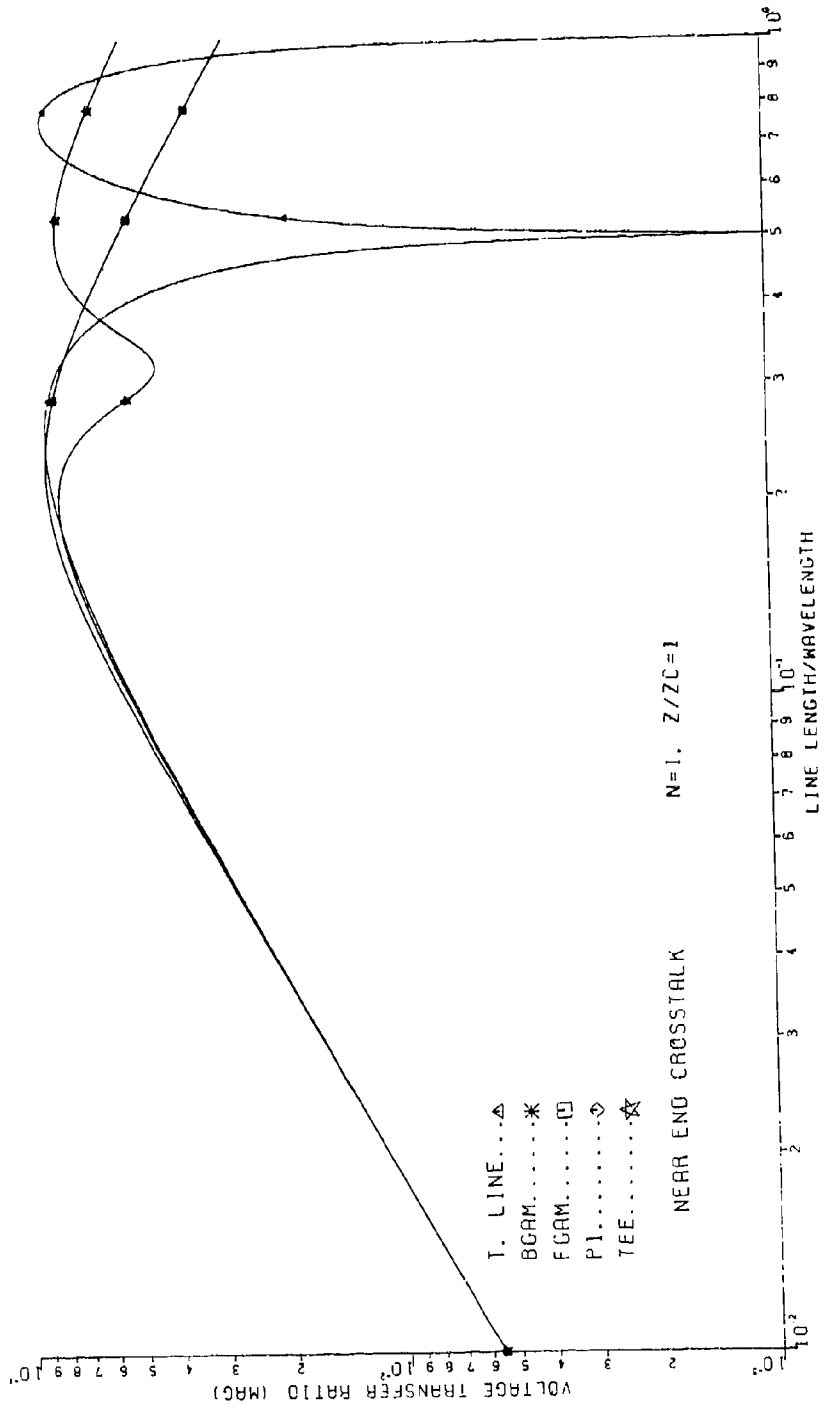
T. LINE...
BGAM.....
F.GAM.....
P1.....
TEE.....
NEAR END CROSSTALK
N=1, Z/ZC=1
LINE LENGTH/WAVELENGTH
VOLTAGE TRANSFER RATIO (MAG)

Figure C-2

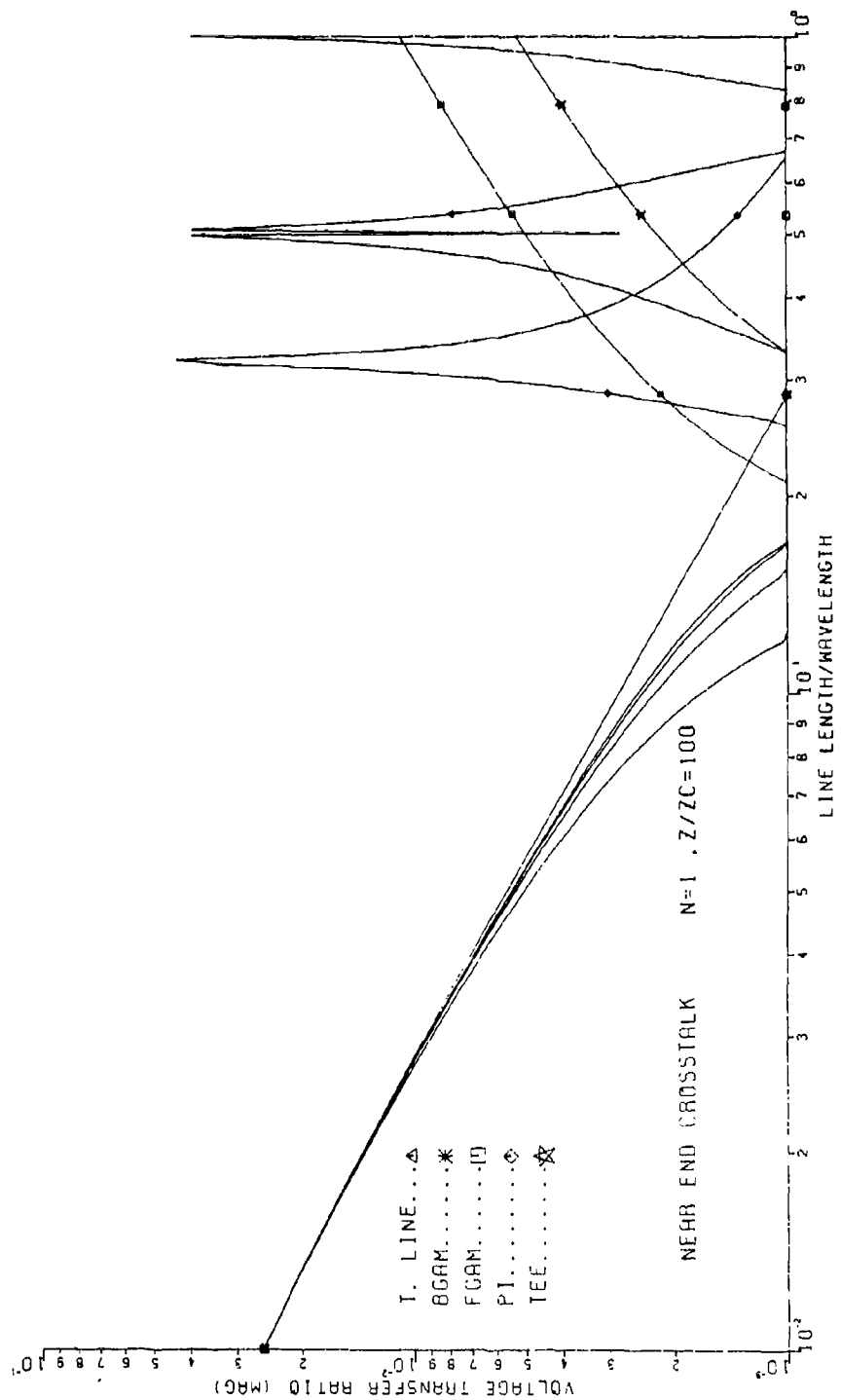
VOLTAGE TRANSFER RATIO (MAG)
LINE LENGTH/WAVELENGTH
NEAR END CROSSTALK
N=1 , Z/ZC=100
T. LINE...
BGAM.....
FGAM.....
PI.....
TEE.....

Figure C-3

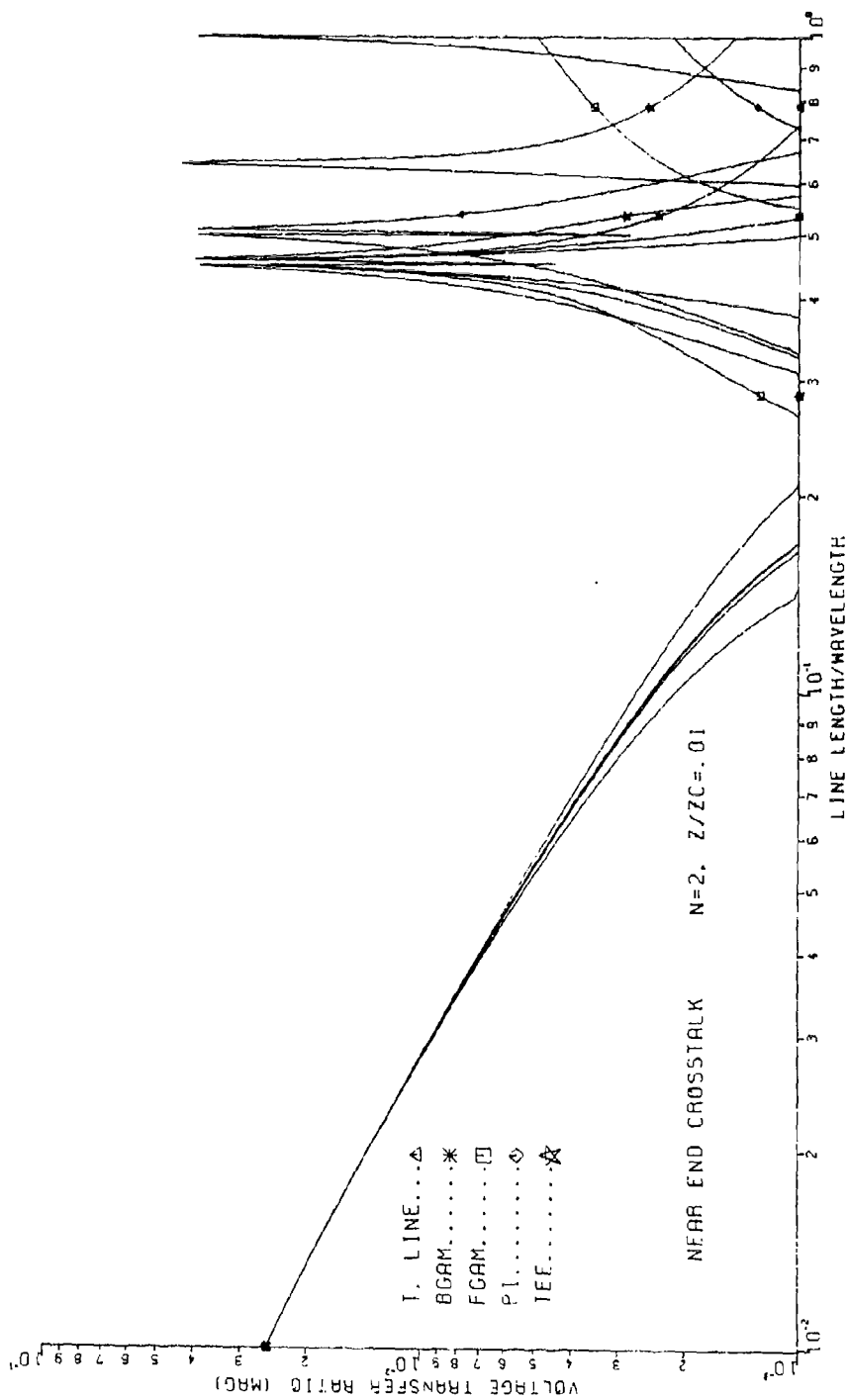
VOLTAGE TRANSFER RATIO (MAG)
LINE LENGTH/WAVELENGTH
NEAR END CROSSTALK N=2. Z/ZC=.01
I. LINE...
BGAM.....
FGAM.....
PI.....
TEE.....

Figure C-4

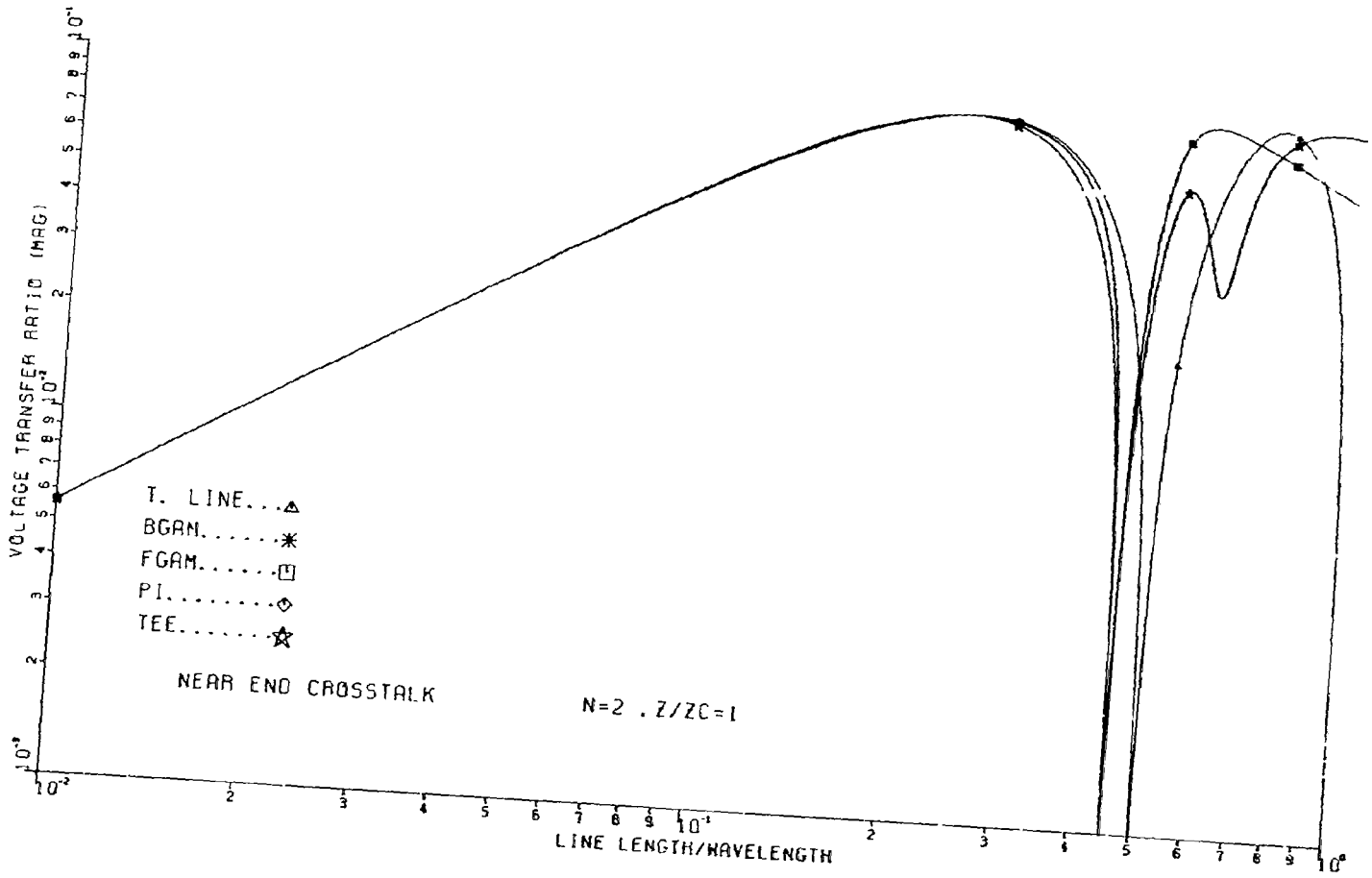
VOLTAGE TRANSFER RATIO (MAG)
T. LINE...
BGAM.....
FGAM.....
PI.....
TEE.....
NEAR END CROSSTALK
N=2 . Z/ZC=1
LINE LENGTH/WAVELENGTH

Figure C-5

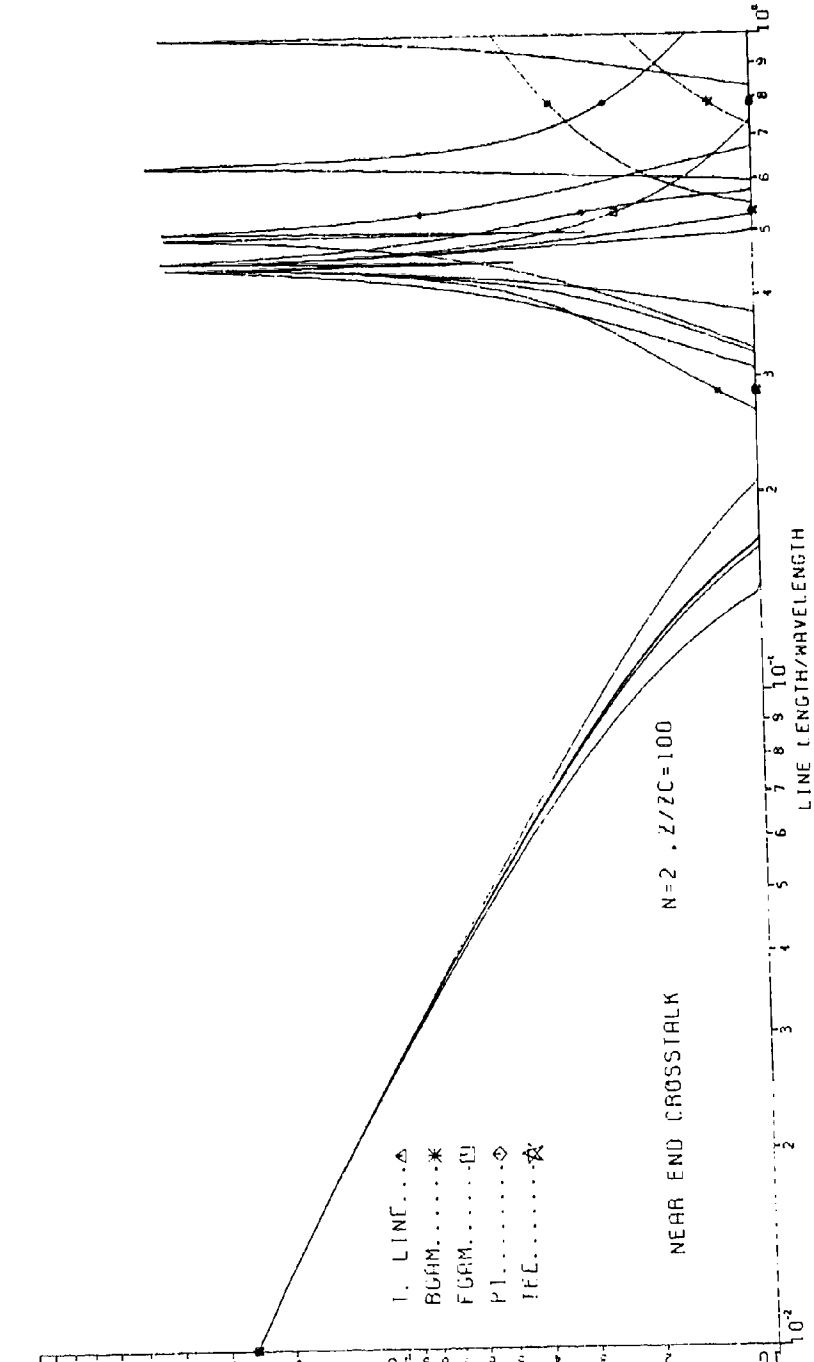
VOLTAGE TRANSFER RATIO (MAG)
LINE LENGTH/WAVELENGTH
NEAR END CROSSTALK
N=2 , Z/ZC=100
T. LINE...
BUHM.....
FORM.....
PI.....
IEE.....

Figure C-6

T. LINE
BGAM
FGAM
PI
IEE
N=3. Z/ZC=.01
NEAR END CROSSTALK
LINE LENGTH/WAVELENGTH
VOLTAGE TRANSFER RATIO (MAG)

Figure C-7

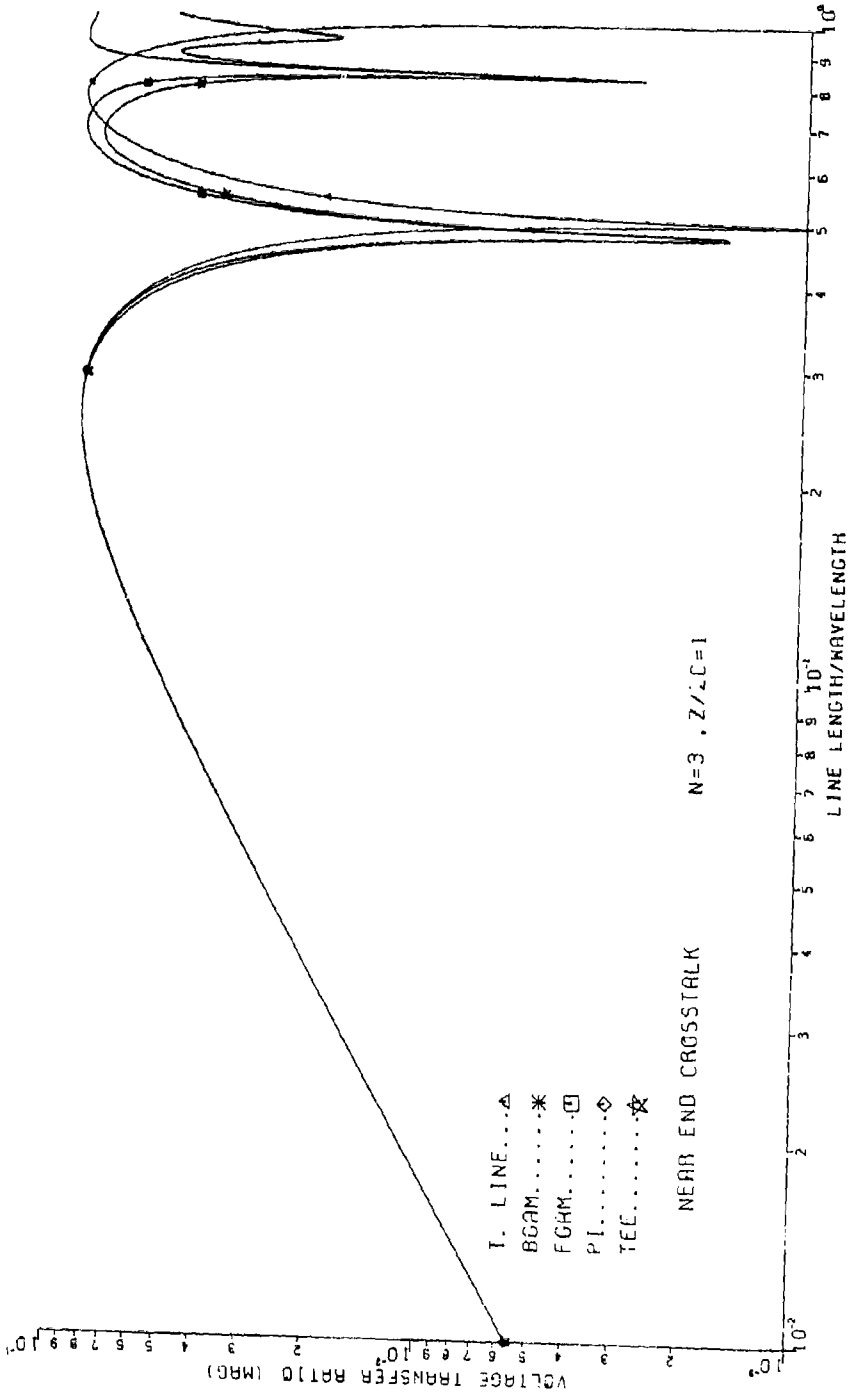
T. LINE
BGAM
FGAM
PI
TEE
NEAR END CROSSTALK
N=3 , Z/λC=1
LINE LENGTH/WAVELENGTH
VOLTAGE TRANSFER RATIO (MAG)

Figure C-8

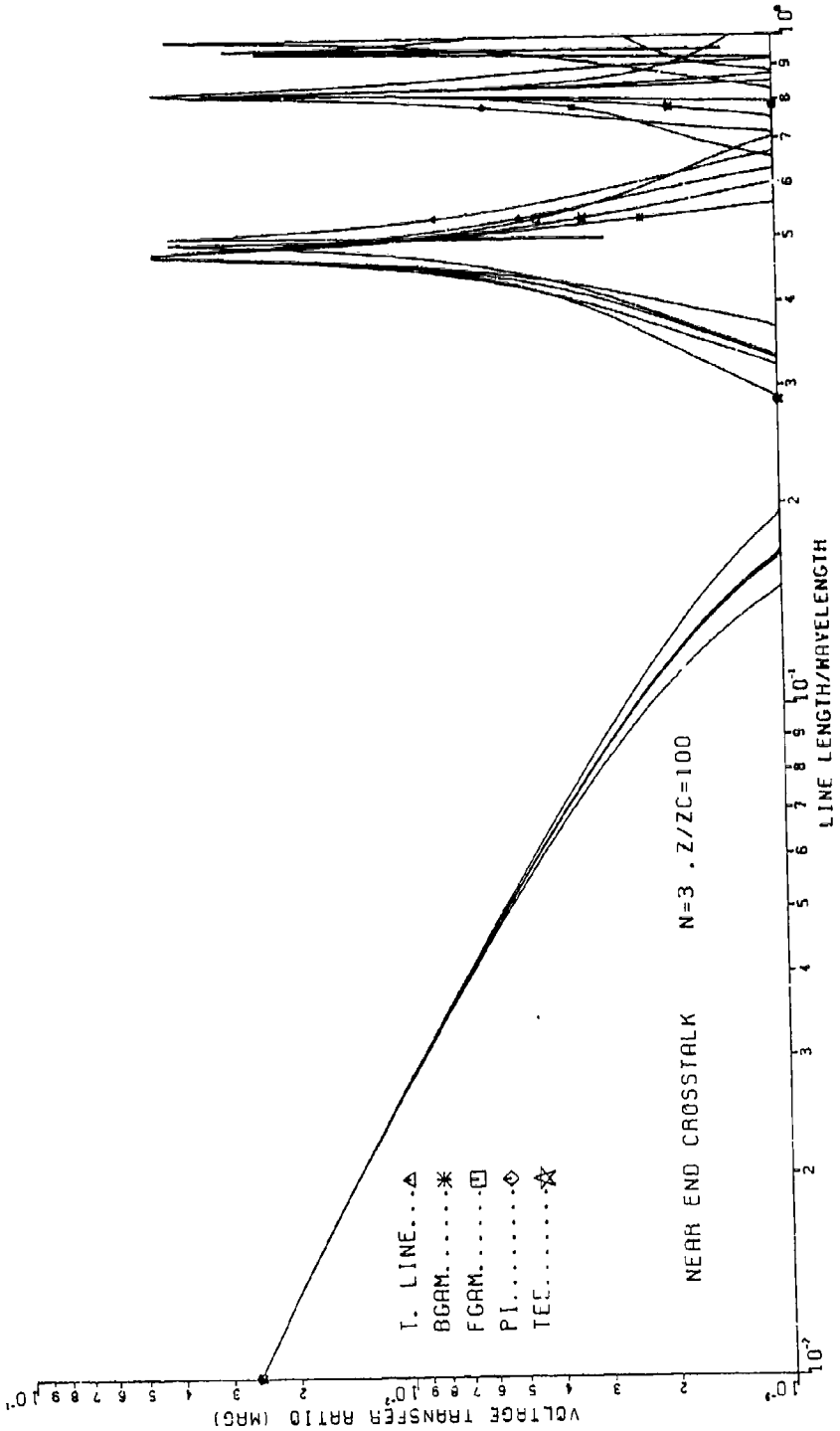
VOLTAGE TRANSFER RATIO (MAG)
LINE LENGTH/WAVELENGTH
NEAR END CROSSTALK
N=3 . Z/ZC=100
T. LINE...
BGAM.....
FGAM.....
PI.....
TEC.....

Figure C-9

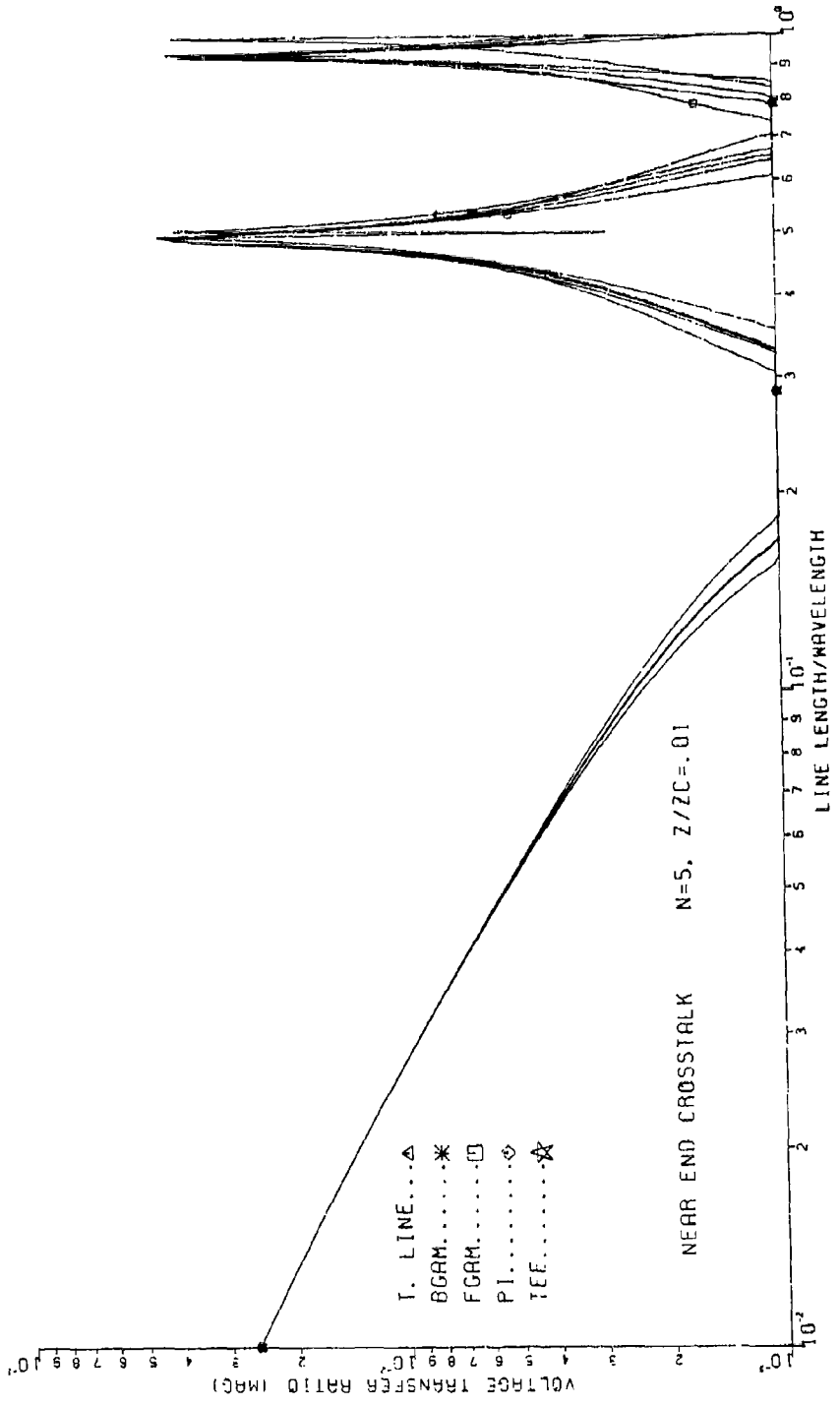
T. LINE...
BGAM.....
FGAM.....
PI.....
TEE.....
NEAR END CROSSTALK
N=5, Z/ZC=.01
LINE LENGTH/WAVELENGTH
VOLTAGE TRANSFER RATIO (MAG)

Figure C-10

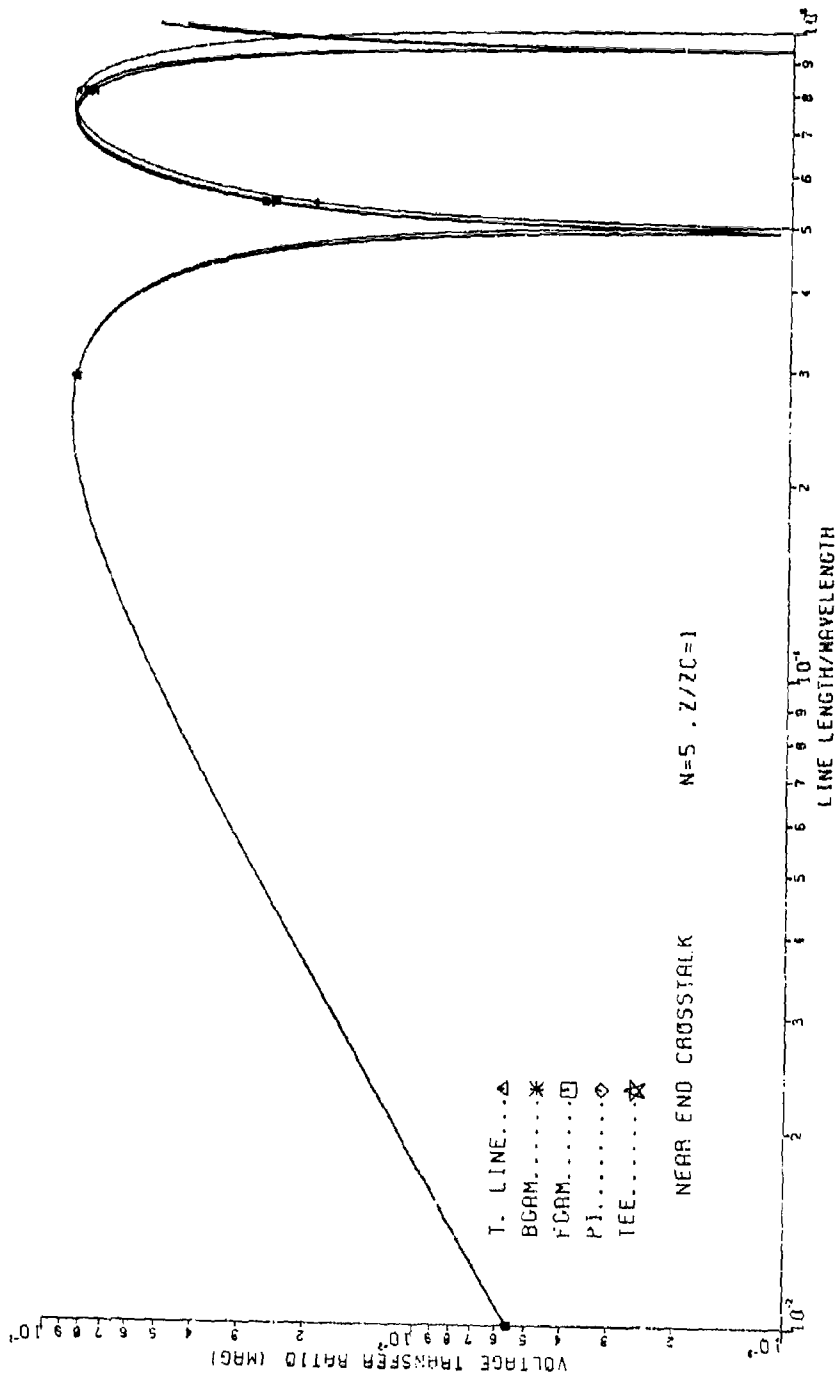
VOLTAGE TRANSFER RATIO (MAG)
LINE LENGTH/WAVELENGTH
T. LINE
BGAM
FGAM
PI
TEE
NEAR END CROSSTALK
N=5 . Z/ZC=1

Figure C-11

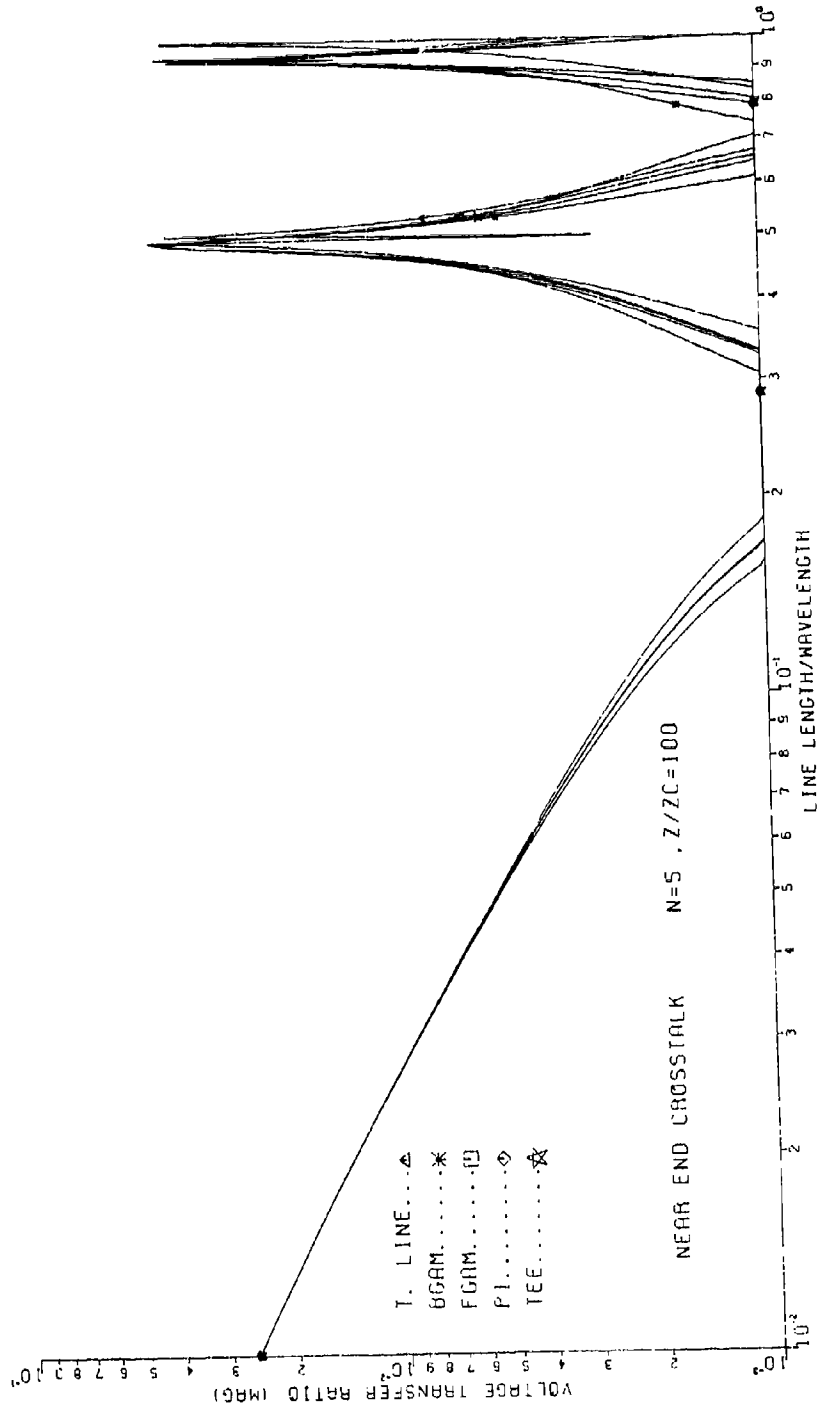
VOLTAGE TRANSFER RATIO (MAG)
LINE LENGTH/WAVELENGTH
NEAR END CROSSTALK
N=5 , Z/ZC=100
T. LINE
BGAM
FGAM
PI
TEE

Figure C-12

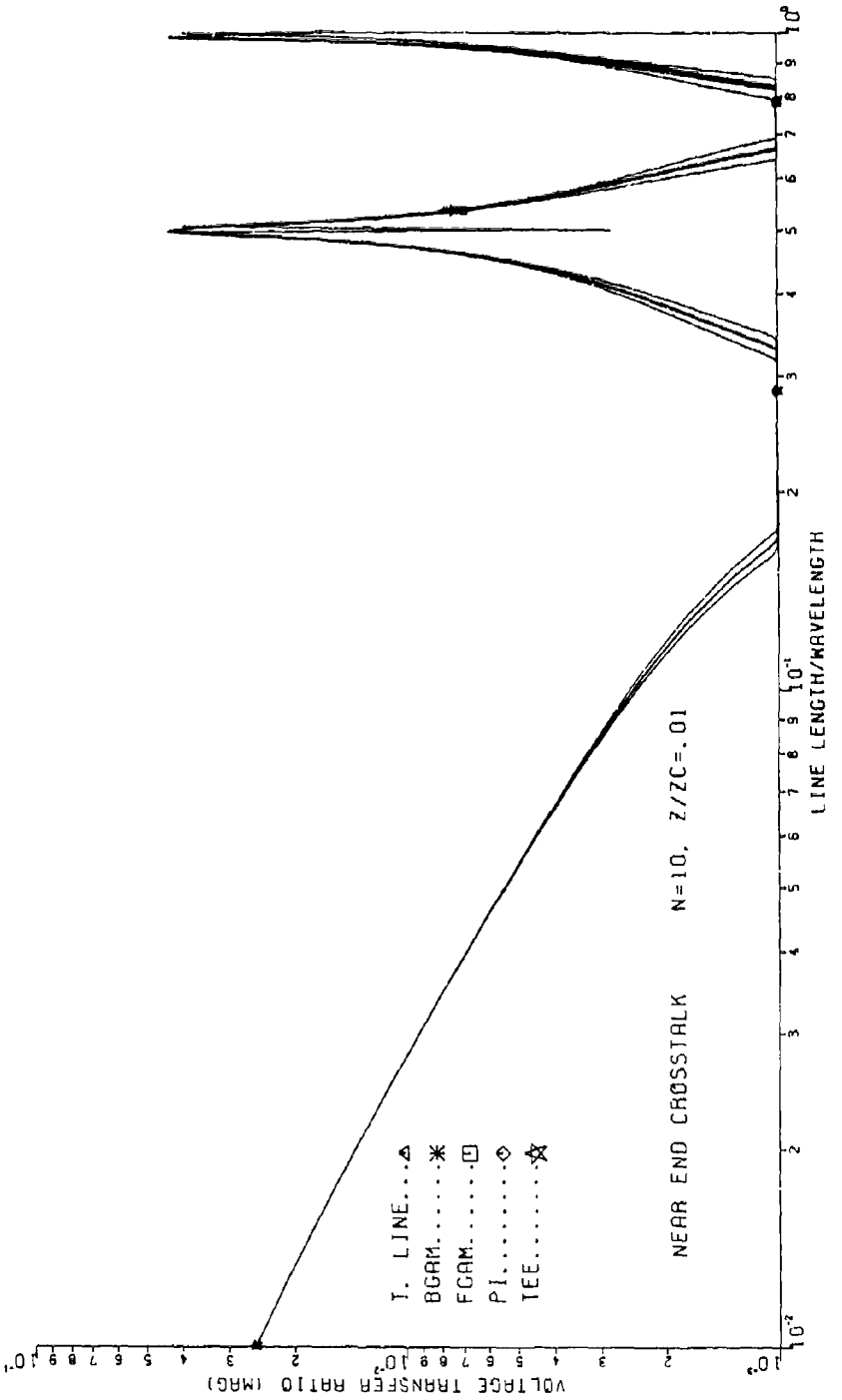
VOLTAGE TRANSFER RATIO (MAG)
LINE LENGTH/WAVELENGTH
NEAR END CROSSTALK
N=10, Z/ZC=.01
T. LINE...
BGAM.....
FGAM.....
PI.....
TEE.....

Figure C-13

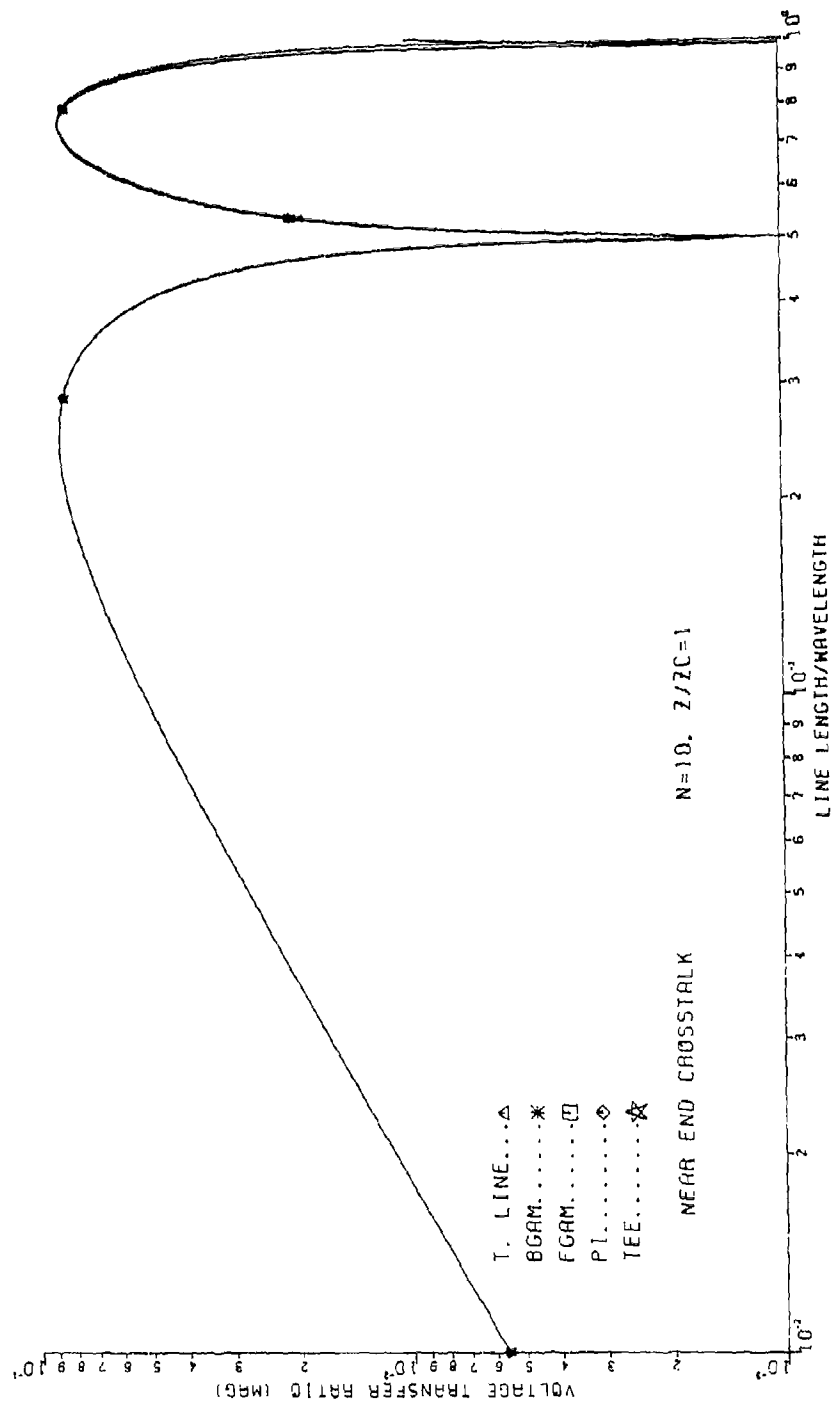
VOLTAGE TRANSFER RATIO (MAG)
LINE LENGTH/WAVELENGTH
T. LINE...△
BGAM.....✳
FGAM.....□
PI.....◇
TEE.....☆
NEAR END CROSSTALK
N=10. Z/ZC=1

Figure C-14

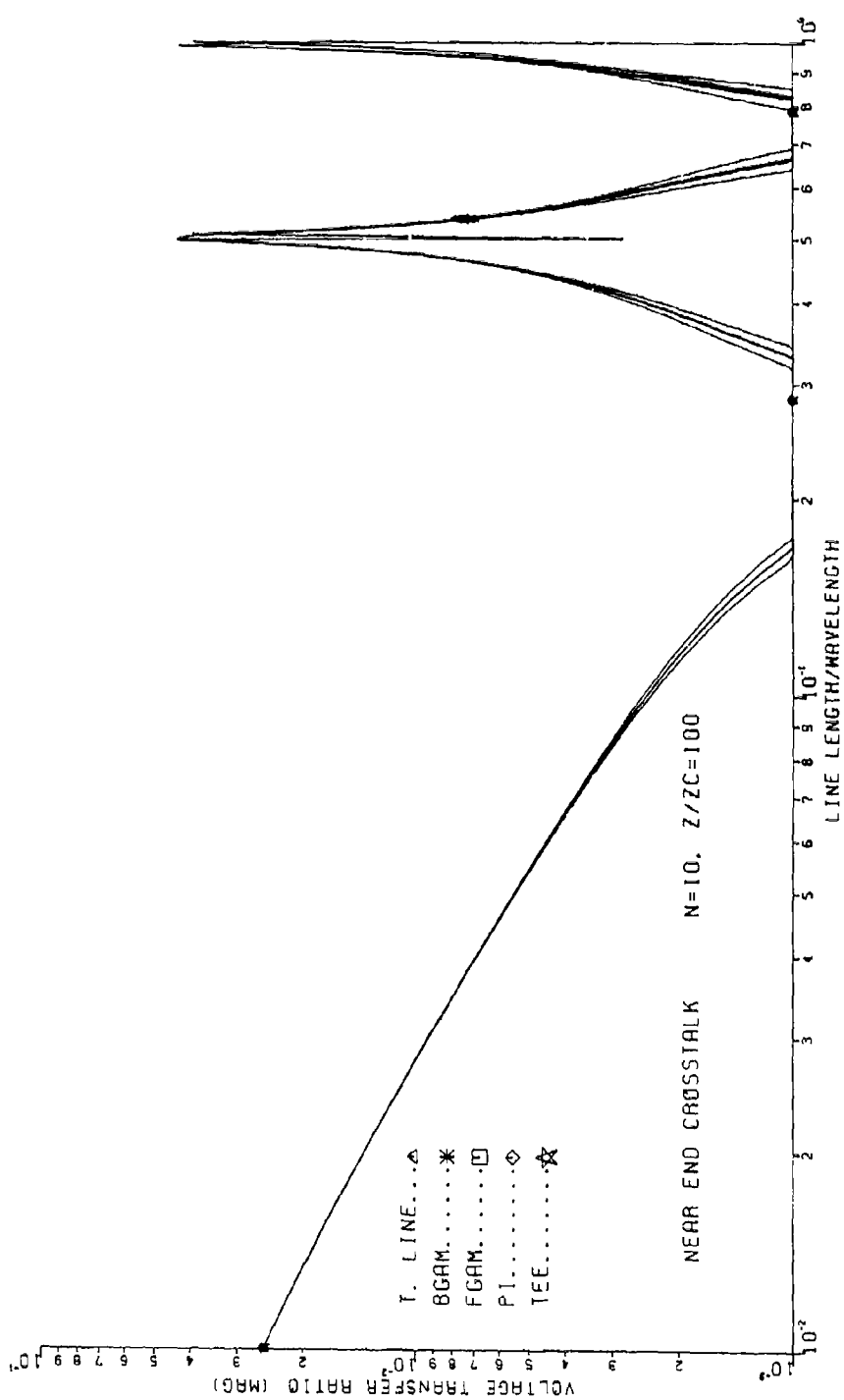
T. LINE
BGAM
FGAM
PI
TEE
NEAR END CROSSTALK
N=10. Z/ZC=100
VOLTAGE TRANSFER RATIO (MAG)
LINE LENGTH/WAVELENGTH

Figure C-15

APPENDIX D

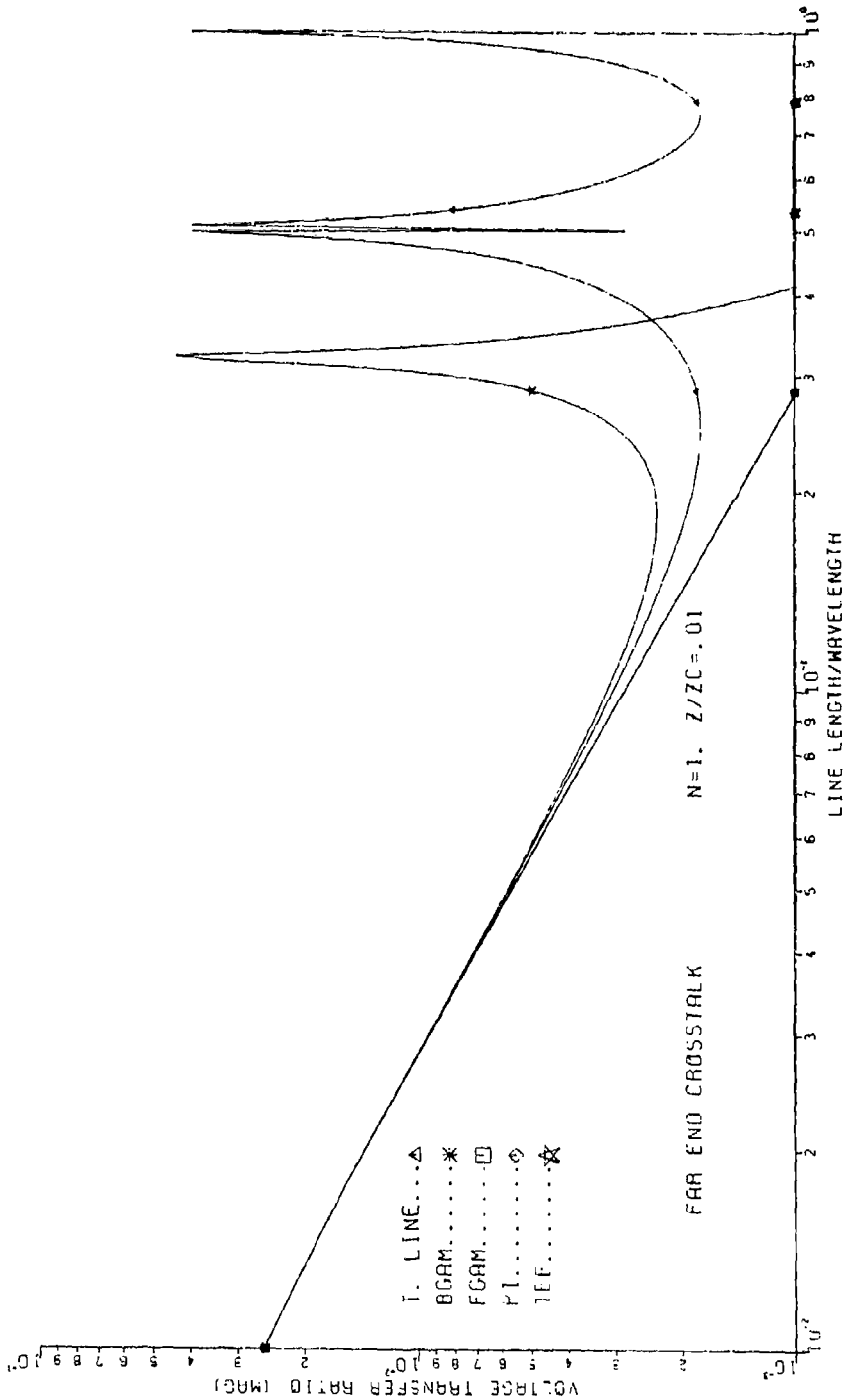

Figure D-1

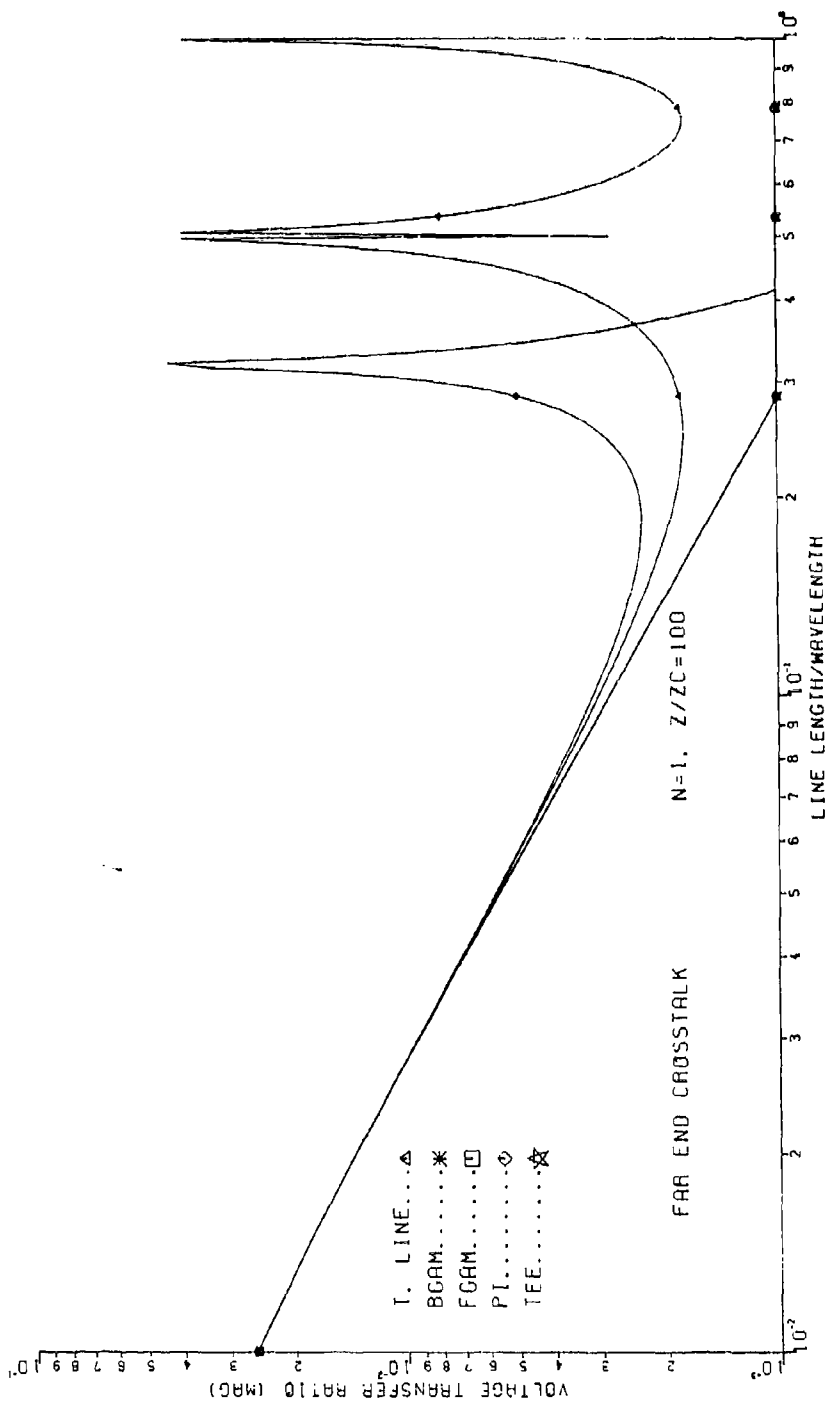
T. LINE
BCAM
FCAM
PI
TEE
FAR END CROSSTALK
N=1. Z/ZC=100
LINE LENGTH/WAVELENGTH
VOLTAGE TRANSFER RATIO (MAG)

Figure D-2

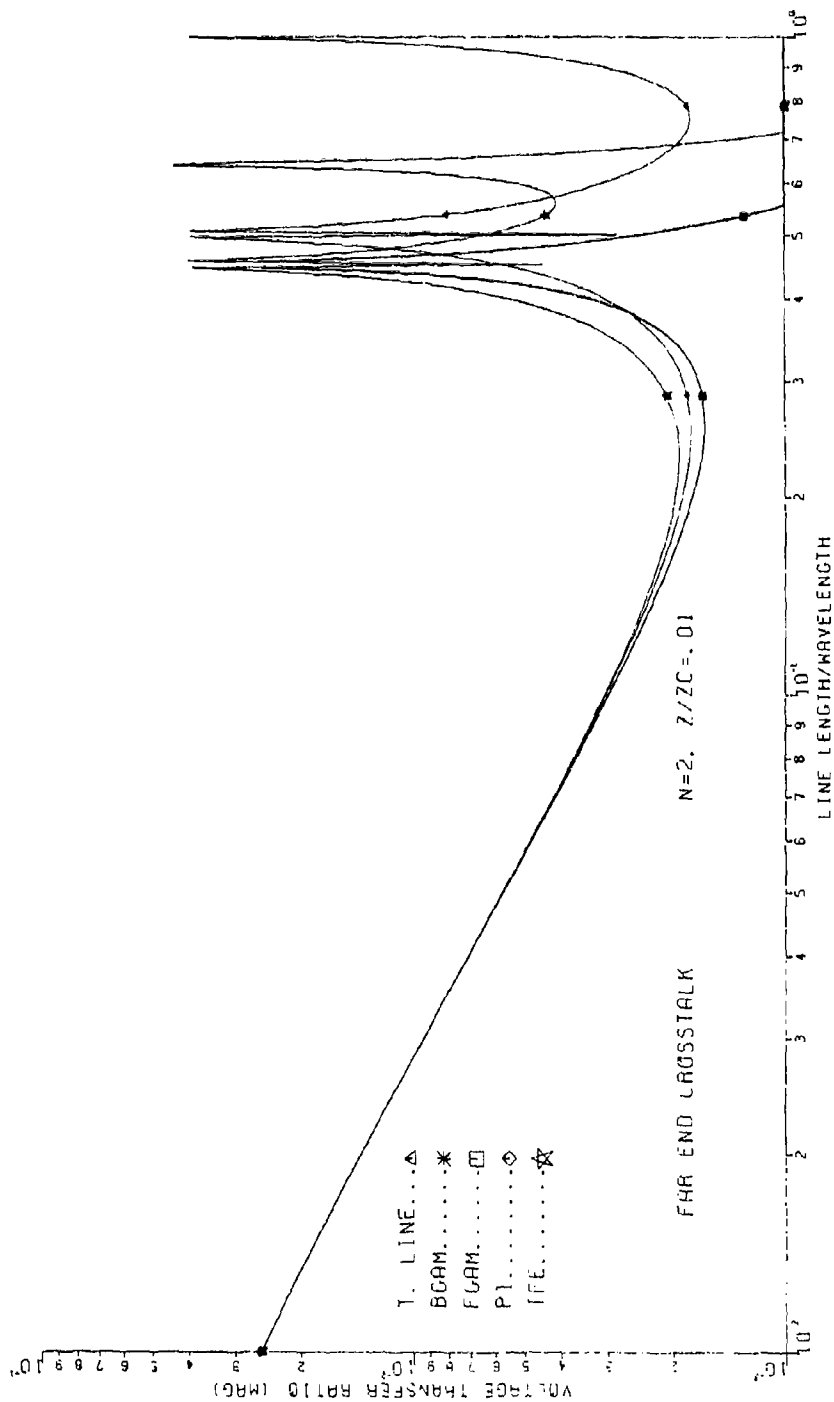
T. LINE
BCAM
FCAM
P1
IFE
FAR END CROSSTALK
N=2, Z/ZC=.01
LINE LENGTH/WAVELENGTH
VOLTAGE TRANSFER RATIO (MAG)

Figure D-3

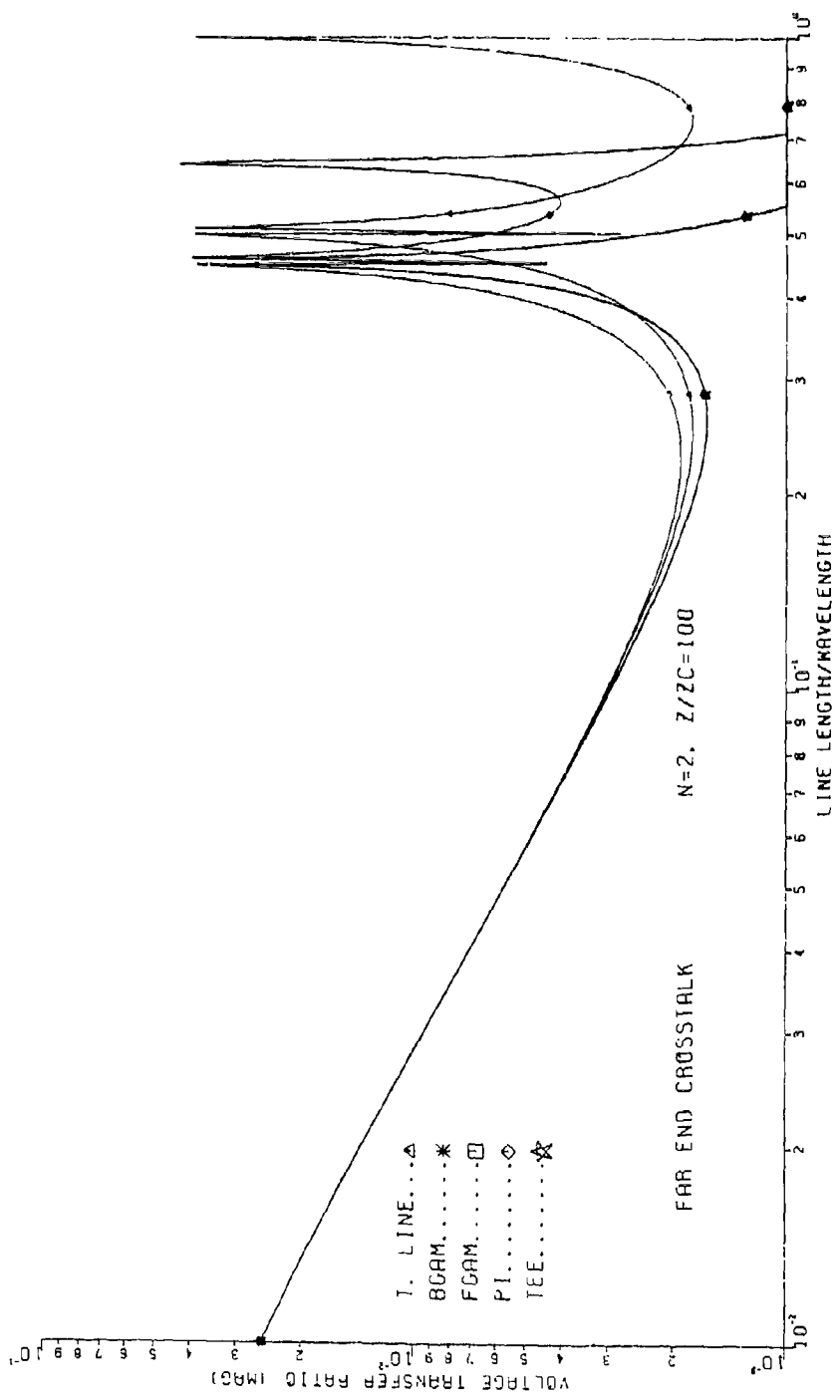
VOLTAGE TRANSFER RATIO (MAG)
LINE LENGTH/WAVELENGTH
FAR END CROSSTALK
N=2. Z/ZC=100
T. LINE...
BOAM.....
FOAM.....
PI.....
TEE.....

Figure D-4

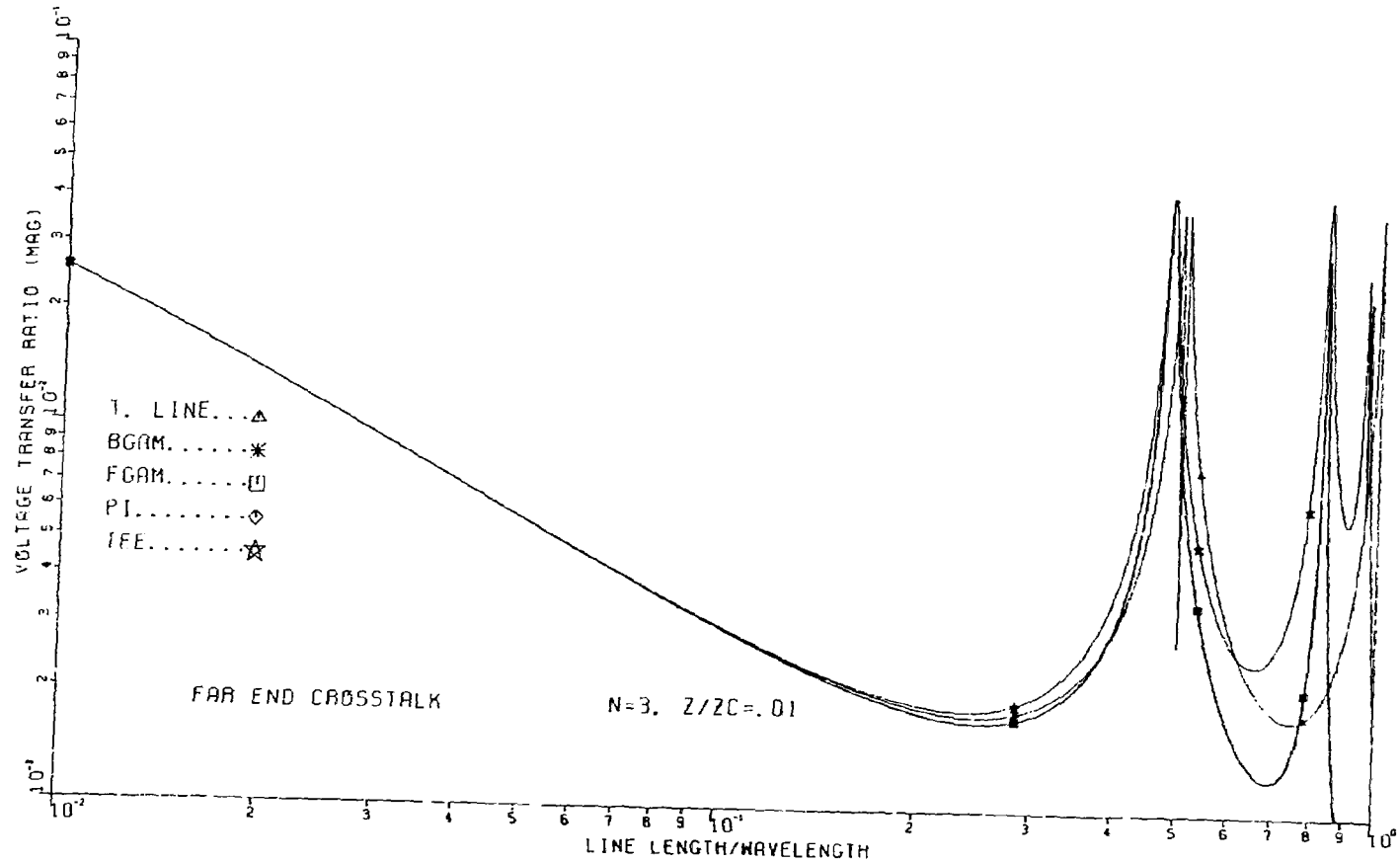
VOLTAGE TRANSFER RATIO (MAG)
T. LINE...
BGAM.....
FGAM.....
PI.....
IFE.....
FAR END CROSSTALK
N=3. Z/ZC=.01
LINE LENGTH/WAVELENGTH

Figure D-5

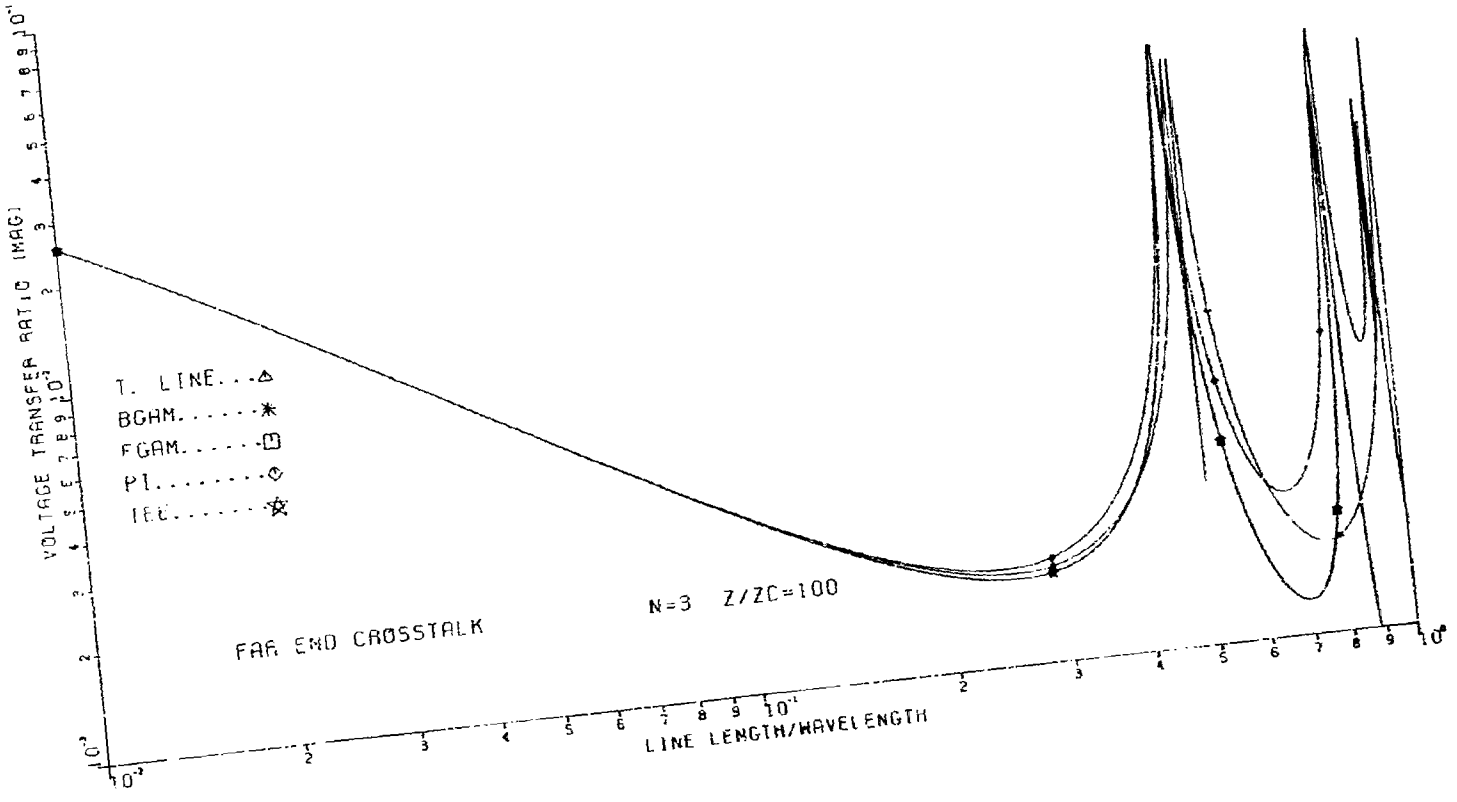
VOLTAGE TRANSFER RATIO (MAG)
T. LINE...
BGAM.....
FGAM.....
PI.....
IEE.....
FAR END CROSSTALK
N=3 Z/ZC=100
LINE LENGTH/WAVELENGTH

Figure D-6

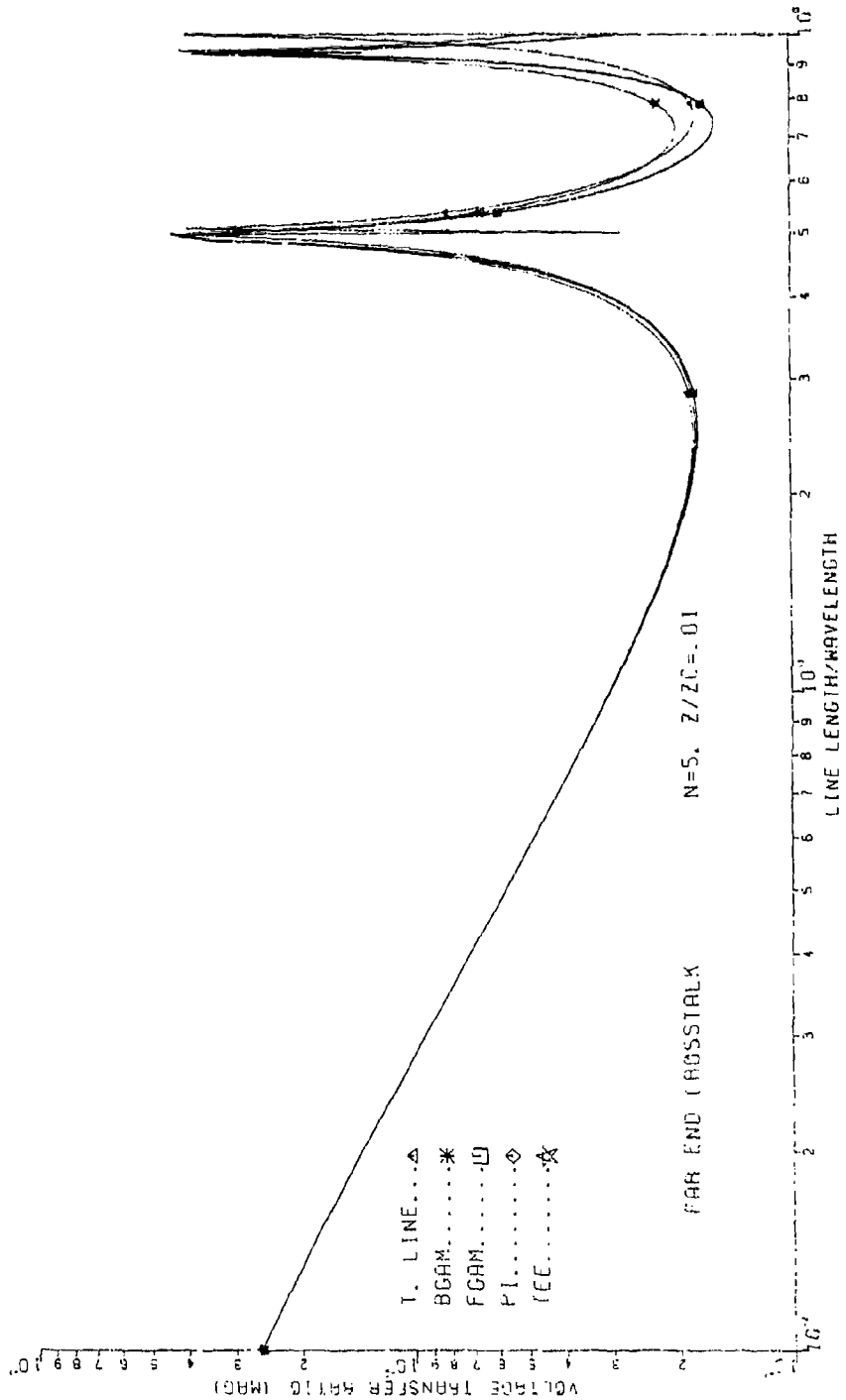
VOLTAGE TRANSFER RATIO (MAG)
LINE LENGTH/WAVELENGTH
FAR END CROSSTALK
N=5. Z/Z0=.01
T. LINE...
BGAM.....
FGAM.....
PI.....
TEE.....

Figure D-7

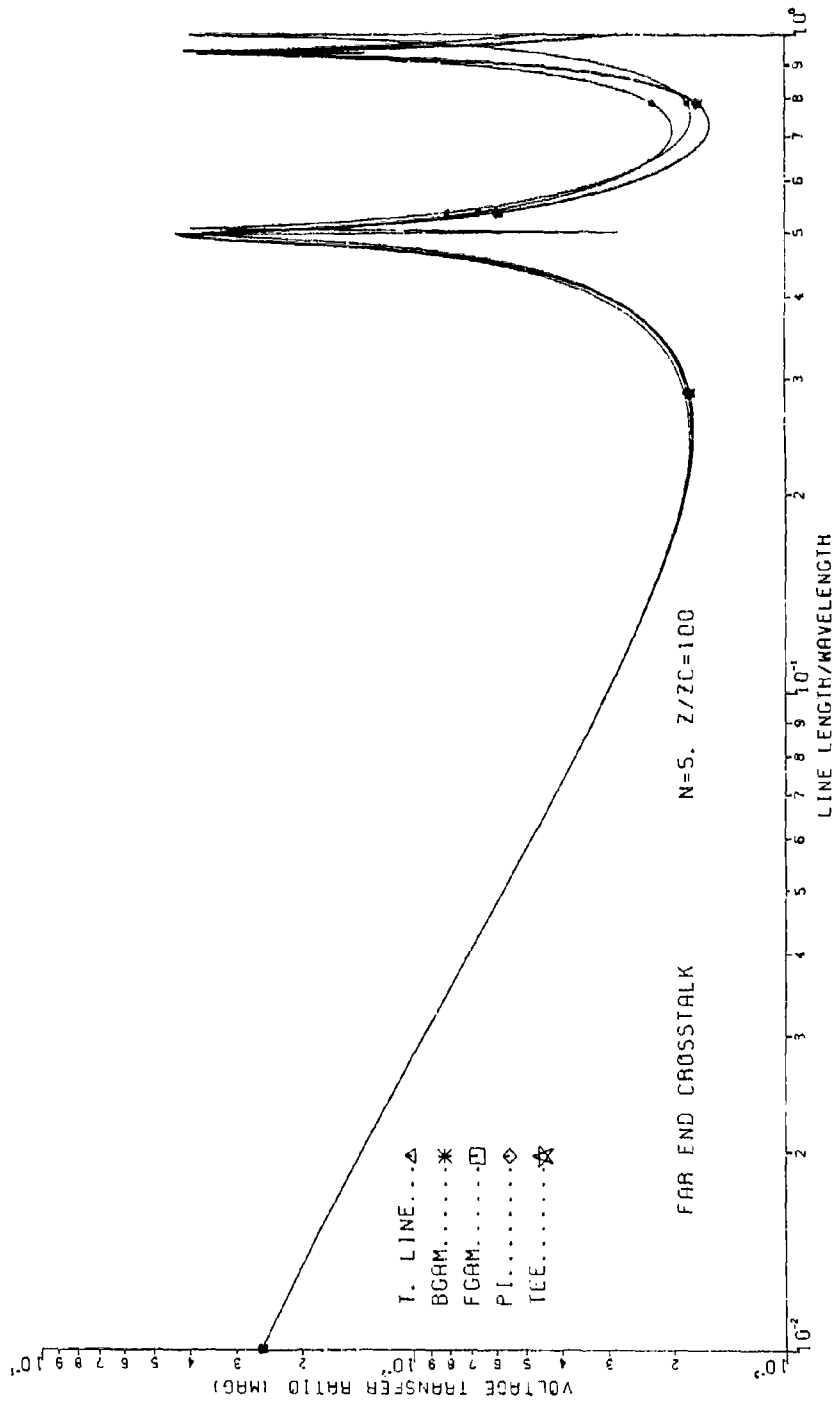
VOLTAGE TRANSFER RATIO (MAG)
LINE LENGTH/WAVELENGTH
FAR END CROSSTALK
N=5. Z/ZC=100
T. LINE.....
BGAM.....
FGAM.....
PI.....
TEE.....

Figure D-8

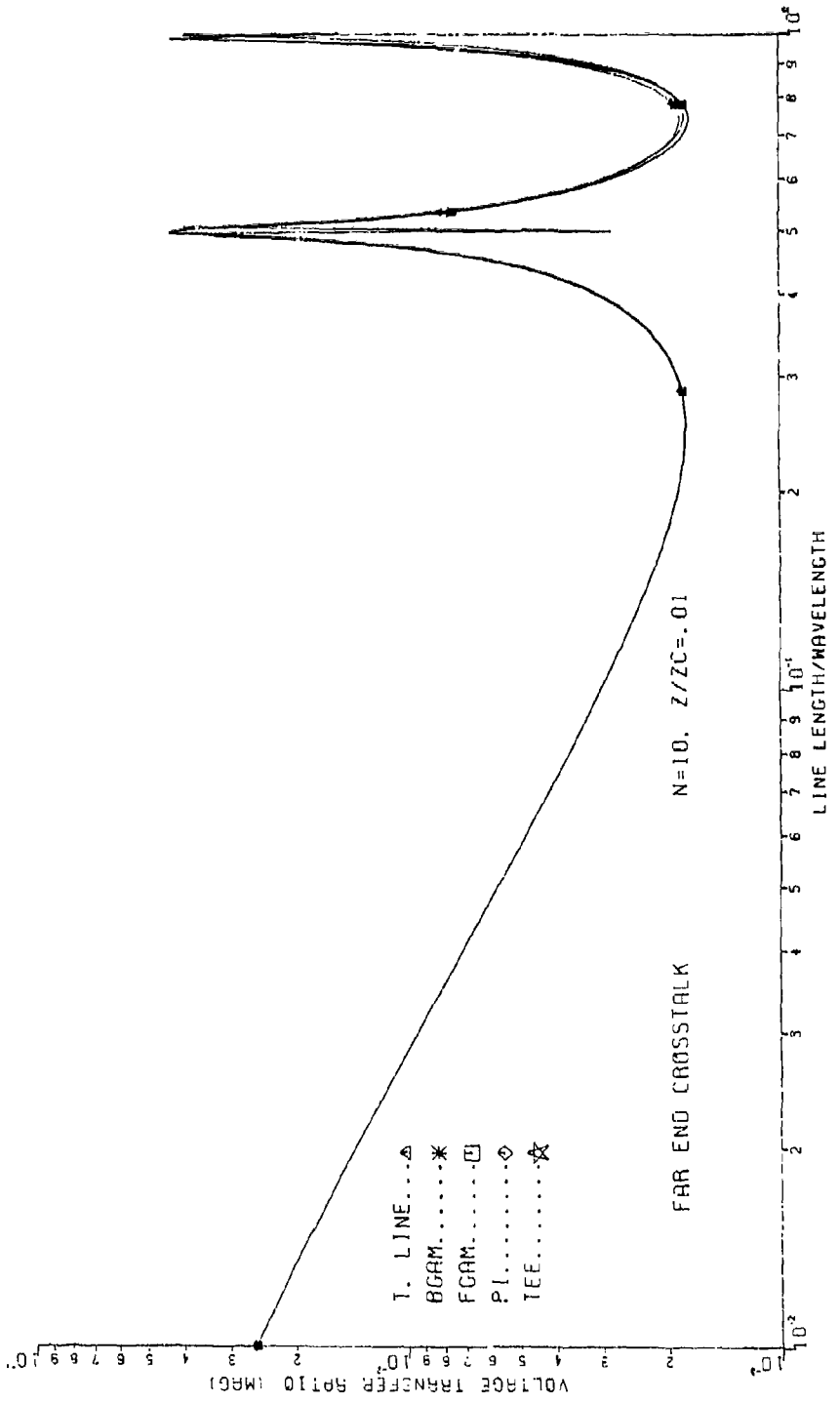
VOLTAGE TRANSFER RATIO (MAG)
LINE LENGTH/WAVELENGTH
FAR END CROSSTALK
N=10. Z/ZC=.01
T. LINE
BGAM
FGAM
PI
TEE

Figure D-9

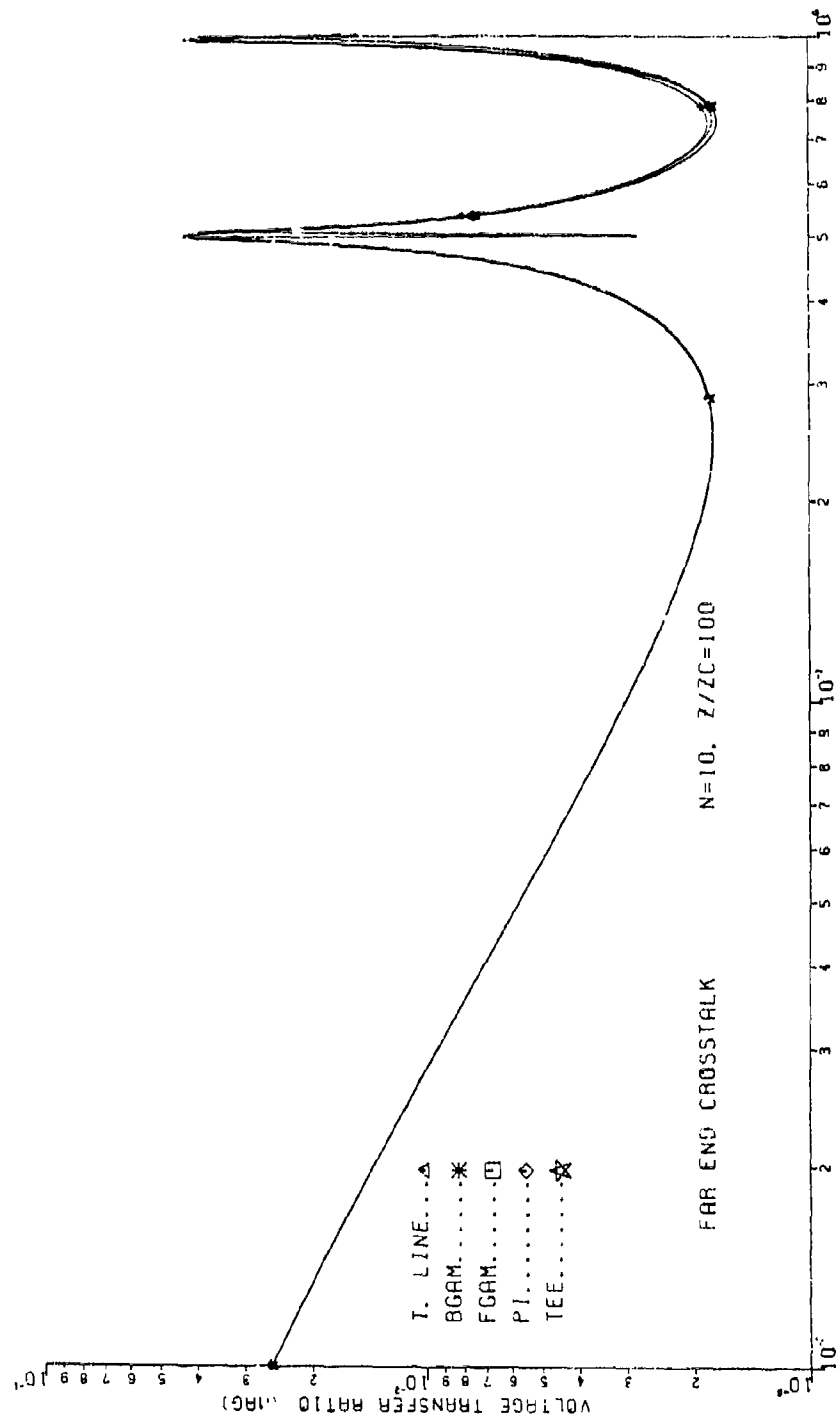
VOLTAGE TRANSFER RATIO (dB)
LINE LENGTH/WAVELENGTH
FAR END CROSSTALK
N=10, Z/ZC=100
I. LINE
BGAM
FGAM
PI
TEE

Figure D-10

APPENDIX E

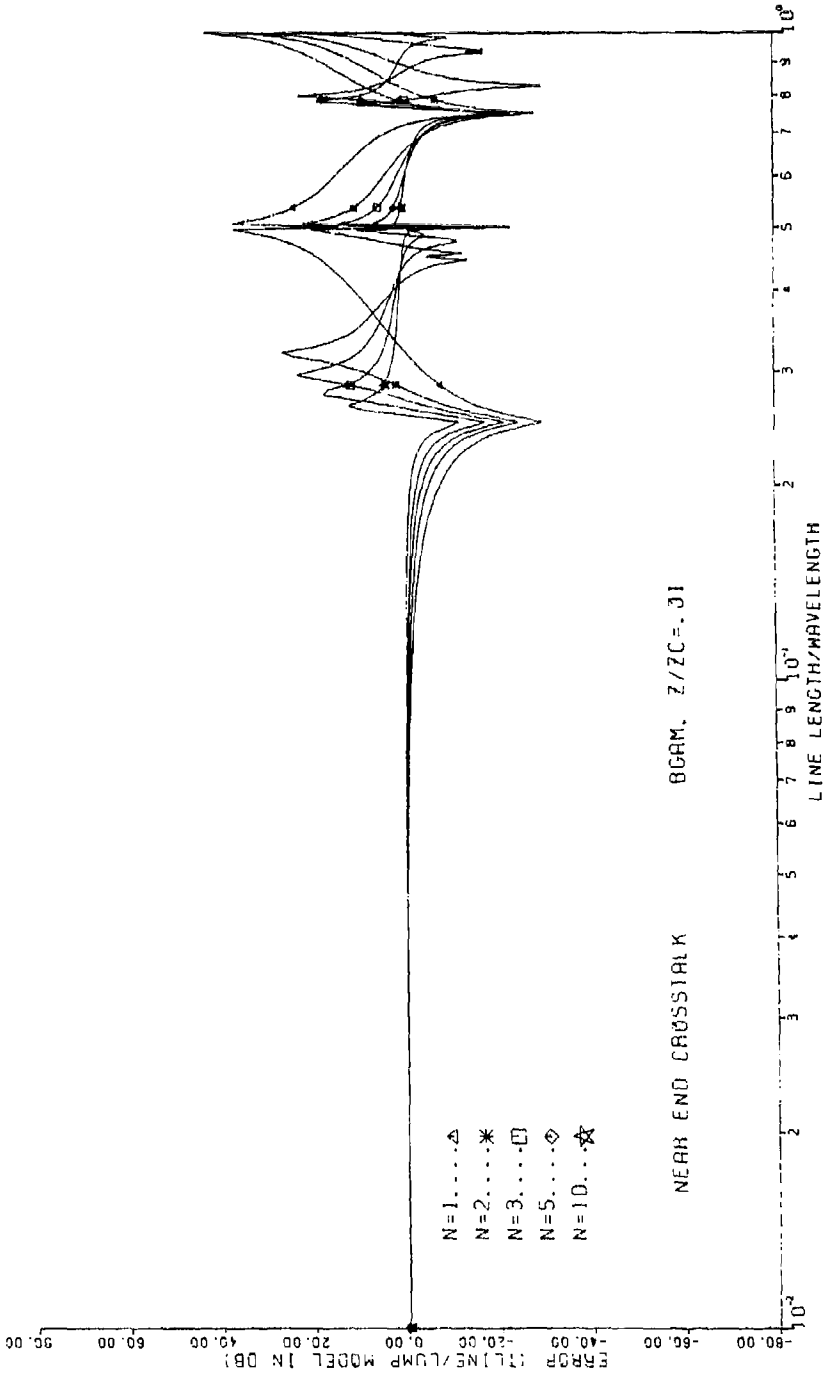

Figure E-1

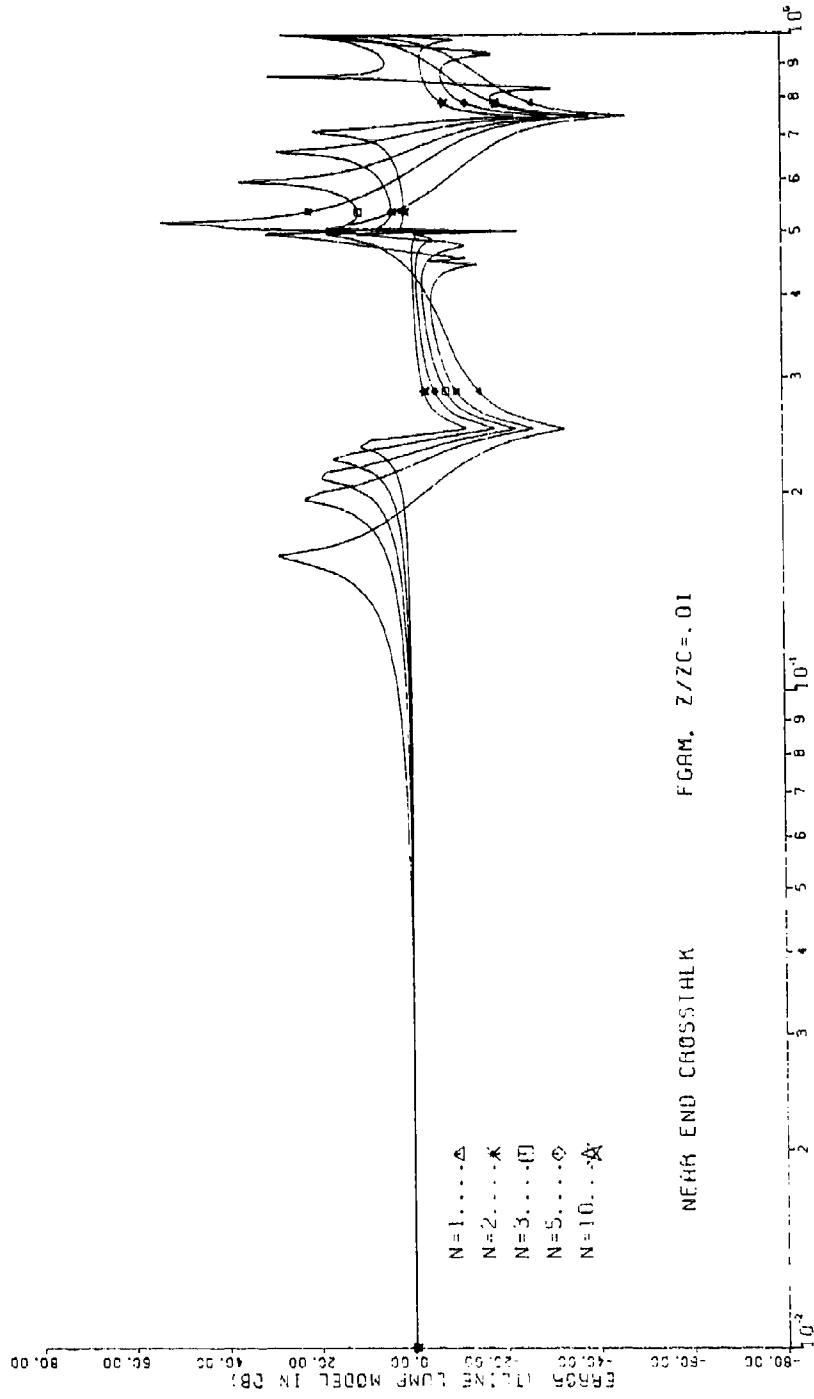
ERROR (LINE LUMP MODEL IN DB)
80.00
60.00
40.00
20.00
0.00
-20.00
-40.00
-60.00
-80.00
10^{-2}
10^{-1}
10^{0}
LINE LENGTH/WAVELENGTH
N=1
N=2
N=3
N=5
N=10
NEAR END CROSSTALK
FGAM. Z/ZC=.01

Figure E-2

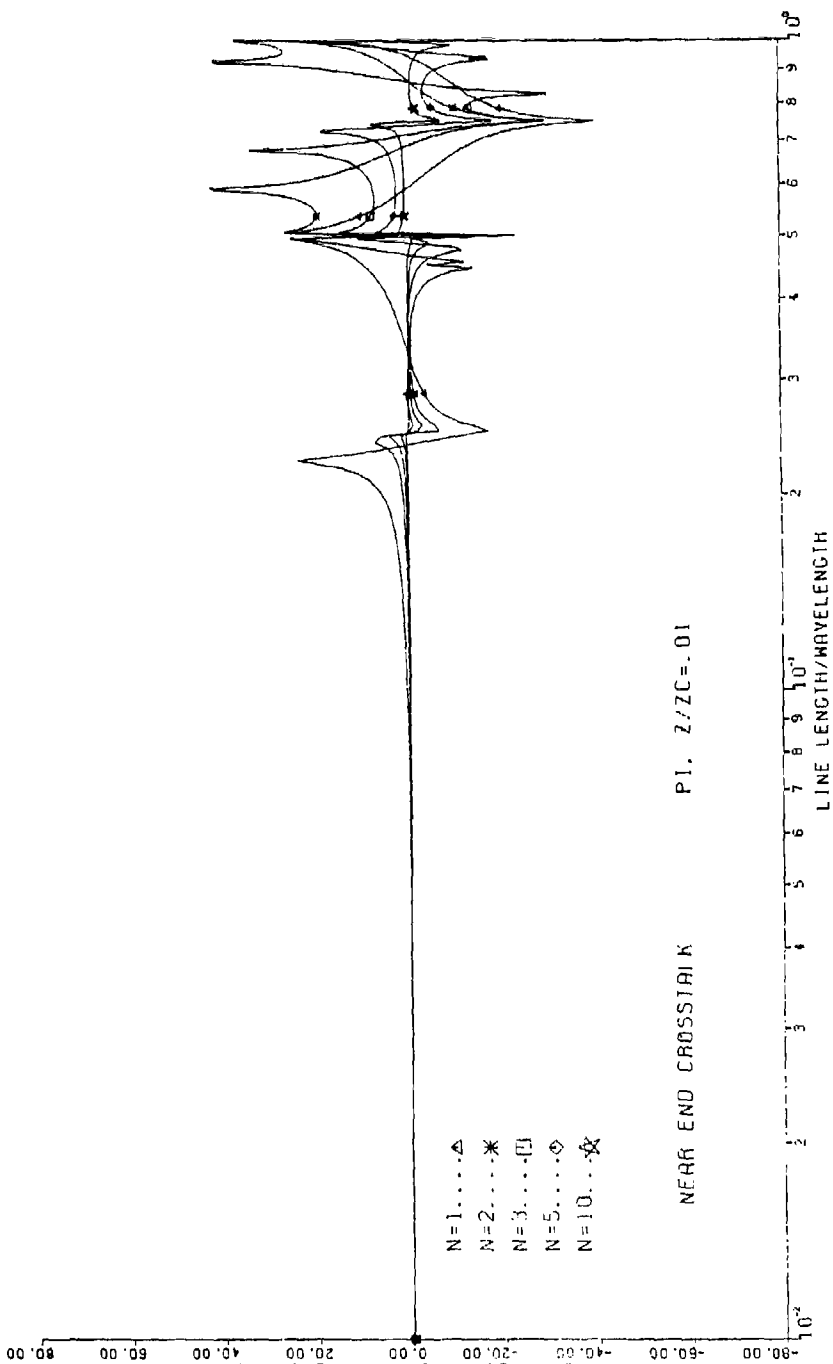
ERROR (LINE/LUMP MODEL) IN DB
80.00
60.00
40.00
20.00
0.00
-20.00
-40.00
-60.00
-80.00
10^{-2}
10^{-1}
10^{0}
LINE LENGTH/WAVELENGTH
N=1
N=2
N=3
N=5
N=10
NEAR END CROSSTALK
P1, Z/ZC=.01

Figure E-3

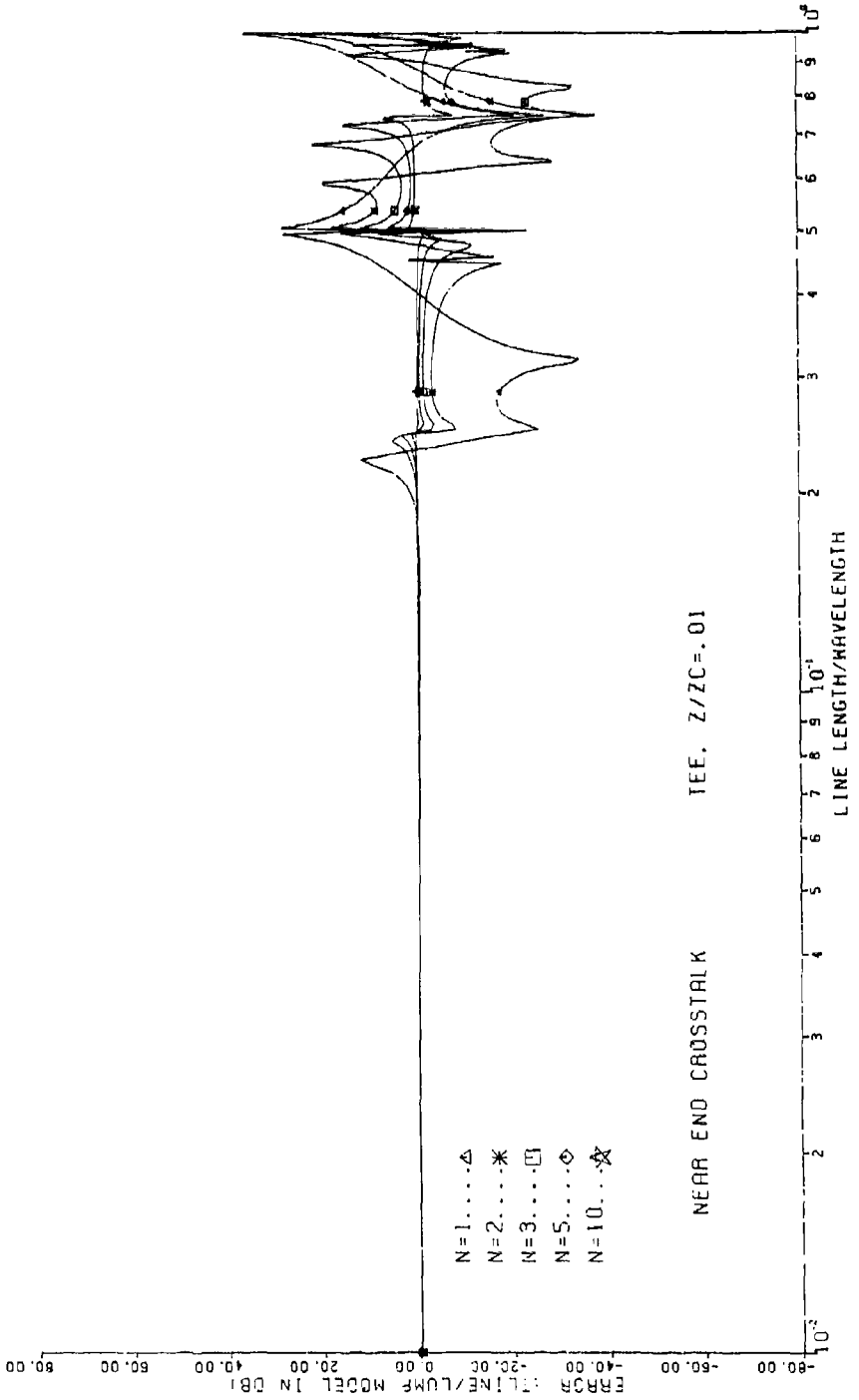
ERROR (LINE/LUMP MODEL) IN DB
80.00
60.00
40.00
20.00
0.00
-20.00
-40.00
-60.00
-80.00
10^{-3}
2
3
4
5
6
7
8
9
10^{-2}
2
3
4
5
6
7
8
9
10^{-1}
2
3
4
5
6
7
8
9
10^{0}
LINE LENGTH/WAVELENGTH
TEE, Z/ZC=.01
NEAR END CROSSTALK
N=1
N=2
N=3
N=5
N=10

Figure E-4

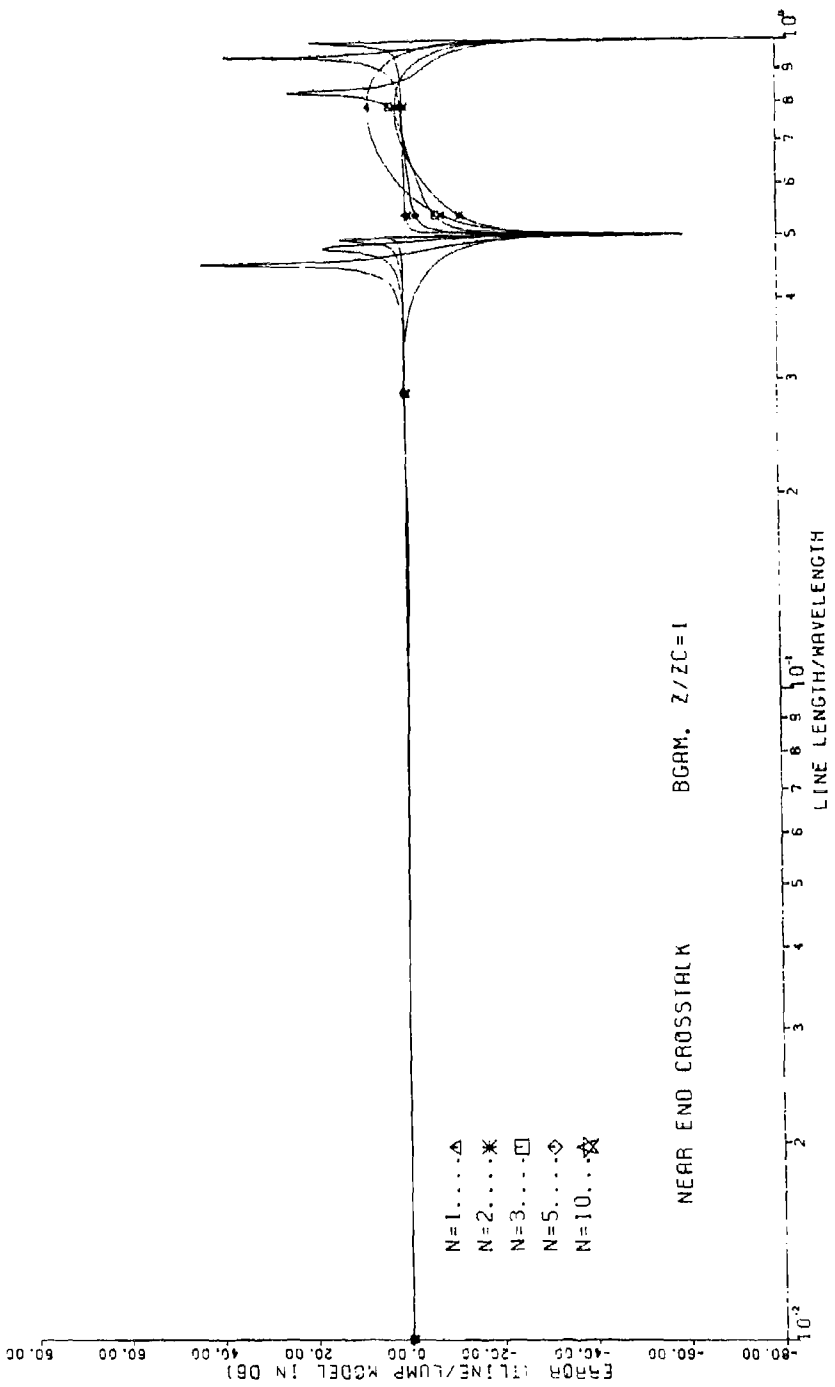
ERROR (LINE/LUMP MODEL IN DB)
60.00
40.00
20.00
0.00
-20.00
-40.00
-60.00
-80.00
10^{-2}
2
3
4
5
6
7
8
9
10^{-1}
2
3
4
5
6
7
8
9
10^{0}
LINE LENGTH/WAVELENGTH
NEAR END CROSSTALK
BGAM. Z/ZC=1
N=1.....△
N=2.....✳
N=3.....□
N=5.....◇
N=10....☆

Figure E-5

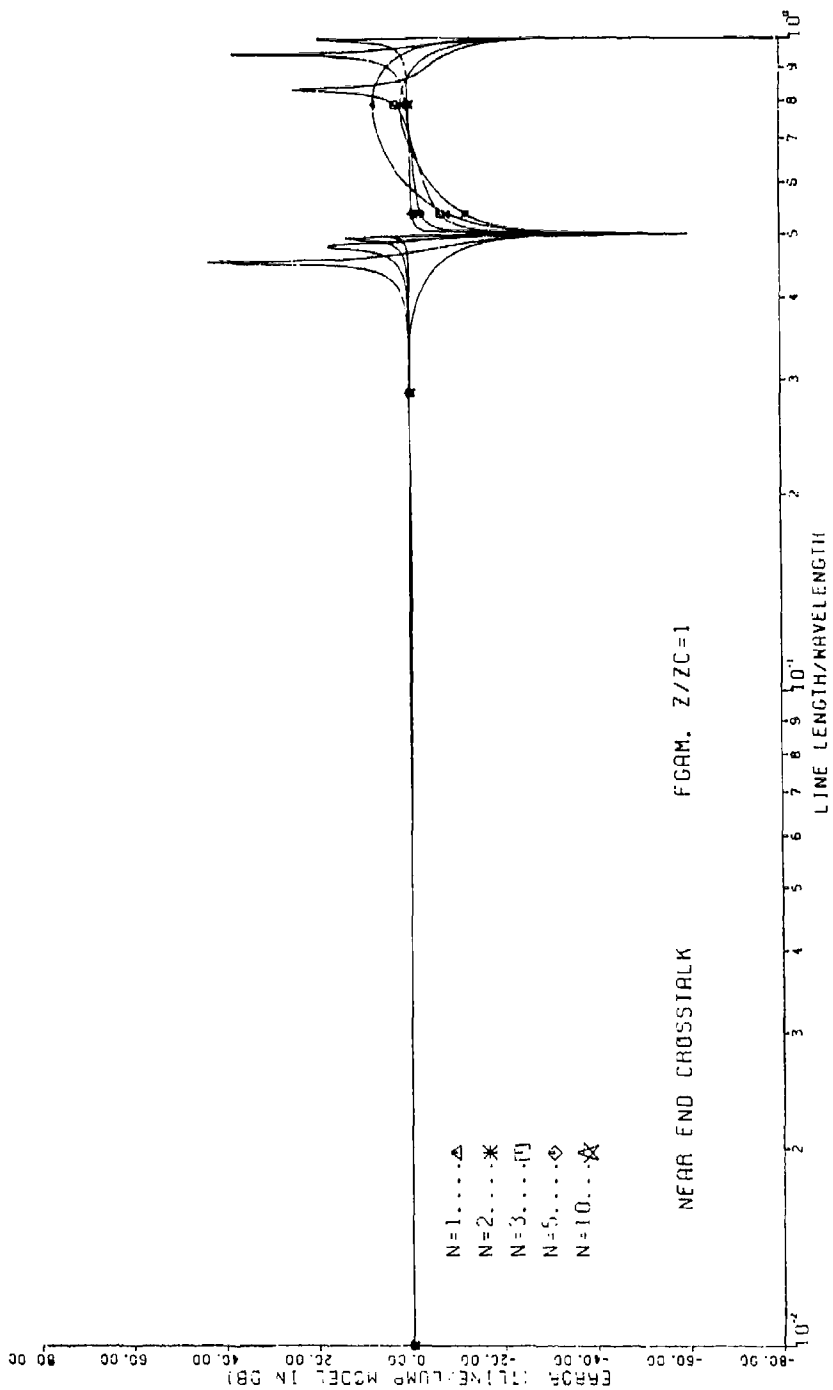
NEAR END CROSSTALK
FOAM. Z/ZC=1
N=1
N=2
N=3
N=5
N=10
LINE LENGTH/WAVELENGTH
ERROR (TLINE/LUMP MODEL) IN DB
80.00
60.00
40.00
20.00
0.00
-20.00
-40.00
-60.00
-80.00

Figure E-6

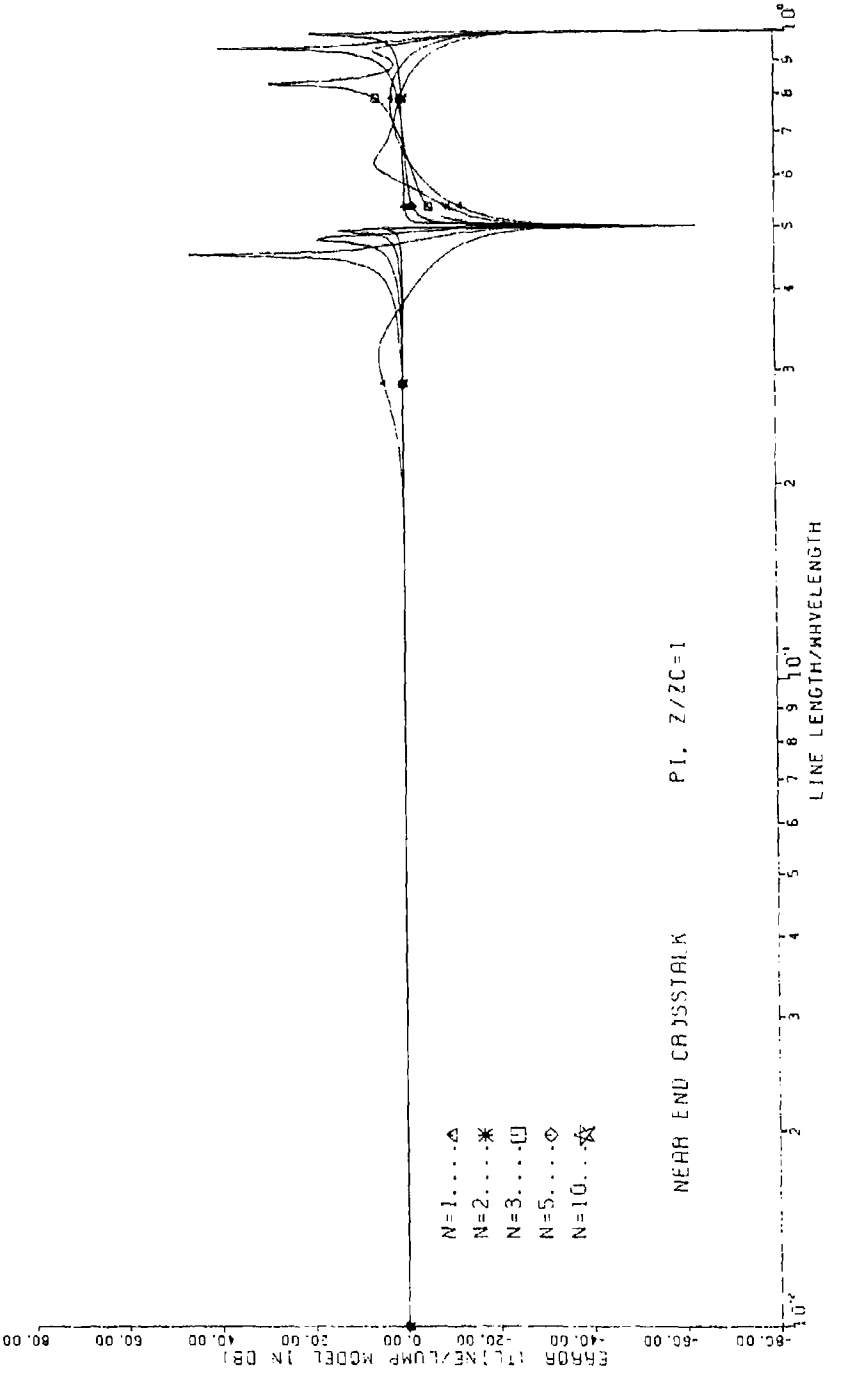
ERROR (TC)NEAR/LUMP MODEL IN DB)
60.00
40.00
20.00
0.00
-20.00
-40.00
-60.00
-80.00
LINE LENGTH/WAVELENGTH
N=1.....
N=2.....
N=3.....
N=5.....
N=10.....
NEAR END CROSSTALK
PI, Z/ZC=1

Figure E-7

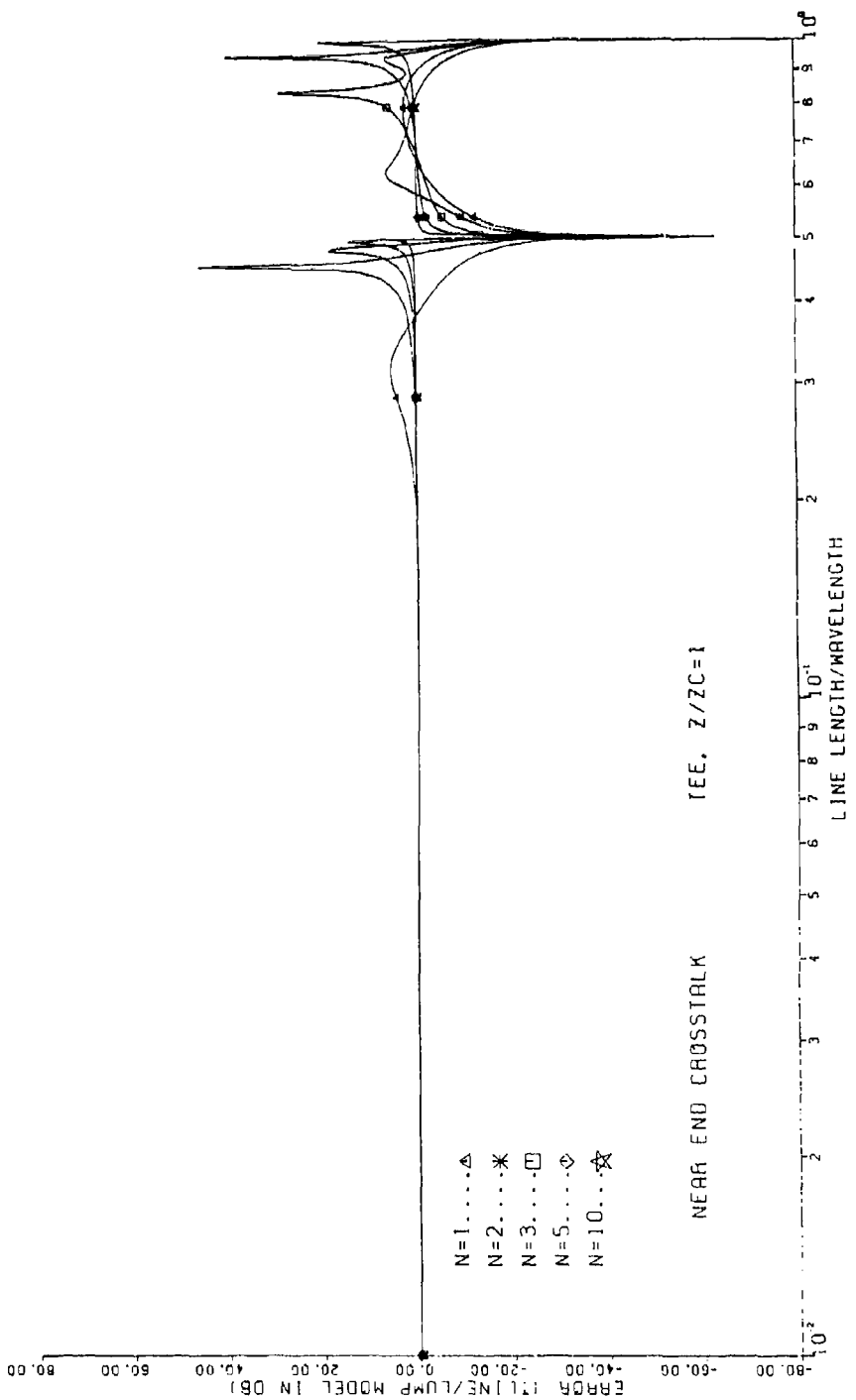
ERROR (LINE/LUMP MODEL IN DB)
80.00
60.00
40.00
20.00
0.00
-20.00
-40.00
-60.00
-80.00
LINE LENGTH/WAVELENGTH
NEAR END CROSSTALK
IEE, Z/ZC=1
N=1
N=2
N=3
N=5
N=10

Figure E-3

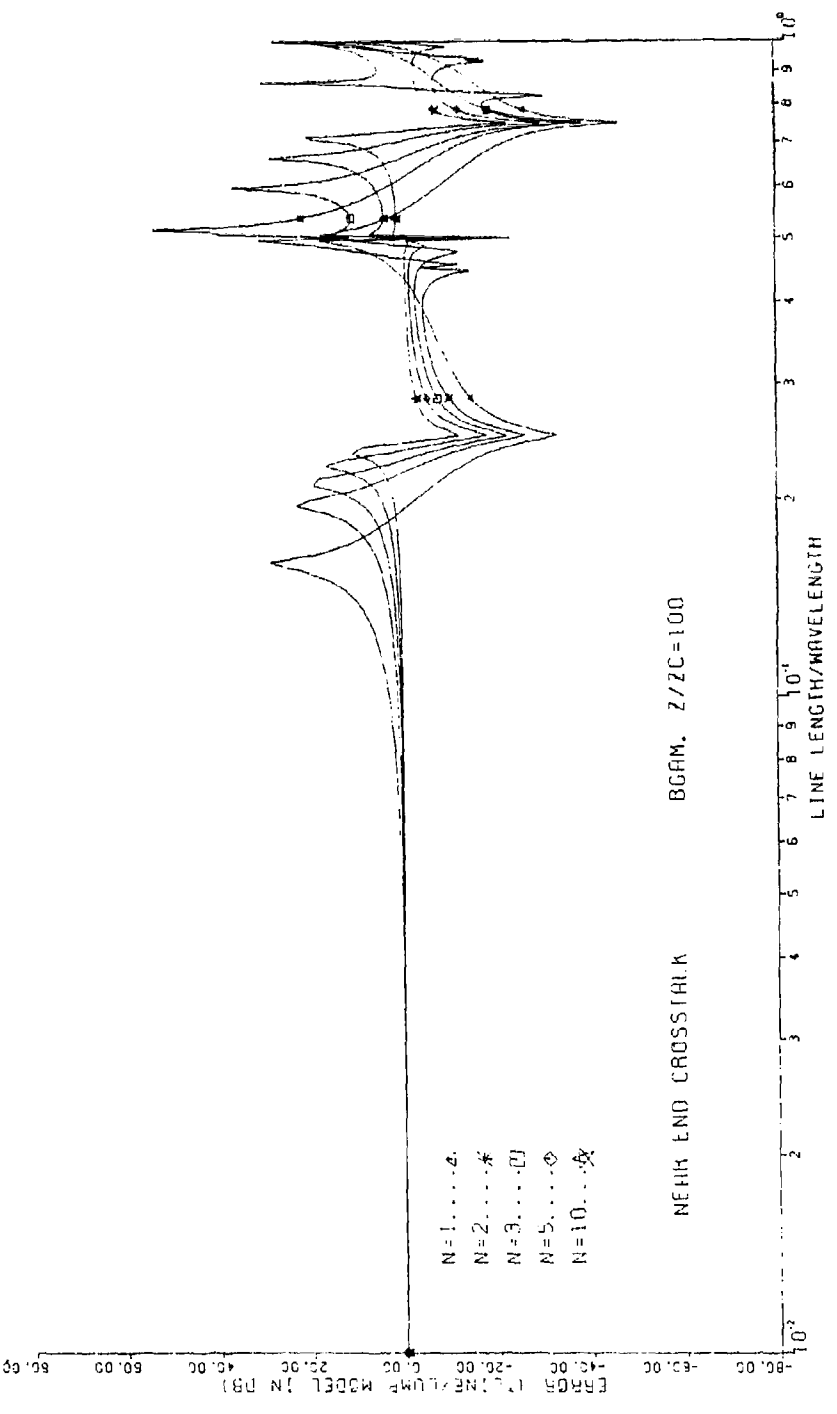
NEAR END CROSSTALK
BGAM. Z/ZC=100
N=1
N=2
N=3
N=5
N=10
LINE LENGTH/WAVELENGTH
ERROR (LINE/LUMP MODEL) IN DB
60.00
40.00
20.00
0.00
-20.00
-40.00
-60.00
10^{-2}
10^{-1}
10^{0}

Figure E-9

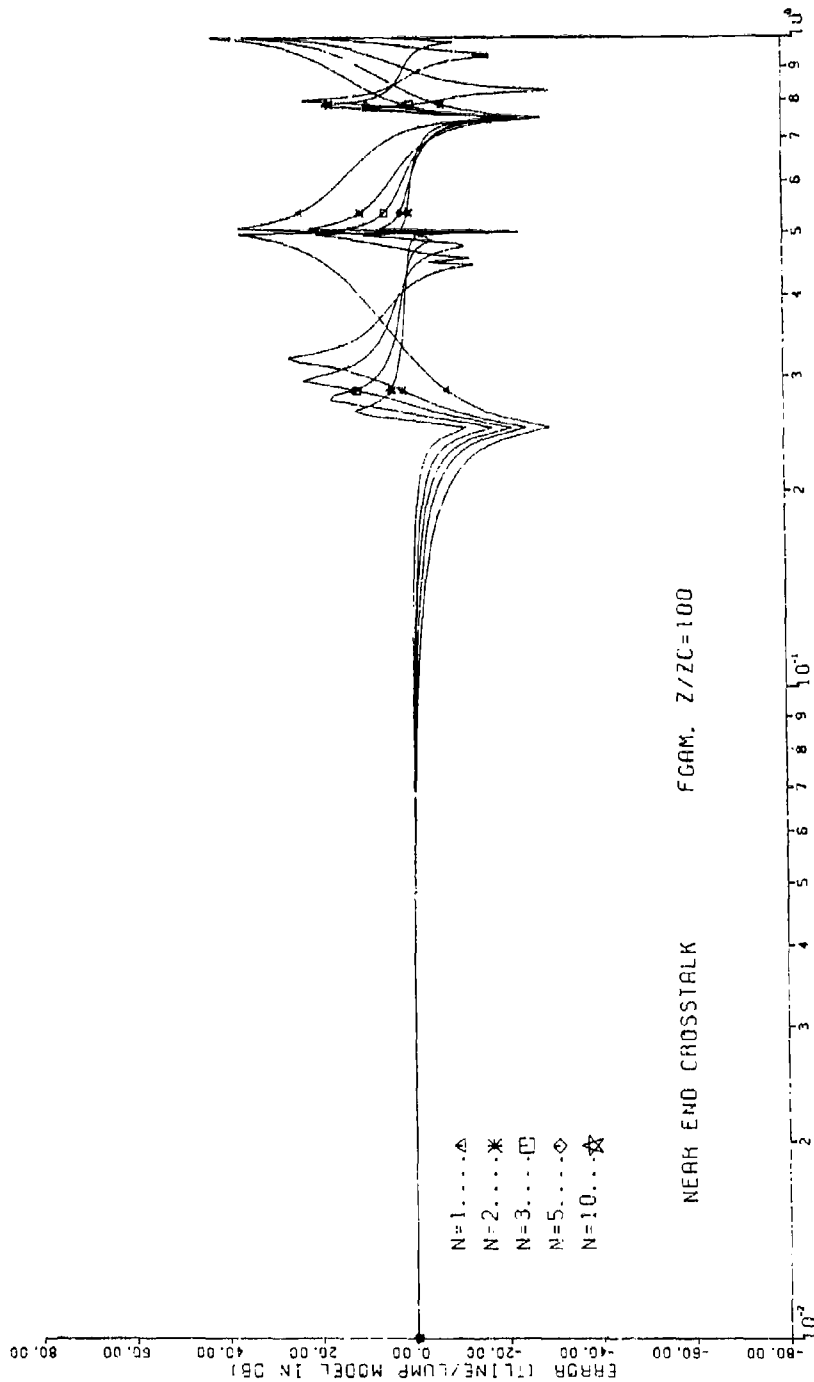
ERROR (LINE/LUMP MODEL IN DB)
LINE LENGTH/WAVELENGTH
NEAR END CROSSTALK
FGAM. Z/ZC=100
N=1
N=2
N=3
N=5
N=10

Figure E-10

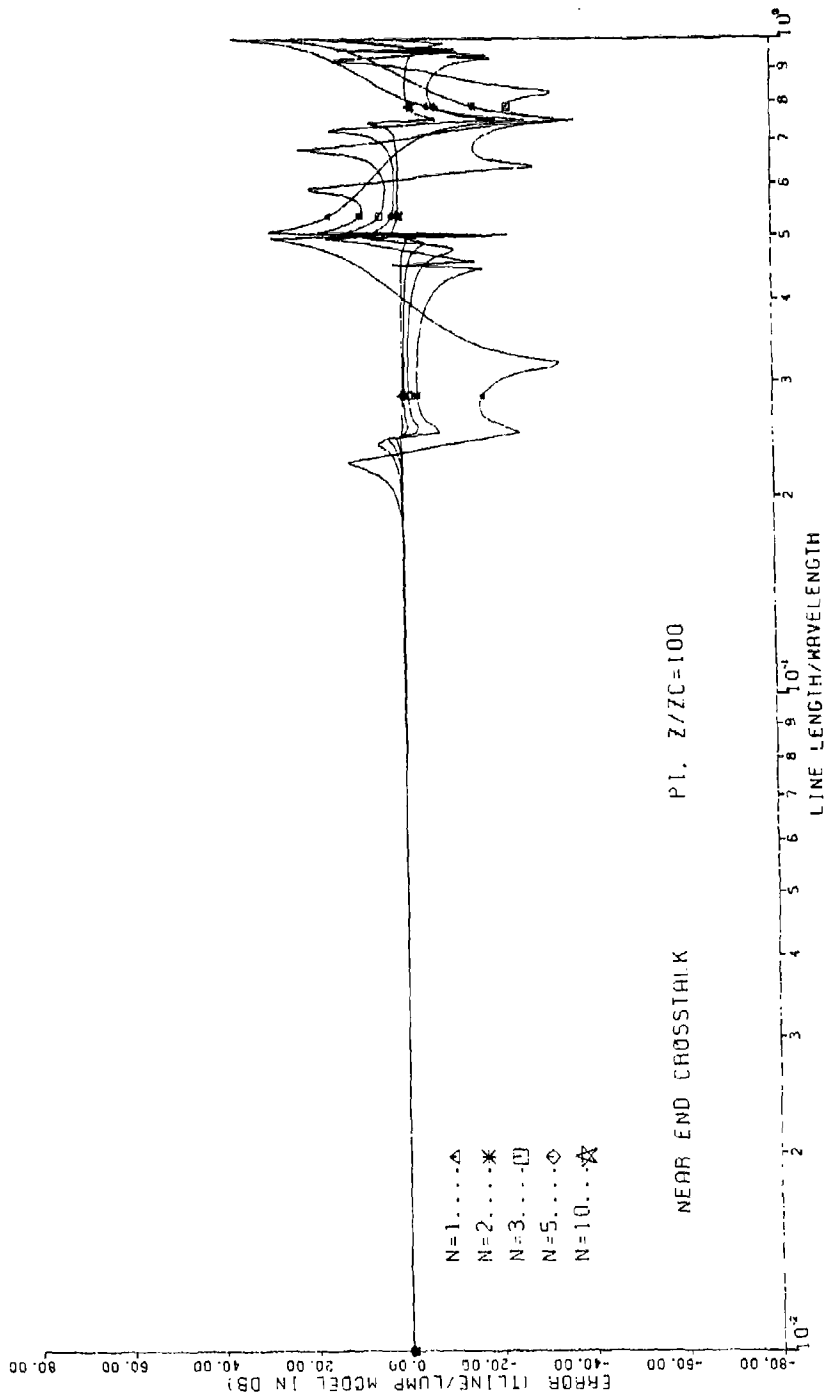
ERROR (TL]NE/LUMP MODEL]N DB)
-80.00
-60.00
-40.00
-20.00
0.00
20.00
40.00
60.00
80.00
10^{-2}
10^{-1}
10^{0}
LINE LENGTH/WAVELENGTH
NEAR END CROSSTALK
PI, Z/ZC=100
N=1.....△
N=2.....✳
N=3.....□
N=5.....◇
N=10.....☆

Figure E-11

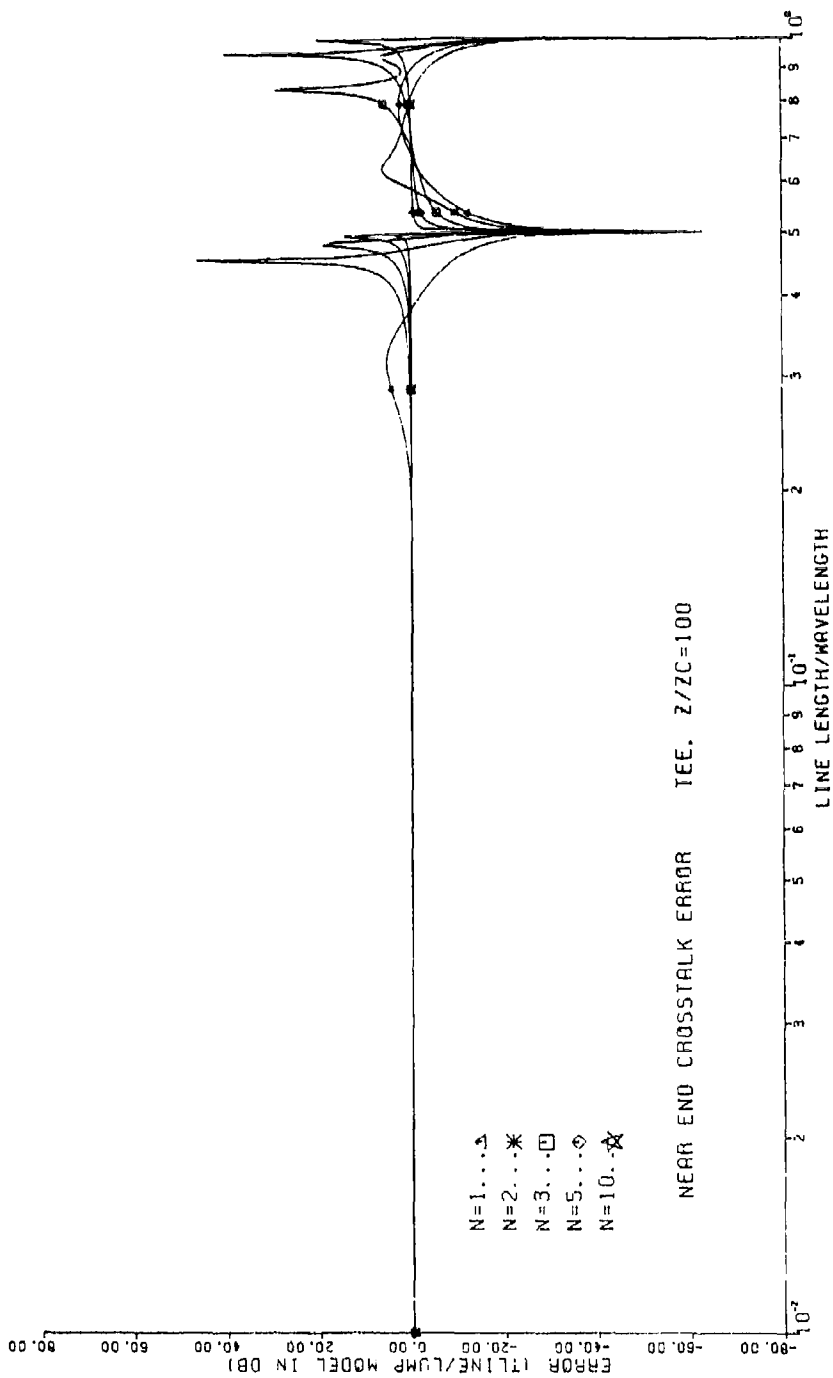
NEAR END CROSSTALK ERROR TEE. Z/ZC=100
N=1.
N=2.
N=3.
N=5.
N=10.
ERROR (TLINE/LUMP MODEL IN DB)
80.00
60.00
40.00
20.00
0.00
-20.00
-40.00
-60.00
-80.00
LINE LENGTH/WAVELENGTH

Figure E-12

APPENDIX F

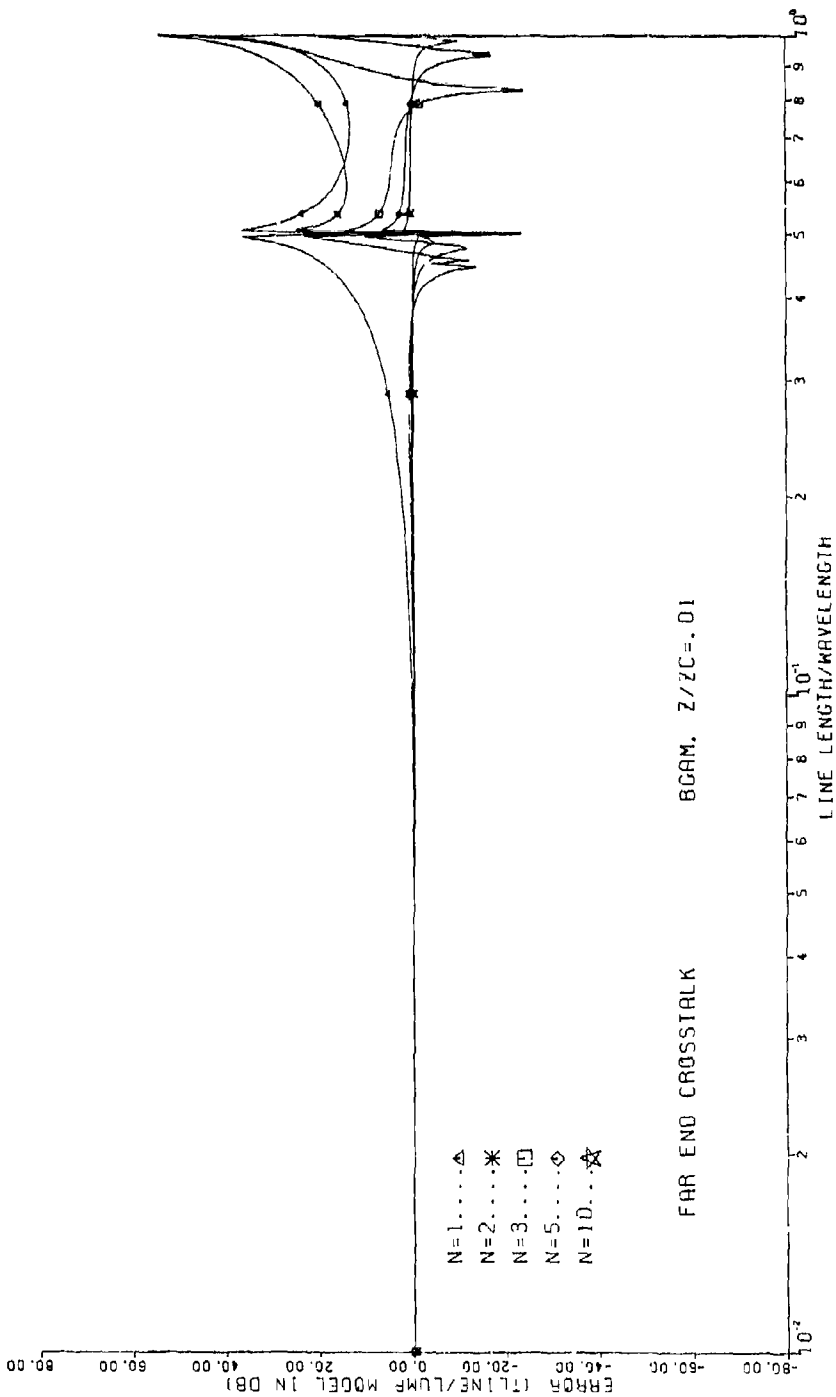

Figure F-1

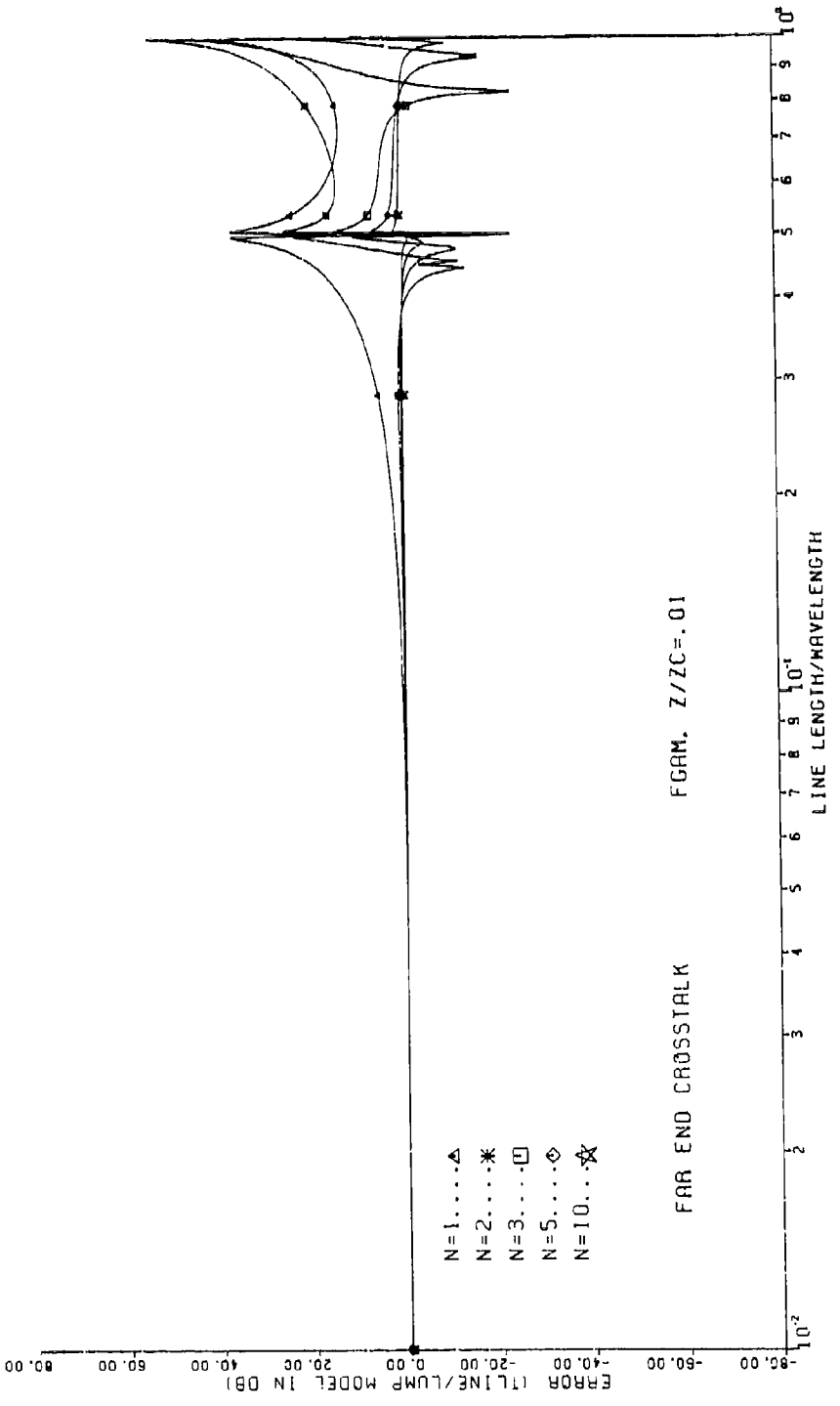
FAR END CROSSTALK
FGAM. Z/ZC=.01
N=1.....△
N=2.....✳
N=3.....□
N=5.....◇
N=10....☆
ERROR (LINE/LUMP MODEL IN DB)
LINE LENGTH/WAVELENGTH

Figure F-2

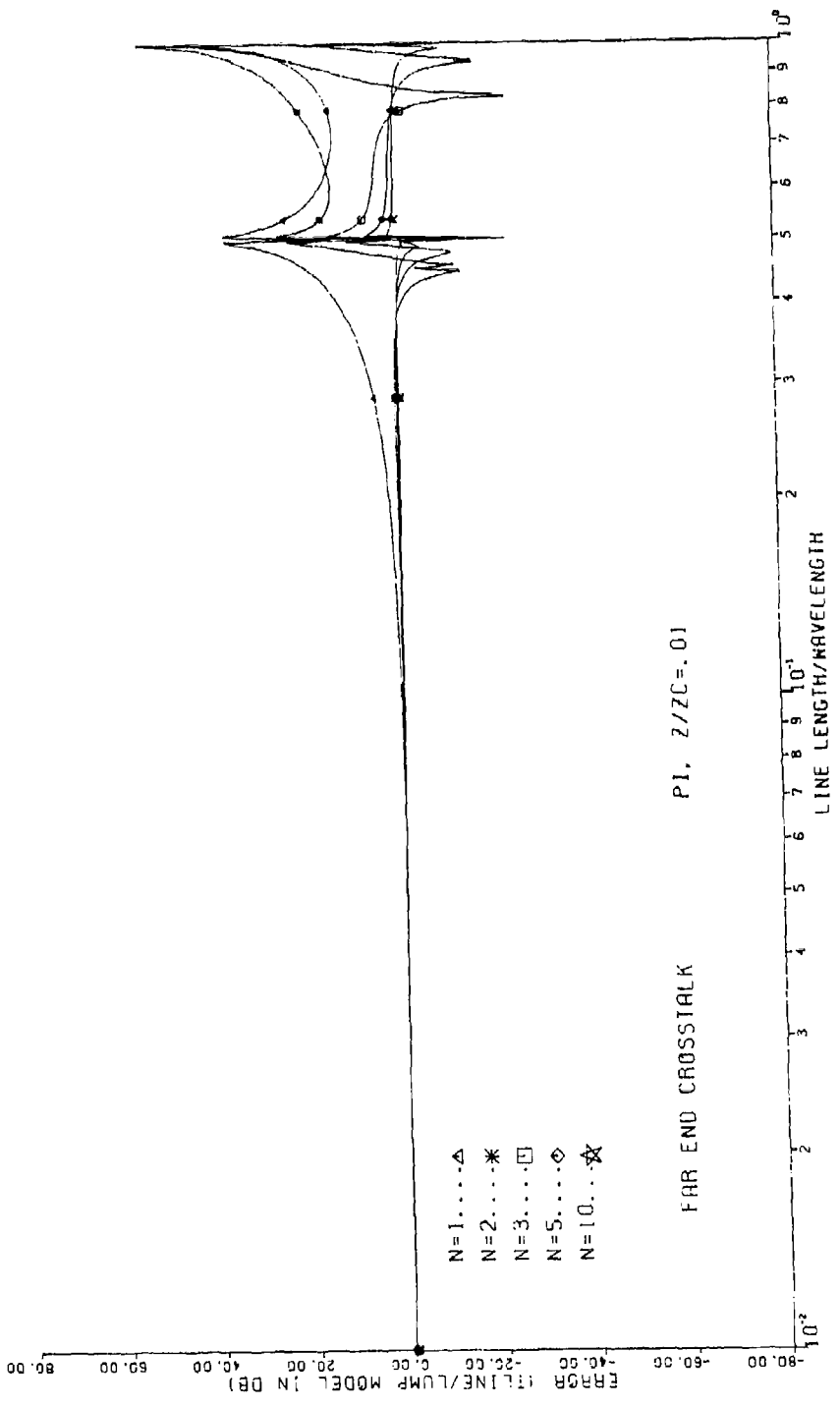
ERROR (LINE/LUMP MODEL IN DB)
80.00
60.00
40.00
20.00
0.00
-20.00
-40.00
-60.00
-80.00
10^{-2}
10^{-1}
10^{0}
LINE LENGTH/WAVELENGTH
FAR END CROSSTALK
P1, Z/ZC=.01
N=1
N=2
N=3
N=5
N=10

Figure F-3

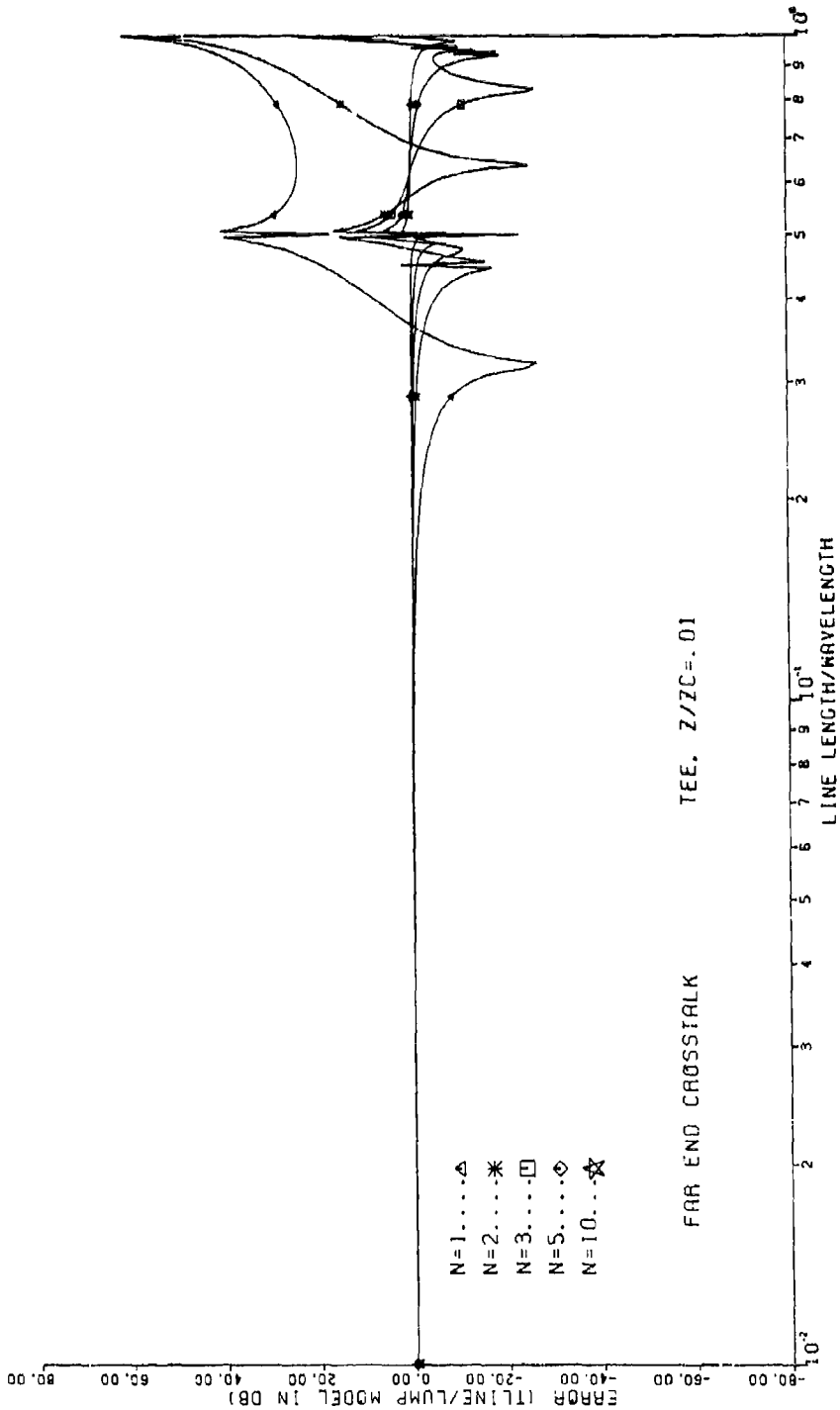
ERROR (LINE/LUMP MODEL IN DB)
80.00
60.00
40.00
20.00
0.00
-20.00
-40.00
-60.00
-80.00
10^{-2}
10^{-1}
10^{0}
LINE LENGTH/WAVELENGTH
FAR END CROSSTALK
TEE. Z/ZC=.01
N=1
N=2
N=3
N=5
N=10

Figure F-4

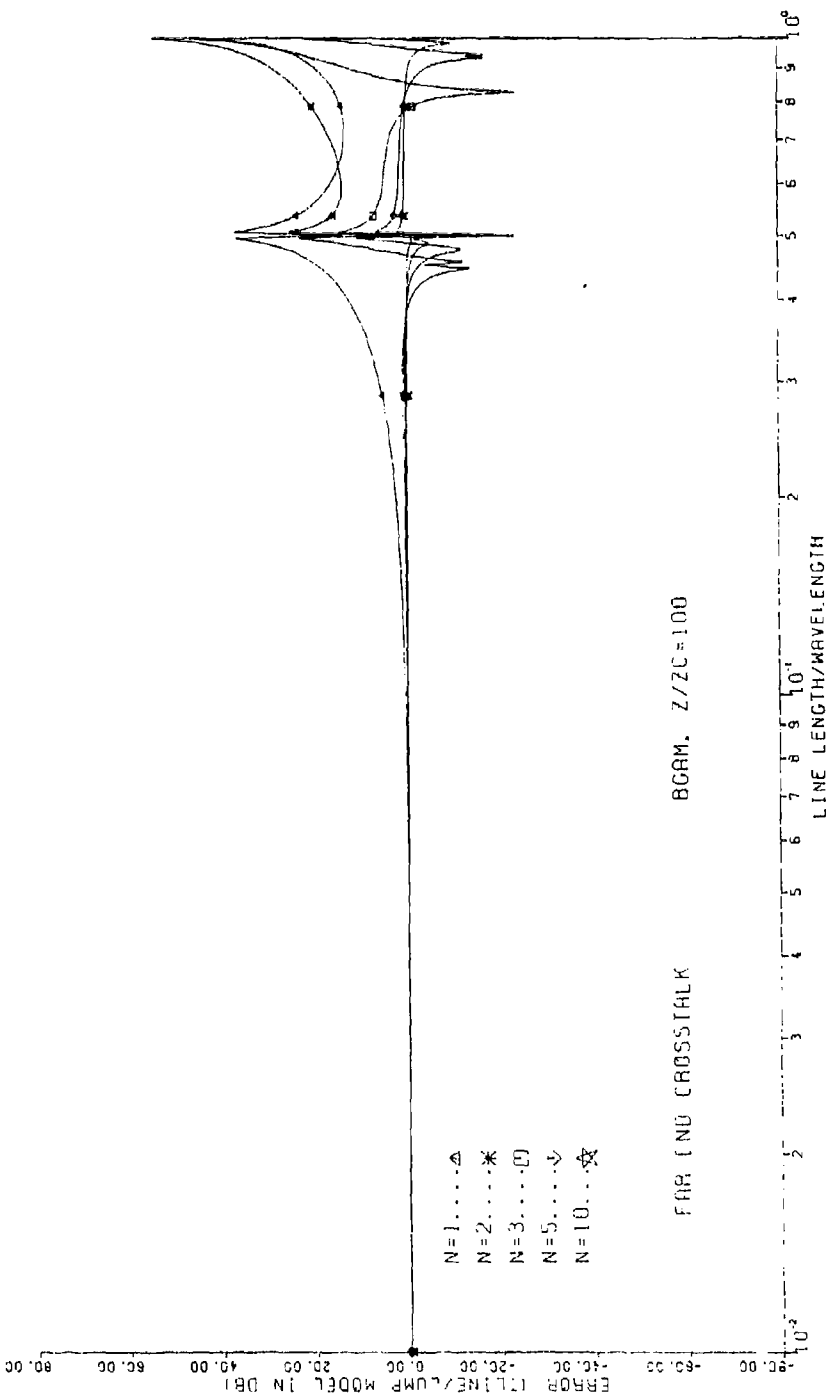
FAR END CROSSTALK
BGAM. Z/ZC=100
N=1.....Δ
N=2.....*
N=3.....□
N=5.....▽
N=10.....☆
ERROR (LINE/LUMP MODEL) IN DB
LINE LENGTH/WAVELENGTH

Figure F-5

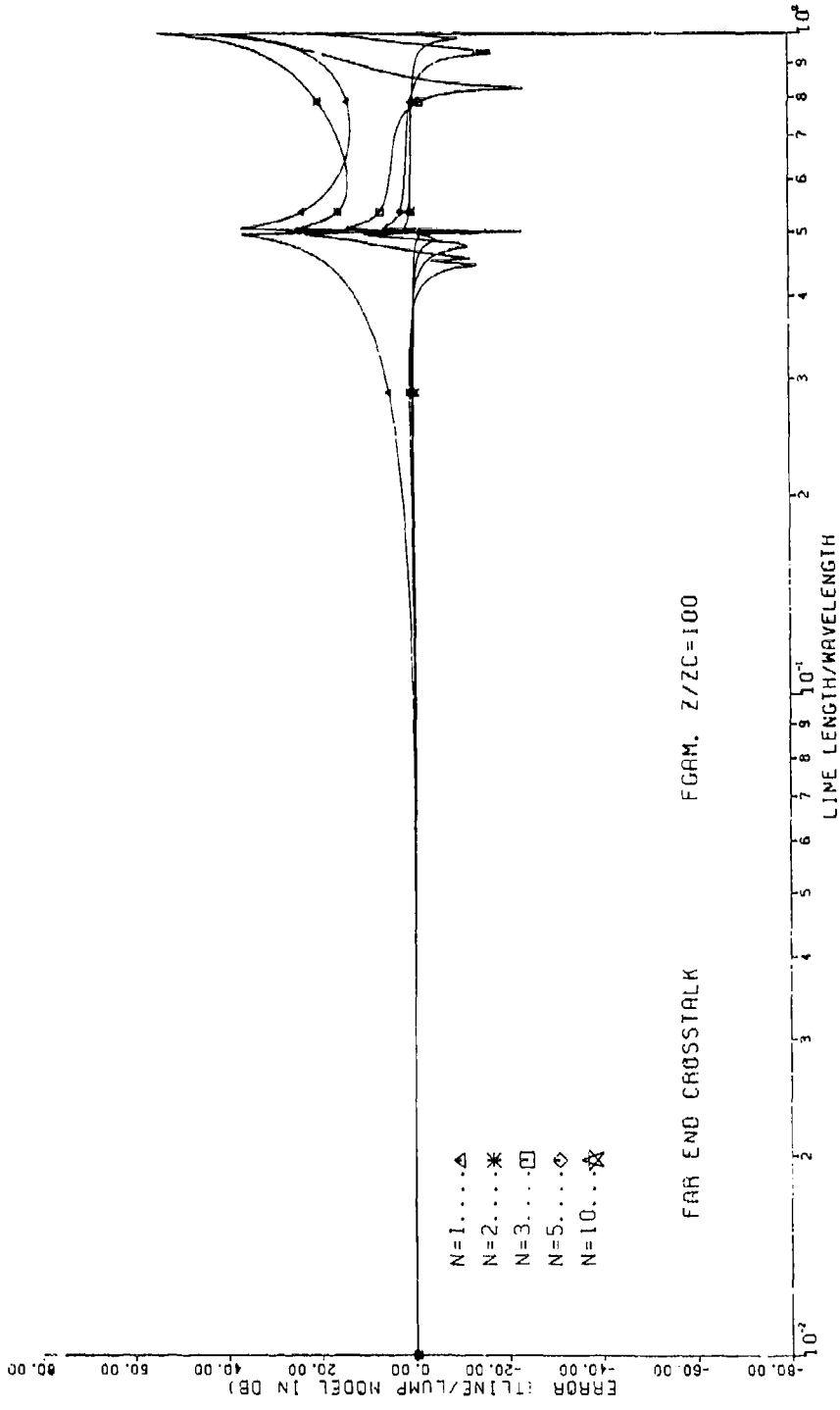
ERROR (LINE/LUMP MODEL IN DB)
80.00
60.00
40.00
20.00
0.00
-20.00
-40.00
-60.00
-80.00
10^{-2}
10^{-1}
10^{0}
LINE LENGTH/WAVELENGTH
FAR END CROSSTALK
FGAM. Z/ZC=100
N=1.....
N=2.....
N=3.....
N=5.....
N=10.....

Figure F-6

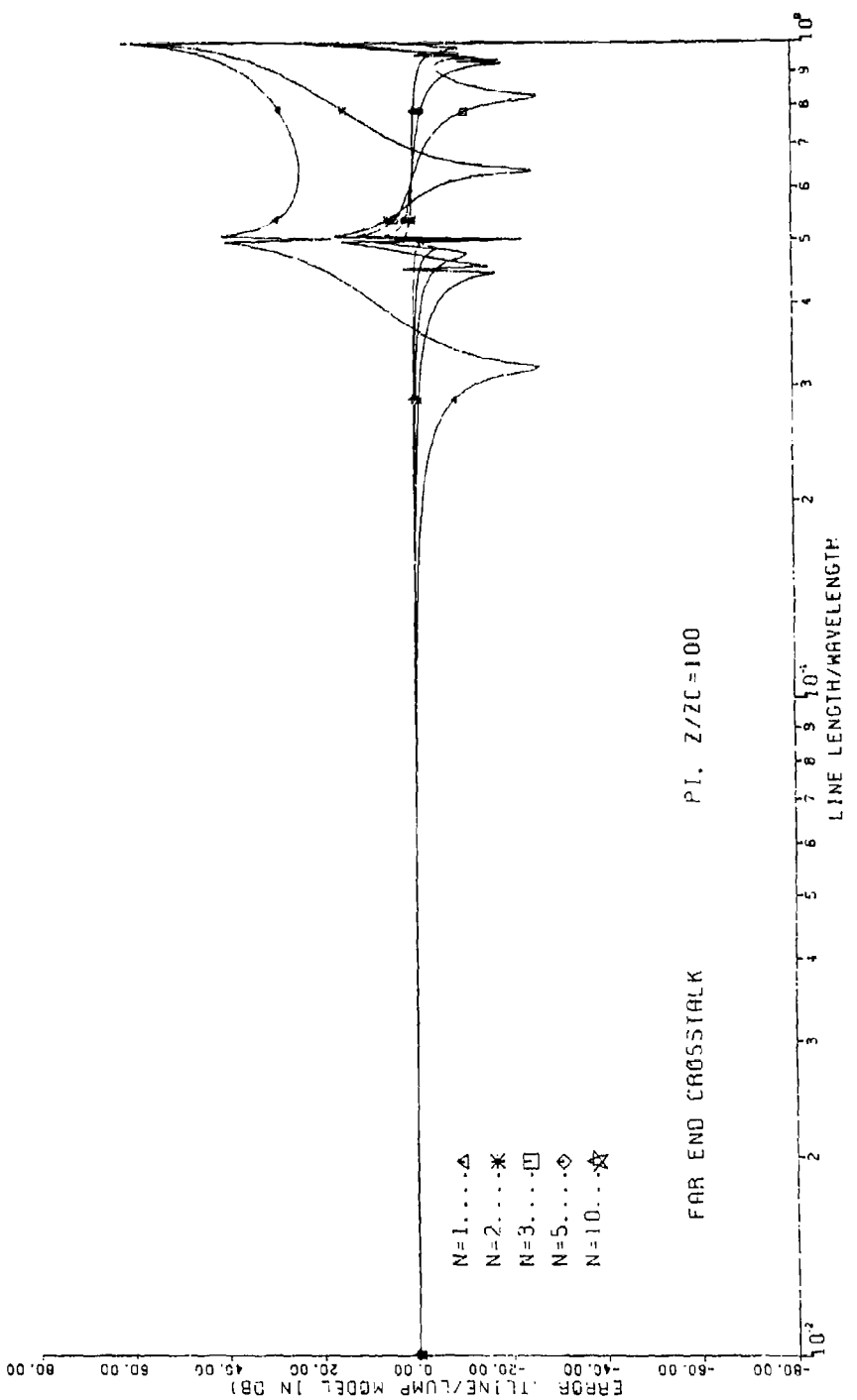
ERROR (LINE/LUMP MODEL) IN DB)
80.00
60.00
40.00
20.00
0.00
-20.00
-40.00
-60.00
-80.00
10^{-2}
2
3
4
5
6
7
8
9
10^{-1}
2
3
4
5
6
7
8
9
10^{0}
LINE LENGTH/WAVELENGTH
FAR END CROSSTALK
PI. Z/ZC=100
N=1.....
N=2.....
N=3.....
N=5.....
N=10.....

Figure F-7

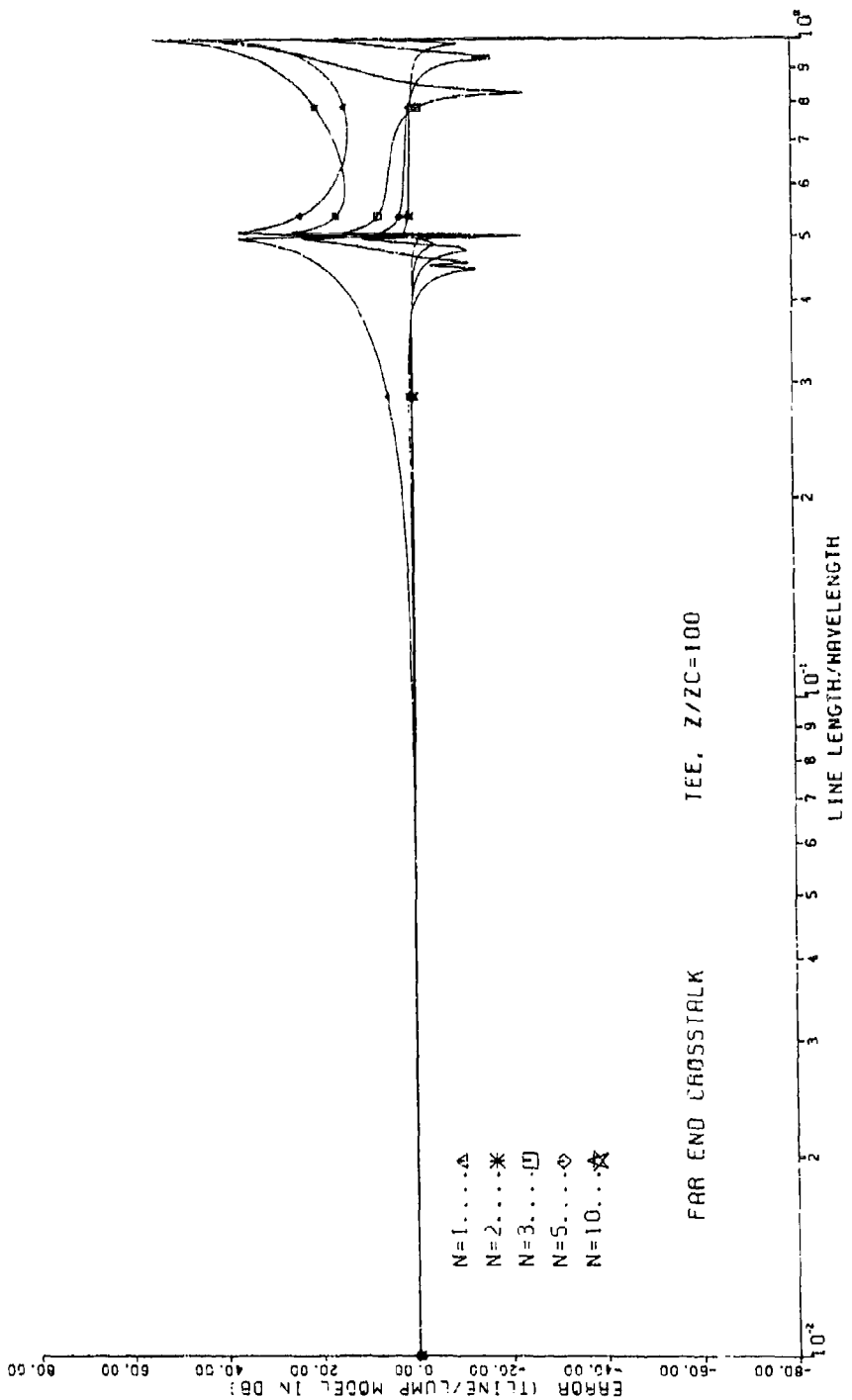
FAR END CROSSTALK
TEE, Z/ZC=100
N=1....△
N=2....✳
N=3....□
N=5....◇
N=10...☆
ERROR (LINE/LUMP MODEL) IN DB
LINE LENGTH/WAVELENGTH
-80.00
-60.00
-40.00
-20.00
0.00
20.00
40.00
60.00
80.00
10^{-2}
10^{-1}
10^{0}

Figure F-8

REFERENCES

[1] C. R. Paul, Applications of Multiconcuctor Transmission Line Theory to the Prediction of Cable Coupling, Vol. I, Multiconductor Transmission Line Theory, Technical Report, RADC-TR-76-101 (A025028), Rome Air Development Center. Griffiss AFB. NY, April 1976.

[2] M. S. Ghausi and J. J. Kelly, Introduction to Distributed-Parameter Networks, Holt, Rinehart, Winston, Inc., NY, 1968.

[3] A. M. Erisman and G. E. Spies, "Exploiting Problem Characteristics in the Sparse Matrix Approach to Frequency Domain Analysis," IEEE Transaction on Circuit Theory, Vol. CT-19, No. 3, pp. 260-264, May 1972.

[4] T. R. Williams, Programming Notes: PCAP 3 (Princeton Circuit Analysis Program), Princeton University, Princeton, NJ, Sept. 1969.

[5] L. W. Nagel, SPICE2: A Computer Program to Simulate Semiconductor Circuits, Memorandum No. ERL-M520, Electronics Research Laboratory, College of Engineering, University of California, Berkeley, Ca, May 1975.

[6] Nonlinear Circuit Analysis Program Documentation, Technical Report, RADC-TR-79245, Vols, I-II, Rome Air Development Center, Griffiss AFB, NY, 1979.

[7] J. C. Bowers and S. R. Sedore, SCEPTRE, A Computer Program for Circuit and Systems Analysis, Prentice-Hall, Inc., Englewood Cliffs, NJ, 1971.

[8] Advanced Statistical Analysis Program (ASTAP), Program Reference Manual, Pub. No. S1120-1118-0, IBM Corporation, Data Processing Division, White Plains, NY, 10604.

[9] G. L. Wilson and K. A. Schmidt, "Transmission Line Models for Switching Studies: Design Criteria II. Selection of Section Length, Model Design and Tests," IEEE Trans. on Power Apparatus and Systems, Vol. 93, No. 1, pp. 389-395, Jan/Feb 1974.

[10] C. R. Paul, "Solution of the Transmission-Line Equations for Three-Conductor Lines in Homogeneous Media," IEEE Trans. on Electrmagnetic Compatibility, Vol. EMC- 20, No. 1, pp. 216-222, Feb. 1978.

[11] C. R. Paul, "On the Superposition of Inductive and Capacitive Coupling in Crosstalk-Prediction Models," IEEE Trans. on Electromagnetic Compatibility, Vol. EMC-24, No. 3, pp. 335-343, August 1982.

MISSION
of
Rome Air Development Center

RADC plans and executes research, development, test and selected acquisition programs in support of Command, Control Communications and Intelligence (C^3I) activities. Technical and engineering support within areas of technical competence is provided to ESD Program Offices (POs) and other ESD elements. The principal technical mission areas are communications, electromagnetic guidance and control, surveillance of ground and aerospace objects, intelligence data collection and handling, information system technology, ionospheric propagation, solid state sciences, microwave physics and electronic reliability, maintainability and compatibility.